Desalination & Water Purification Research and Development Program Report No. XXX

Optimization of Electrode Design for Electrodialysis Reversal

Prepared for Reclamation Under Agreement No. R10AC80283

By

Masoume Jaberi, Abbas Ghassemi

U.S. Department of the Interior
Bureau of Reclamation
Technical Service Center
Water and Environmental Services Division
Water Treatment Engineering Research Team
Denver, Colorado

August 2015

MISSION STATEMENTS

The mission of the Department of the Interior is to protect and provide access to our Nation's natural and cultural heritage and honor our trust responsibilities to Indian tribes and our commitments to island communities.

The mission of the Bureau of Reclamation is to manage, develop, and protect water and related resources in an environmentally and economically sound manner in the interest of the American public.

Disclaimer

The views, analysis, recommendations, and conclusions in this report are those of the authors and do not represent official or unofficial policies or opinions of the United States Government, and the United States takes no position with regard to any findings, conclusions, or recommendations made. As such, mention of trade names or commercial products does not constitute their endorsement by the United States Government.

Acknowledgements

I would like to acknowledge The Desalination and Water Purification Research and Development Program, U.S. Bureau of Reclamation, for their financial support to carry out this research project.

Contents

Page

Glossary

List of Abbreviations

AEM	Anion Exchange Membrane
ANOVA	Analysis of Variance
BGNDRF	Brackish Groundwater National Desalination Research Facility
CE	Current Efficiency
CEM	Cation Exchange Membrane
DC	Direct Current
ED	Electrodialysis
EDR	Electrodialysis Reversal
GPM	Gallon Per Minute
HMI	Human-Machine Interface
IC	Ion Chromatography
LCD	Limiting Current Density
LSI	Langelier Saturation Index
MED	Multiple Effect Distillation
MEE	Multi-Effect Evaporation
MLR	Multi Linear Regression
MMF	Multi Media Filterage
MSF	Multi-Stage Flash
NMSU	New Mexico State University
RO	Reverse Osmosis
SEC	Specific Energy Consumption
TDS	Total Dissolved Solids
VC	Vapor Compression
VIF	Variance Inflation Factor
ZLD	Zero-Liquid Discharge

Executive Summary

The worsening global scarcity of freshwater threatens worldwide peace and prosperity, which are intimately tied to the availability of clean, fresh water (J. E. Miller, 2003). One approach for alleviating this threat is desalination, which can turn brackish and saline water sources into freshwater, and electrodialysis reversal (EDR) is a proven and widely used technology that can desalinate brackish waters in inland areas such as the southwestern United States. In a significant advantage over other membrane-based systems like reverse osmosis, EDR's ability to clean itself renders the system resistant to scaling and fouling and allows it to operate at high levels of water recovery. In a further benefit, this system typically requires less energy than thermal distillation to desalinate brackish water, leading to a reduction in overall desalination costs.

To identify the operating limits of EDR and find the parameters that maximize its performance, this research investigated the performance sensitivity and limitations of EDR for treating brackish groundwater through careful experimental and statistical analyses of selected electrical, hydraulic, and chemical variables. Experimental evaluation was performed using a pilot-scale EDR system and natural feedwaters at the Brackish Groundwater National Desalination Research Facility in Alamogordo, NM; statistical analyses were carried out using SAS software. Based on the experimental results and statistical analyses, multi-linear regression models were developed for EDR systems for removal ratio, current, and specific energy consumption.

Chapter 1 - Introduction

1.1 Background

Water is the essential substance for life on earth, and the demand for it is increasing rapidly. There is about 1.4 billion km3 of water on earth, but less than 3% of it is freshwater, and most of that is inaccessible since it is locked up in ice caps and glaciers. The remaining 23% of freshwater is held as groundwater, surface water, in plants, and in the atmosphere (P. H. Gleick, 1993).

The lack of fresh water prevents economic development, results in environmental degradation, and causes political instability. This challenge has forced many governments to look for technologies that conserve water and improve the efficiency of water use.

Many areas that are facing the highest water stress have access to groundwater resources, but the quality of the groundwater often renders it unsuitable for human consumption: the main disadvantage of groundwater reservoirs is the high amount of dissolved solids such as calcium, magnesium, iron, sulfate, sodium, chloride, and silica. Before water from these supplies can be used for drinking, agriculture, industrial applications, and myriad other purposes, such groundwater has to be desalinated (Elsaid, Bensalah, & Abdel-wahab, 2012).

Desalination is a process by which excess salts are removed from saline water to make it suitable for human consumption and other uses.

The global online capacity for desalination plants has increased from 5.1 million m^3/day in 1980 (Pankratz, 2012), to more than 80 million m^3/day in 2013 (International Desalination Association, 2013). Saudi Arabia is currently the world leader in desalination production capacity at approximately 16% of the global capacity, followed by the United States at approximately 13% (Greenlee, Lawler, Freeman, Marrot, & Moulin, 2009).

However, although there are plentiful sources of saline water, the high costs of desalination and other forms of advanced water treatment have limited the use of these technologies (J. E. Miller, 2003). There are currently 16,000 desalination plants on the planet, but their total capacity is only about 1% of the freshwater used every day in just the United States (P. Gleick, 2012; J. E. Miller, 2003; Pankratz, 2012). This capacity is expected to double over the next 20 years with a predicted $20 billion in spending (Brady, Kottenstette, Mayer, & Hightower, 2009; Martin-lagardette, 2003), but large-scale desalination systems are fairly recent technological developments, dating back only to the mid-1900s, and there are still significant research opportunities for improving the energy consumption, cost, and reliability of desalination technologies.

1.2 Desalination

Desalination is defined as a process for removing various salts from saline water to produce fresh water. There are multiple desalination technologies, but the applicability of each one is heavily dependent on the type of water to be desalinated. Water is typically characterized by the amount of total dissolved solids (TDS), and based on that, there are different water types including:

- Fresh water, with less than 1,000 mg/L TDS,
- Brackish water, with between 1,000 and 5,000 mg/L TDS,
- Highly brackish water, with between 5,000 and 15,000 mg/L TDS,
- Saline water, with between 15,000 and 30,000 mg/L TDS,
- Seawater, with between 30,000 and 40,000 mg/L TDS, and
- Brines, with greater than 40,000 mg/L TDS

In addition to water type, the other main factors in choosing the best desalination technology for a particular application include the availability of energy, the intended use for the produced water, and the required treatment capacity. The basic types of desalination techniques are categorized into two main groups: (a) thermal technologies, and (b) membrane.

The driving force of thermal processes is heat, which is used to induce a phase change in water, causing it to evaporate and leave dissolved solids behind. Because of the energy needed to achieve this, thermal techniques are not usually used for brackish water treatment due to their high cost. However, these technologies produce water with very low levels of TDS, and they are used extensively in the Middle East where there are abundant sources of fossil fuels. Some examples of thermal desalination technologies include multiple stage flash distillation (MSF), multiple effect distillation (MED), multi-effect evaporation (MEE), and vapor compression (VC).

The other main category of desalination approaches, membrane based technologies, is usually divided into two groups based on the driving force, which can be either pressure or electricity. Pressure driven processes include reverse osmosis (RO), nanofiltration, microfiltration, ultrafiltration, and forward osmosis; electrically-driven membrane processes include electrodialysis (ED) and electrodialysis reversal (EDR) (Shaffer & Mintz, 1966).

RO is currently the most popular desalination technology comprising 60% of the total global desalination capacity in 2012 (Pankratz, 2012). However, in comparison to the widely used RO technology, ED has higher water recovery (the fraction of feed water that becomes product water). Low recovery rate prevents widely implementation of RO to desalinate brackish ground waters, because the disposal of large volumes of waste is environmentally and financially unfeasible (Subcommittee, 2004; Nicot & Chowdhury, 2005). The other advantage of ED over RO is greater resistance to scaling and fouling, which makes them particularly promising technologies for brackish water treatment (Murray, 1995).

Electrodialysis (ED) is an electrically driven membrane process in which ions are selectively transferred through ion-exchange membranes under the electric potential of DC voltage. Since the driving force for separation is an electric field, ED only removes charged components from solution. ED cannot safely remove

organic elements that do not carry an electrical charge, but it can be used on waters with high levels of silica that would foul pressure-driven membranes.

Electrodialysis Reversal (EDR) was introduced in the 1970's as an innovative modification of existing ED technology (Elsaid, Bensalah, & Abdel-wahab, 2007). EDR works the same way as ED, except that the polarity of the DC power is reversed at specified time intervals, allowing for a 'self-cleaning' of the membrane surfaces. With the reversal modification, EDR process has proven to operate at higher solution concentrations of dissolved solids, suspended solids, scale-prone salts, and non-ionic species (such as silica) with higher recovery rates and low chemical pretreatment than other desalination technologies (Reahl, 2006).

1.3 Research Challenge

Fueled by rapid population growth, much of the Southwest United States is witnessing an increased demand on their limited freshwater supply, and looking towards their extensive brackish water as part of the mix of available resources to address this issue. Texas and Arizona have an estimated 2.7 billion acre-feet and 600 million acre-feet of brackish water, respectively. In New Mexico, there is a significant amounts of brackish groundwater., but three-quarters of this brackish water has salinities high enough to require treatment before it can be used for most purposes (Eden, Glass, & Herman, 2011; National Ground Water Association, 2010).

The challenge of balancing water scarcity and increasing water demands has drawn attention toward utilizing technology to produce drinking water from non-potable resources. However, the implementation of large-scale inland desalination is hindered by the relatively high cost of treating brackish waters (Staff, 1996; Strathmann, 2004; Lee, Hong, Han, Cho, & Moon, 2009; Jefferies & Comstock, 2001).

Electrodialysis Reversal (EDR) has been used for half a century to desalinate brackish and saline waters for potable use and shows promise as a viable brackish water treatment process for two primary reasons: it can achieve greater product recovery than RO, and it is more robust than RO with respect to feed turbidity, feed silica concentration, and biological growth (*i.e.*, ion-exchange membranes can tolerate a mild chlorine dose) (AWWA, 1995; Reahl, 2006).

While the brackish water desalination using EDR process has been successfully implemented in a few situations, there is lack of wide approach that identifies the various operating aspects of EDR and finds the parameters that maximize its performance,

Therefore, our research challenge is to conduct a complete investigation of performance sensitivity and limitations of EDR for treating brackish groundwater through careful experimental and statistical analyses of selected electrical, hydraulic, and chemical variables.

1.4 Research Objective

One goal of this research was to systematically and quantitatively analyze

the performance of a pilot-scale EDR plant in the treatment of several brackish groundwaters under various electrical, hydraulic, and chemical conditions; another goal was to determine the operating conditions that contribute to higher removal ratios and lower energy consumption.

More specifically, the objectives of this research were to:

1. Experimentally determine the sensitivity of EDR to hydraulic, electrical, and chemical operational parameters;
2. Determine and compare how the three electrode designs (full, recessed, and tapered) affect EDR performance;
3. Identify the operating parameters that maximizes the performance of EDR;
4. Perform statistical analyses of the investigated parameters (electrical, hydraulic, and chemical) to determine their impacts on EDR performance.

The hypothesis for this research is that EDR desalination systems perform differently under different operating and design conditions, including applied stack voltage, flow rate, source water salinity, and electrode design.

1.5 Research Approach

These goals were accomplished using an existing infrastructure in order to be most economical. We used an existing 1-stage pilot-scale EDR owned by NMSU and located at the Brackish Groundwater National Desalination Research Facility (BGNDRF) in Alamogordo, NM. In order to do the investigations on the operating factors, the experiments were done where the effects of operating variables: feed flow rate, feed salinity, voltage and type of electrode were verified.

The introduction presented here is followed in Chapter 2 by a review of EDR technologies and operations. Then, Chapter 3 details the experimental methodology including the experimental location, experimental set-up, and a detailed summary of the data collection procedure. In Chapter 4, a discussion of experimental results is presented in response to the objectives. Finally, a summary of the conclusions resulting from this research is also presented in Chapter 4.

Conclusions

The following is a brief overview of the conclusions and recommendations made based on the results of the experiment; a more detailed discussion is given in sections 4.3 and 4.4.

- EDR performance depends on operating conditions such as, stack voltage, flow rate and feed salinity. However, the design of the electrodes has no significant effect on EDR performance.
- Brackish groundwater experiments demonstrated that stack voltage applications in the range of 30-40 Volts and feed flow rates in the

range of 7-11 GPM effectively separated up to 70% of the initial feed salinity in the range of approximately 1000-5500 mg/L at single-stage EDR recovery of 80%.

- The rate of separation and current are approximately proportional to the applied voltage.
- The specific energy consumption increases with increasing the applied voltage.
- A decrease in the rate of separation was observed with increases in the feed flow rate, which increase the stack superficial velocity leading to a decrease in residence time.
- An increase in flow rate causes an increase in the energy required for pumping, and consequently an increase in total energy.
- Specific energy consumption decreases with increases in the feed flow rate while product water volume increases when feed flow rate increases.
- As the concentration of solution increases, the removal ratio drops when feed concentration increases.
- Since current is proportional to feed conductivity, the specific energy consumption increases as feed water becomes more saline.
- In order to increase the removal ratio, lower feed concentrations, higher voltages, and lower flow rates should be utilized.
- In order to reduce the specific energy consumption, lower voltages, lower feed concentrations, and higher flow rates are suggested.
- The data gathered in these experiments are from conditions that still left salinity levels above 1,000 μS/cm in the product water. Therefore, real-world desalination processes would require further treatment to bring the quality of the produced water to acceptable levels.
- Given that specific energy consumption is strongly determined by the removal ratio, further salt removal to produce truly potable water would significantly increase the specific energy consumption of the systems.
- As a consequence of an expanded hydrodynamic boundary layer and concentration boundary layer, the system is likely to experience progressively poorer electrochemical/hydrodynamic behavior.
- As the removal ratio increases, there is a higher likelihood of salt precipitation in the hydrodynamic/concentration boundary layer.
- Additional testing should be conducted before designing industrial-scale systems due to the preceding reasons.

Recommendations

- Expansion of the EDR experiment could be made to study how additional operating conditions, such as temperature and recovery ratio, affect EDR performance.
- The experiments could be done with more than one hydraulic stage to improve the removal ratio and study how energy consumption changes when more stages are added.
- The models for the pilot-scale plant could be extended to simulate full-scale EDR systems. This would allow them to quantify limitations in the tradeoff between energy consumption and removal ratio associated with voltage application and feed flow rate, making it possible to optimize the design of EDR systems.

Chapter 2 - Literature Review

In this chapter, the principles of electrodialysis reversal are described and

the thermodynamic basics for separation and overall mass transfer are explained. Then, the chapter moves on to describe the coupled hydraulic/electrochemical behavior of the system. This is followed by an introduction to basic performance metrics of each EDR system, including energy consumption, desalting ratio, current efficiency and recovery ratio. Lastly, the chapter moves on to present and explain strategies that contribute to improved EDR performance.

EDR is an electrochemical separation process that selectively removes dissolved solids, based on their electrical charge, by transferring the brackish water ions through a semipermeable ion exchange membrane charged with an electrical potential (Younos & Tulou, 2009). The ions are transferred through ion exchange membranes by means of a direct current (DC) voltage. The process uses a driving force to transfer ionic species from the source water toward a cathode (positively charged ions) and anode (negatively charged ions) to a concentrate wastewater stream, creating a more dilute stream (Walker, 2010). The overall schematic for the EDR process is shown in Figure 2.1.

2.1 EDR System Description

As illustrated in Figure 2.2 (Hanrahan, 2013), EDR works as follows. First, the influent source water is split into three streams: feed in, concentrate makeup, and electrode in. The feed in stream, which receives the largest portion of the source water, enters the dilute flow-paths and is demineralized until it exits the stack as product water. A smaller portion of the source water becomes the concentrate makeup stream, which combines with the concentrate recycle at the suction end of the concentrate pump and enters the concentrate flow-paths as the concentrate in stream. This water is progressively concentrated until going to waste as concentrate blowdown, and the remainder enters the concentrate recycle. The source water flows in parallel only through demineralizing compartments, whereas the concentrate stream flows in parallel only through concentrating compartments. The last part of the source water becomes the electrode in stream. This stream is dosed with acid and continuously circulates through the space provided by heavy spacers in order to prevent scaling by neutralizing the hydroxyl ions at the cathode and flushing the electrode chambers of precipitates and gases such as oxygen, hydrogen, and chlorine, which are formed as part of the electrochemical reactions at the surface of the electrodes.

Within the electrode chambers, different oxidation and reduction reactions will occur, depending on the polarity of the electrode. When DC potential is applied across the electrodes, the following processes take place (Murray, 1995):

At the cathode, pairs of water molecules dissociate, producing two hydroxyl (OH–) ions plus hydrogen gas (H_2). This reaction, shown in Equation 2.1, is called the reduction of water by the half reaction:

$$2H_2O + 2e^- \rightarrow 2OH^- + H_{2(g)} \qquad \text{Eq.2.1}$$

As a result, hydroxide raises the pH of the water, causing calcium carbonate

($CaCO_3$) precipitation.

At the anode, pairs of water molecules break down to produce four hydrogen ions (H^+), one molecule of oxygen (O_2), and four electrons (e^-), a process which is called the oxidation of water by the half reaction. This is shown in Equation 2.2.

$$H_2O \rightarrow 2e^- + \frac{1}{2}O_{2_{(g)}} + 2H^+ \qquad \text{Eq. 2.2}$$

The acid produced by this reaction tends to dissolve any calcium carbonate present to inhibit scaling. In this reaction, in the case of having chloride at the anode, the oxidation of chloride results in chlorine gas (Cl_2) formation, as shown in Equation 2.3.

$$2Cl^- \rightarrow 2e^- + Cl_{2_{(g)}} \qquad \text{Eq. 2.3}$$

Flows from the two electrode compartments do not mix with other streams. Concentrate from the electrode stream is sent to a degasifier to remove and safely dispose of any reaction gases. In many applications, after being passed through the degasifier, concentrate from the electrode stream is recycled back to the feed in order to increase the overall recovery of the system (Valero, Barceló, & Arbós, 2010).

2.2 Polarity Reversal Phenomenon

Across all ED/EDR systems and almost all membrane-based desalination processes, membrane fouling is a major problem. In this phenomenon, suspended solids that carry electrical charges adhere to the surface of the membranes and drastically increase membrane resistance, significantly reducing membrane efficiency.

Despite the almost universal prevalence of the membrane fouling problem, this difficulty has been largely overcome in EDR through periodic reversals in the polarity of the electrodes. This reversal tends to expel charged particles that have precipitated onto the membranes. This process, which is called "clean in place" or simply electrodialysis reversal (Pilat, 2001; Reahl, 2006), is illustrated in Figure 2.3. (Allison, 2008).

While the source water flows in the chambers between the cationic and anionic membranes, the DC voltage supplied by the cathode draws anions toward the cathode through the anion exchange membrane (AEM). Over time, the cathodic attraction leads anions to accumulate on the AEM surface, forming a barrier termed a "fouling layer." Polarity reversal disrupts the fouling layer by driving the negatively charged components away from the AEM and back into the feed stream, restoring membrane properties to their pre-fouling condition (H.-J. Lee et al., 2009).

In addition to the polarity reversal, the flows of the hydraulic streams at the

stack inlet and outlet are also reversed. The hydraulic streams in an EDR stack consist of concentrate streams and dilute streams, and when the EDR stack is operating with reversed polarity, the concentrate cells become the diluate cells, and vice versa. The interval between polarity reversals can range from several minutes to several hours.

For a short period of time while the polarity and streams are being reversed, the salinity of the diluate stream exceeds the salinity levels required of the product water. To avoid producing unacceptable product water, a more complicated flow control process is required. Therefore, the outlet for the product water is monitored by a concentration sensor that regulates a 3-way valve. When conductivity passes a pre-determined threshold, the valve shunts product water with overly high salinity into the brine stream. This is continued until the feed stream has completed replaced the concentrate stream in the newly-diluate flow path, resulting in the production of permeate water with acceptable quality. At this point, the conductivity sensor at the outlet detects salinities below the required threshold and returns the product stream to the product tank.

In the use of EDR systems, some of the product water is always lost into the waste stream during polarity reversal. Usually, this loss varies between 2 and 4% of the volume of product water in industrial EDR plants (AWWA, 1995). Although such loss may not be acceptable when feed solutions contain high value products (e.g., in particular applications within the food and drug industry), product water loss generally is not a problem in the desalination of brackish water.

Overall, periodically reversing the polarity of the electrical field in the EDR process results in several positive impacts to the operation of the system (Katz, 1979):

- The polarization films are broken up several times every hour, which avoids scaling;
- Newly precipitated scales are dissolved before they can damage the membrane;
- As the directional movement of colloidal particles is reversed, slime formation on the membrane surface is reduced; and
- Drawbacks resulting from the need to continuously add chemicals (e.g., antiscalants and acids) are eliminated.

2.3 EDR Stack Components

The basic structure of an EDR stack consists of electrode chamber and cell pairs, as shown in Figure 2.4.

2.3.1 Electrode Chamber

Each electrode compartment consists of an electrode, an electrode water-flow spacer, and a heavy cation membrane. This spacer prevents the electrode waste from entering the main flow paths of the stack and typically is thicker than a normal spacer, which increases water velocity to prevent scaling (Ionics, 1984).

In order to withstand a greater degree of hydraulic pressure difference between the electrode streams and the adjacent flow-paths, heavy cation exchange membranes are required. These membranes have all the properties of regular cationic membranes but are twice as thick (Valerdi-Perez, Berna-Amoros, & Ibanes-Mengual, 2000).

Another component, the electrode, is located at each end of the membrane stack and conducts electric current into the stack. Because of the corrosive nature of the anode compartments, electrodes are usually made of titanium and plated with platinum.

The life span of an electrode is dependent on the amperage applied to the electrode and the ionic composition of the source water. High amperages and large amounts of chlorides in the source water reduce electrode life (AWWA, 1995).

Generally, electrode life in the last decade varied with the application and type of feed water, the capability of the operators, and other factors. Over time, material science has been developing new techniques for plating and deposition, and electrode materials have changed over the years as experience and process understanding have increased. For instance, with the advent of EDR, Ionics, Inc., undertook an extensive research and development program designed to produce an electrode that has a reasonable life, is reasonably inexpensive, and is relatively electrically efficient. (Purification & Program, 2003).

2.3.2 EDR Cell Pair

Each assembled stack is composed of the two electrodes and groups of cell pairs. A cell pair consists of the following (Valero & Arbós, 2010):

- Anion permeable membrane,
- Concentrate spacer,
- Cation permeable membrane, and
- Dilute stream spacer.

This basic cell pair is repeated until it is capped on both ends by the electrode compartments, which consist of: a heavy flow-path spacer, a heavy cation-exchange membrane, and an electrode (Figure 2.5).

2.3.2.1 Ion-Exchange Membranes

Typically, ion-exchange membranes are dense hydrophobic polymers, such as polystyrene, polyethylene, or polysulfone, which are fixed with charged functional groups (Walton, 1962). There are two different types of ion-exchange membranes, which are classified based on the ions that they interact with in solutions: (1) cation-exchange membranes (CEMs), which contain negatively charged groups fixed to the polymer matrix; and (2) anion-exchange membranes (AEMs), which contain positively charged groups fixed to a polymer matrix.

Figure 2.6 (Strathmann, 2010) schematically illustrates the matrix of a CEM with fixed anions and mobile cations. In a cation-exchange membrane, the fixed anions are in electrical equilibrium with mobile cations in the interstices of the polymer. For a CEM, the mobile cations and anions are called counter-ions and co-ions respectively. The co-ions are excluded from the membrane matrix because of their electrical charge, which is identical to that of the fixed ions. In other words,

CEMs are preferentially permeable to cations. AEMs, conversely, carry positive charges fixed on the polymer matrix. AEMs exclude cations, and therefore are preferentially permeable to anions (Tanaka, Uchino, & Murakami, 2012). The extent of exclusion from an ion-exchange membrane depends on the properties of both the membrane and the solution (Strathmann, 2010).

In addition to classifying the membranes based on their ionic functionality, it is useful to distinguish them, according to their structure, as homogeneous or heterogeneous (Walton, 1962). Homogeneous membranes are prepared by introducing an ion-exchange moiety directly into the structure of the polymer, leading to a relatively even distribution of charged groups over the entire membrane matrix. Heterogeneous membranes are prepared by mixing a fine ion-exchange resin powder with a binder polymer and pressing and sintering the mixture at an elevated temperature. This results in a structure where the ion-exchange groups are clustered and very unevenly distributed in membrane matrix as shown in Figure 2.6 a) and b) (Strathmann, 2004).

Generally, to produce commercial cation membranes, the polymer film is sulfonated and cross-linked in a sulfuric acid solution, producing $-SO_3H$ groups attached to the polymer. The $-SO_3H$ groups ionize in water, producing a mobile counter ion (H^+) and a fixed charge ($-SO_3^-$). Additionally, commercial AEMs usually have fixed positive charges from quaternary ammonium groups ($-NR_3+OH^-$), which repel positive ions (Strathmann, 2011).

The most desired properties of ion-exchange membranes are: high permselectivity, low electrical resistance, good mechanical and form stability, high chemical and thermal stability, and low production costs (Toshikatsu Sata, 2004). In other words, to contribute to the success of EDR plants treating saline water, both AEMs and CEMs must possess common properties including: low electrical resistance; insolubility in aqueous solutions; semi-rigidity for ease of handling during stack assembly; ability to operate in temperatures above 46 ºC; resistance to osmotic swelling; long life expectancies; resistance to fouling; ability to be hand-washed; and resistance to change in pH from 1 to 10, allowing the use of strong acid solutions to remove scales and metal hydroxide deposits (Miller, 2009).

In general, EDR technologies have a membrane life of 7 to 10 years, after which membranes must be replaced. Bacterial growth and hot spots or voltage short circuits inside the stack will damage membranes, requiring stack disassembly and the replacement of membranes and spacers, which is tedious and time consuming, particularly if not all membranes in a stack are to be replaced. In order to extend membrane life, improve product quality, and reduce power consumption, cleanings-in-place can be effective (Purification & Program, 2003).

2.3.2.2 Spacers

Spacers typically are made of polypropylene or low density polyethylene and are positioned in the spaces between the membranes that represent the flow paths of the diluate and concentrated streams. These spacers are called dilute and concentrate spacers, respectively. The spacers match the ion-exchange membrane area and are generally about 1 mm thick.

The spacers not only separate the membranes, they both direct the flow of

water uniformly across the exposed face of the membrane and create independent flow-paths through the stack (Balster, Stamatialis, & Wessling, 2009). The identical spacers rotate 180° between membranes; as a consequence, all the demineralized streams are combined with each other and all the concentrated streams are combined with each other, allowing the separation of the product and concentrate streams as seen in Figure. 2.7 (Strathmann, 2010). Various spacer designs such as the sheet flow or tortuous path flow are used in practical applications, as illustrated in Figure 2.7 (Scott, 1996).

Generally, the main difference in spacer models is the number of flow paths, which determines water velocity across the membrane stack and the contact time of the source water with the membrane.

The "sheet flow spacer" consists of an open frame with a plastic screen separating the membranes. In these spacers, the compartments are vertically arranged and the process path is relatively short. These compartments give better support for thinner membranes. The second type of spacers, "tortuous flow spacers" are horizontally arranged and folded back upon themselves. These spacers have a long, narrow channel for the flow path, providing much longer flow path. The feed flow velocity in the stack is relatively high, which provides better control over concentration polarization and allows higher limiting current densities. Despite this, the pressure loss in the feed flow channels is still quite high (*Process Technologies for Water Treatment*, 2013; Scott, 1996).

The spacer geometry dictates the proper usage of the available membrane area and the mobility of the feed water along the membrane surfaces. In general, spacers increase the turbulence and promote the mixing of the water, the use of the membrane area, and the transfer of ions. Turbulence resulting from spacers also breaks up particles or slime on the membrane surface, attracts ions to the membrane surface, and increases the availability of ions near the membrane surface, which in turn decreases concentration polarization (Chiapello & Bernard, 1993).

Velocity is an important design parameter for spacer choice because both the amount of desalting that occurs across the membranes and the amount of turbulence are a function of the solution velocity through the spacer, and higher velocity results in higher turbulence (A. A. Von Gottberg & Manager, 2010).

On the first impression, it seems that we should increase the velocity as much as we can. However, the operating velocity in an EDR stack is limited by the pressure drop along the spacer, which also increases with increasing turbulence. Additionally, to prevent external leakage, the maximum inlet pressure of the stack is limited. In conclusion, the optimal spacer provides a balance between promoting turbulence and minimizing the pressure drop (Valero et al., 2010).

2.4 Mass Transport in EDR Stack

In membrane processes, the transport rate is determined by the driving force or forces acting on the individual components and their mobility and concentration in the membrane. The driving force for the transport of a component A from a phase (') to a phase (") through a membrane can be expressed as a gradient in its

concentration, its electrical potential, and its pressure (Figure 2.8) (Strathmann, 2011).

As indicated in Figure 2.8, depending on the driving force and the transport mechanism in the membrane, three different forms of transport are distinguished:

2.4.1 Diffusion

A mass transport process is referred to as diffusion and described by Fick's laws when the individual components move independently of each other under the driving force of a chemical potential gradient. The permeation rate in a diffusion process depends on its diffusion coefficient, which is determined by friction between the diffusing component and other components in a mixture (Philibert, 2005).

2.4.2 Migration

A mass transport is referred to as migration and described by Ohm's law when charged components move through a matrix under the driving force of an electrical potential (ϕ) difference. The migration rate depends on the electrical potential gradient and the mobility of the components in the matrix, which itself is directly related to its diffusion coefficient and is determined by the friction between the migrating component and other components in a mixture (Verbrugge & Hill, 1990).

2.4.3 Convection

A mass transport process is referred to as convection when bulk flow occurs under the driving force of a hydrostatic pressure difference. The flow velocity depends on the hydrostatic pressure difference and hydrodynamic permeability coefficient, determined by the friction between the solution and the matrix.

In membrane processes, all three forms of mass transport can contribute to the overall flux. However, one transport form generally is dominant while the others contribute to a lesser extent to the overall mass flux. In microfiltration and ultrafiltration, the convection of a bulk solution is the dominant form of transport while diffusion is generally insignificant. In reverse osmosis, mass transport through the membrane occurs mainly by the diffusion of individual molecules through a more-or-less homogeneous membrane matrix, but convection can become significant with high flux membranes. In EDR cell pairs, migration of ions in an electric field is the dominant form of transport (Strathmann, Giorno, & Drioli, 2000).

The transport of a particular ion (i), within an EDR system can be approximated by the Nernst-Planck Equation (Equation 2.4) which is the summation of the diffusion, electromigration, and convection fluxes.

$$\mathrm{Ji} = -\mathrm{z_i u_i C_i F \nabla \varphi} - \mathrm{D_i \nabla C_i} + \mathrm{C_i v} \qquad \text{Eq. 2.4}$$

where J is the molar flux of species i, z is the sign and magnitude of the charge of the ion, u_i is mobility, C is the molar concentration of species i, F is the Faraday

constant (which is a product of Avogadro's number, N_A, and the elementary charge, q_e), $\nabla\varphi$ is the electric potential difference, D is the ionic diffusivity, and v is the fluid velocity (Moon, Sandí, Stevens, & Kizilel, 2004).

Then, the molar flux of species i is described as in Equation 2.5, where i_i is the current density species i.

$$J_i = \frac{i_i}{z_i F} \qquad \text{Eq. 2.5}$$

The total electrical current density (i_t) passing through the ED stack is the summation of the fluxes of all charged species in solution (Moon et al., 2004), as shown in Equation 2.6.

$$i_t = \sum_i i_i = F \sum_i z_i J_i \qquad \text{Eq. 2.6}$$

The fraction of the current that a particular ion carries is called the transport number(t_i), defined in Equation 2.7:

$$t_i = \frac{i_i}{i_{tot}} = \frac{z_i J_i}{\sum_i z_i J_i} \qquad \text{Eq. 2.7}$$

where:

$$\sum_i t_i = 1 \qquad \text{Eq. 2.8}$$

In an ideal system, the rate of separation of ions is proportional to the electrical current density. However, in reality, the number of salt ions separated is less than the electrical equivalent of the current density (Kim, Walker, & Lawler, 2012; Sadrzadeh, Kaviani, & Mohammadi, 2007; Shaposhnik, 1997). Inefficiencies with the ion-exchange membranes, the loss of current through manifolds, and concentration polarization across the ion-exchange membranes can significantly diminish the current efficiency, and each of these sources of inefficiency will be discussed in the following sections (Bard, Faulkner, Swain, & Robey, 1944; Mandersloot & Hicks, 1966; Stuttgart, 2002).

2.5 Electrodialysis Reversal Challenges

The EDR process faces several challenges, especially concentration polarization, scaling and fouling, and limiting current density. These obstacles are discussed in Sections 2.5.1 through 2.5.3.

2.5.1 Concentration Polarization

Let us consider a basic system consisting of an ion-exchange membrane separating two aqueous solutions of 1:1 electrolyte at bulk concentrations of $C_\circ$ and $\acute{C}_\circ$ with the same temperature and pressure, as illustrated in Figure 2.9 (Valerdi-Pérez, López-Rodríguez, & Ibáñez-Mengual, 2001).

When an electric potential is applied, there are two types of currents in the system: one, in the membrane, is comprised solely by counter-ions, and the other one is in the solution because of the co-ions and counter-ions in the solution and in contact with the membrane.

Assuming that the transfer number of chloride ions in solution is t_i while it is $\bar{t}_i$ in the membrane and the solution volumes are so large that bulk concentrations are not affected by the passage of current, the subsequent results follow. At current density i $(\mathrm{mA/cm^2})$, an electrical flow of chloride ions will take place within the membrane equal to $\bar{t}_i \, i/F$ $(\mathrm{meq/s.cm^2})$, and within the solution, equal to $t_i \, i/F$ $(\mathrm{meq/s.cm^2})$, where F is Faraday's constant (96.5 $\mathrm{A.s/meq.}$). The difference between t_i and $\bar{t}_i$ leads to an unbalanced electrical transfer, and a net shortage of $(\bar{t}_i - t_i) \, i/F$ $(\mathrm{meq/s.cm^2})$ occurs. Therefore, the solution concentration of sodium chloride drops in the region, and nonelectrical diffusion of sodium chloride salt takes place into the immediate vicinity.

At steady state, interfacial concentration is determined by equating the diffusion into the region with net electrical transfer out of the region:

$$\frac{D_s \, (C_0 - C_1)}{\delta} = \frac{(\bar{t}_i - t_i) \, i}{F} \qquad \text{Eq. 2.9}$$

where D_s is the diffusion coefficient of the salt (cm^2/s), C_0 is the bulk solution concentration ($meq./cm^3$), C_1 is the solution concentration at the membrane surface ($meq./cm^3$), δ is the solution film thickness (cm) across which the concentration gradient exists, and F is Faraday's constant.

The passage of current causes a reduction in the electrolyte concentration on one side of the membrane, a phenomenon known as depletion layer (C_1) that arises due to differences in the mobility of the counterions in the two phases of membrane and solution. Alternately, the concentration of the electrolytes increases on the opposite side of the membrane (C_2), a phenomenon that is called the concentration layer. Consequently, a concentration gradient is formed in the boundary layers on both sides of the membrane, which results in polarization layers. In these layers, the electric potential gradient drives cations and anions in opposite directions, whereas the concentration gradient drives both types of ions in the same direction – an effect known as diffusion (Tanaka, 1991; Ślezak et al., 2005).

The magnitude of the concentration gradient adjacent to a CEM would be different than the concentration gradient adjacent to an AEM due to the differences between the diffusivities of cations and anions (Walker, 2010).

Concentration polarization in EDR cells leads to an accumulation of ions on the membrane surface facing the concentrate cell and a depletion of ions at the

membrane surface in the diluate compartment. Both of these occurrences are problematic, as shown subsequently.

2.5.2 Scaling and Fouling: A Concentrate Problem

Brackish groundwater often has relatively high concentrations of calcium, magnesium, carbonate, and sulfate, leading to the supersaturation of one or more salts within the concentrate stream. The precipitation of salts is most likely to occur in the concentrate diffusion boundary layer where concentration polarization causes an accumulation of ions on the membrane surface facing the concentrate cell, which can decrease the mass-transfer efficiency, increase electrical resistance, and damage the membrane.

The supersaturation of a solution with respect to a particular compound can be described by the Langelier Saturation Index (LSI). For a water sample containing Calcium Carbonate, LSI is dependent on pH, alkalinity, calcium concentration, total dissolved solids, and water temperature, and is calculated as the difference between the actual pH (pH_{act}) of the solution and the pH under which precipitation of the given ion concentrations would occur (pH_{eq}).

Thus, a negative LSI means the water is under saturated with calcium carbonate and will tend to dissolve solid calcium carbonate, an LSI close to zero indicates water is not quite saturated with calcium carbonate and would not be strongly scale forming, and a positive LSI shows that the water is over saturated with calcium carbonate and will tend to deposit calcium carbonate, forming scales.

2.5.3 Limiting Current Density: A Dilute Problem

As the concentration gradient phenomenon explained in Section 2.5.1 continues, the interfacial concentration C_1 falls to zero eventually (as indicated in Figure 2.9) and the depletion layer resistance tends to infinity. After this point, the current density value reaches a limiting value called limiting current density (LCD) and therefore,

$$i_{lim} = \frac{D_s F C_\circ}{\Delta t_i \delta} \qquad \text{Eq. 2.10}$$

where $\Delta t_i = \bar{t}_i - t_i$, or the difference between the counter-ion transport number in the membrane and the solution, $t_i = {J_i F}/{i}$ and $\bar{t}_i = {\bar{J}_i F}/{i}$ (univalent ions); i is the current density; J_i and $\bar{J}_i$ are flux associated with ions in the bulk solution and membrane, respectively; D_s is the electrolyte diffusion coefficient; and δ is the boundary layer's thickness (Valerdi-Pérez et al., 2001).

In an ion-exchange membrane surface, if the bulk dilute concentration is raised or if the diffusion boundary layer thickness is dropped, then the limitation on electrical current is increased, allowing the maximum rate of desalination (Walker, 2010).

Concentration polarization has been studied widely, and current-voltage curves have been developed to reflect the relationship between the current through the membrane and the corresponding voltage drop over that membrane and its

adjacent boundary layers. According to the classical theory of concentration polarization for ion-exchange membranes, the steady-state current-voltage response shows three sections as illustrated in Figure 2.10 (Długołęcki, Anet, Metz, Nijmeijer, & Wessling, 2010).

At low voltage values, the resistance of the stack is constant - i.e., the current intensity and imposed voltage are linearly dependent according to Ohm's law. Therefore, the first region is called the Ohmic region. In the second region, the current varies very slowly with voltage, denoting an almost unconstrained current applied voltage ("plateau") that corresponds to the limiting current (Helfferich, 1962). When the LCD is reached, the cell resistance increases drastically and an increase in the applied voltage does not lead to a significant increase in the current density until, at a certain applied voltage, the current density increases again with the applied voltage (Rubinstein & Shtilman, 1979). In the post-limiting current region, the current intensity once again increases with the applied voltage. In this section, the current density is referred to as overlimiting current density and is caused by the transport of H^+ and OH^- ions which are generated at the membrane/solution interface by water dissociation. The water dissociation affects the current utilization and can lead to a drastic pH-value decrease in the diluate and an equally drastic pH increase in the concentrate solution, which may cause the precipitation of carbonates and sulfates of calcium and magnesium (Ibanez, Stamatialis, & Wessling, 2004).

In an EDR stack, a commonly used technique to decide maximum operating current that can be used without coupled effects with concentration polarization of the membranes, the relationship between the applied potential and the current intensities have to be achieved.

Traditionally, LCD is the point where the current (I) -potential (V) and cell resistance (R) - 1/current curves deflect from linearity, as shown in parts a) and b), respectively, of Figure 2.11 (H. J. Lee, Strathmann, & Moon, 2006). However, this does not always yield unambiguous estimates of the limiting condition when applied to a practical electrodialysis apparatus (Valerdi-pcrez, 2001).

Considering that the aim of ED is to obtain high desalting efficiency, the optimal operating current may be obtained by combining the curves for V/I-I and η-I (where η is removal ratio) as shown in Figure 2.12 (Meng et al., 2005). The feasibility of the combined method was assessed, and this method proved to be more efficient and simple compared to the traditional V-I curve.

Since the basic function of EDR is to obtain a high desalting efficiency and since there is a maximum desalting ratio with current change, the maximum point of the removal ratio under the optimal operating current can be considered a limiting factor (Meng et al., 2005).

It is evident from studies that limiting current densities depend on the concentration of the solution (J.-H. Choi, Lee, & Moon, 2001; Długołęcki et al., 2010), the flowrate (E. Choi, Choi, & Moon, 2002; Tsiakis & Papageorgiou, 2005; VALERDI-PÉREZ et al., 2000), and temperature (Hwang & Lai, 2007). Therefore, the limiting current can be determined empirically. In the case of the EDR pilot plant located at the Brackish Groundwater National Desalination Research Facility (BGNDRF) in Alamogordo, NM, R. V. Chintakindi (2010) studied the operating

parameters and indicated that the limiting current is in a relationship with the aforementioned factors in the manner shown by Equation 2.11:

$$I_{lim} \propto C_f U^{0.8} T^{0.67} \qquad \text{Eq. 2.11}$$

The results prove that the resistance of ion exchange membranes strongly depends on the solution concentration. We observe a very strong increase in membrane resistance with decreasing concentration, leading to an increase in the LCD. The LCD is also influenced by the liquid flow rate, because higher solution flow rates generate turbulence in the bulk of the streams and reduce the diffusion boundary layer thickness at the membrane surface. This results directly in an increased LCD. Furthermore, resistance in general strongly depends on the temperature, and the diffusion boundary layer resistance decreases with increasing temperature due to the increase in ion mobility with increasing temperature. In result, temperature increases could increase the LCD.

In this study, the LCD has been experimentally measured and the operating current ranges have been determined considering the limitations in order to avoid challenges associated with concentration polarization.

2.6 EDR Process Performance Metrics

Several metrics may be used to evaluate the performance of the EDR process. These metrics – removal ratio, recovery ratio, specific energy consumption (SEC), and current efficiency – are discussed in Sections 2.6.1 to 2.6.4 of the present work.

2.6.1 Chemical Efficiency: Removal Ratio

The ability of a desalination process to remove salt from a feed stream and produce a product stream of lower salinity measures the technical feasibility of that process. The degree to which that technical goal is accomplished by a desalination process is quantified by the removal ratio (R), which represents the "chemical efficiency" of the system. The removal ratio is defined by Equation 2.12:

$$R = 1 - \frac{C_p}{C_f} \qquad \text{Eq. 2.12}$$

where C_p is the salt concentration of the dilute effluent (typically in the units of mass of salt per volume of solution), and C_f is the salt concentration of the feed solution (Tanaka, 2015).

The degree of desalination that can be achieved in passing the feed solution through a stack is a function of the solution concentration, the applied current density, and the residence time of the solution in the stack. If the degree of desalination or concentration that can be achieved in a single pass through the stack is insufficient, several stacks are operated in series (Strathmann, 2010). A typical removal ratio for a single-stage EDR system is between 50% and 99%, depending

on the source water quality and product water specifications (American Water Works Association, 1995).

2.6.2 Hydraulic Efficiency: Recovery Ratio

Another aspect of the EDR desalination process is its "recovery ratio" which is considered to be a form of hydraulic efficiency defined by Equation 2.13:

$$r = \frac{Q_p}{Q_f} \qquad \text{Eq. 2.13}$$

where Q_p is the volumetric flow rate of the product and Q_f is the volumetric flow rate of the feed (Valero & Arbós, 2010). In a single stage of an EDR stack, where the geometries of the diluate and concentrate cells as well as the linear flow velocities are identical, the recovery rate is 50%. This operation results in a similar pressure in the concentrate and diluate cells. However, in EDR processes, the system often is intentionally operated so that the concentrate cells have a slightly lower pressure than the diluate cells. This prevents trans-membrane pressure and contamination of the diluate stream from leaks.

If the amount of product volume that can be achieved in a single path through the stack is insufficient, part of the diluate or concentrate can be fed back to the feed solution. With such an approach, EDR systems can achieve water recovery rates of up to 95%, which reduces feed water costs and waste water discharge (Strathmann, 2010); however, high-recovery EDR desalination is limited by the scaling tendency of salts in the concentrate stream.

2.6.3 Electrical Efficiency: Specific Energy Consumption (SEC)

Another evaluation metric for the desalination process efficiency is SEC, which quantifies how much energy is consumed by the desalination process to produce a given volume of product water. SEC can be calculated by Equation 2.14:

$$SEC = \frac{E_t}{V_p} \qquad \text{Eq. 2.14}$$

where SEC is specific energy consumption (kWh/m^3), E_t is the total energy consumption (kWh), and V_p is the product volume (m^3) (Stuttgart, 2002).

For full-scale membrane desalination systems with feedwaters ranging from brackish water to sea water, the SEC typically ranges from 1-10 kWh/m^3, depending on source water TDS, process technology, recovery ratio, and removal ratio. To be compared, the equivalent SEC of a full-scale thermal process such as MED and MSF typically ranges from 20-40 kWh/m^3 (Walker, 2010).

The total energy E_t required in an EDR process is the summation of two terms, as shown in Equation 2.15:

$$\mathrm{E_t} = \mathrm{E_{des}} + \mathrm{E_p} \qquad \text{Eq. 2.15}$$

where E_{des} is the electrical energy needed to transfer the ionic components from one solution through the membranes into another solution, and E_p is the energy required to pump the solutions through the EDR unit.

The energy consumption due to electrode reactions and the energy required for operating the process control devices can generally be neglected in large industrial-size plants, since the electrical and pumping typically are the dominant energy consumers in the process (Strathmann, 2010).

Generally, the SEC for EDR is a function of cell geometry, feed water linear flow and electro-chemical characteristics, membrane properties, concentration potential, total area resistance of the membranes, and electrical resistance of the solutions (Myint, Ghassemi, & Nirmalakhandan, 2011).

2.6.3.1 Direct Energy Requirements

The actual desalination process in EDR occurs when the required energy is given by the current passing through the stack multiplied with the total voltage drop encountered between the electrodes (E. Choi et al., 2002).

$$\mathrm{E_{des}} = \mathrm{I_{st}}\mathrm{U_{st}}\mathrm{t} \qquad \text{Eq. 2.16}$$

Furthermore:

$$\mathrm{U_{st}} = \mathrm{I_{st}}\mathrm{R_{st}} \qquad \text{Eq. 2.17}$$

where E_{des} is the energy consumed in a stack for the transfer of ions from a feed to the concentrate solution, I_{st} is the current passing through the stack, U_{st} is the voltage applied between the electrodes, and R_{st} is the stack resistance, defined as:

$$R_{st} = R_{AEM} + R_{CEM} + R_c + R_d \qquad \text{Eq. 2.18}$$

Four resistances can be taken into account in a single cell: R_{CEM}, the resistance of cation exchange membranes; R_{AEM}, the resistance of anion exchange membranes; R_d, the resistance of dilute compartments; and R_c, the resistance of concentrate compartments (Myint et al., 2011). The electrical resistance of a solution can be expressed as a function of concentration as shown in Equation 2.19 (Sadrzadeh & Mohammadi, 2009).

$$R = \frac{h}{\kappa A} \qquad \text{Eq. 2.19}$$

Here, κ is the electrical conductivity (S/m), h is the thickness of the dilute or concentrate solution compartment (m), and A is the effective area of the ion exchange membrane (m^2). The electrical conductivity is an aggregate of the ionic composition as shown in Equation 2.20:

$$\kappa = \sum_{\mathrm{i}} C_i \lambda_i |z_i| \qquad \text{Eq. 2.20}$$

For species i, λ_i is the molar conductivity (Sm^2/mol), z_i is the valence, and C_i is the concentration (mol/m^3) (Anderko & Lencka, 1997).

It is evident that the required desalination energy is a function of the stack resistance, the amount of the produced water, and the feed and dilute concentration.

2.6.3.2 Pumping Energy Requirement

An EDR unit requires pumps to circulate the diluate, the concentrate, and the electrode rinse solution through the stack. The energy required for pumping these solutions is determined by the volumes of the solutions to be pumped and the pressure drop, as expressed by Equation 2.21:

$$E_p = k_{eff}(Q_d \Delta p_d + Q_c \Delta p_c + Q_e \Delta p_e) \qquad \text{Eq. 2.21}$$

Here, E_p is the total energy for pumping the diluate, the concentrate, and the electrode rinse solution through the stack per unit diluate water, k_{eff} is an efficiency term for the pumps, Q_d, Q_c and Q_e are the volume flow rates of the diluate, the concentrate, and the electrode rinse solution through the stack, and $\Delta p_d, \Delta p_c,$ and Δp_e are the pressure difference between the inlet and outlet of dilute, concentrate, and electrode rinse solution, respectively (E. Choi et al., 2002; Mcgovern, Zubair, & V, 2014; Turek & Dydo, 2001; Zhou & Tol, 2005).

Since the volume of the electrode rinse solution is very small compared to the volumes of the diluate and concentrate, the energy consumption due to the pressure loss in the electrode rinse solution is negligible in most practical applications.

The pressure losses in the various cells are determined by the solution flow velocities and the cell design. The energy requirements for circulating the solution through the system may dominate over the direct energy consumption for solutions with rather low salt concentrations (Strathmann, 2010).

2.6.4 Electrical Efficiency: Current Efficiency (CE)

CE is an important parameter that determines the optimum range of applicability of ED and is a measure of how effectively ions are transported across the ion exchange membranes for a given applied current. CE is calculated using the Equation 2.22:

$$CE(\%) = \frac{Q_p F (C_f - C_p)}{N I_{st}} * 100 \qquad \text{Eq. 2.22}$$

Here, Q_p is the volume flow (m^3/s); F is Faraday constant, equal to 96.5 A s /eq; C_f is feed concentration (mol/m^3 or eq/m^3), C_p is product concentration (mol/m^3 or eq/m^3), I_{st} is the current passing through the stack (A), and N is the number of cell pairs in the stack (Sadrzadeh & Mohammadi, 2009).

In any practical EDR system, it is generally found that the amount of current required to produce a given amount of desalting exceeds the requirement that can be calculated on the basis of current flow through ideal membranes. Several

undesirable phenomena occurring in the EDR cell pairs may contribute to low current efficiency in an EDR stack:

- Back diffusion phenomena due to non-perfect permselectivity of membranes (Turek, 2002);
- Shunt or stray current running in the non-active cell areas (Veerman, Post, Saakes, Metz, & Harmsen, 2008);
- Electrical leakage through the manifolds due to short circuit between electrodes (Mandersloot & Hicks, 1966); and
- Osmotic and electro-osmotic water transport through the membranes (Shaposhnik, 1997).

Literature review on the investigation of CE values for different ED and EDR processes indicates that CE values were most frequently observed in the range of 60-80 (Demircio, Kabay, & Gizli, 2001; Demircioglu, Kabay, Kurucaovali, & Ersoz, 2002; A. A. Von Gottberg & Manager, 2010; Ions, Rod, & Is, n.d.; H.-J. Lee et al., 2009; Meng et al., 2005; Rosenberg & Tirrell, 1957; Sadrzadeh et al., 2007; Sadrzadeh & Mohammadi, 2009; T Sata, 1986; Shaposhnik & Grigorchuk, 2010; Shaposhnik, 1997; Turek & Dydo, 2001; Turek, 2002; Veerman et al., 2008). However, values both higher and lower than this have been reported. For instance, Turek & Dydo (2001) reported a current efficiency of 90% for the removal of natrium chloride through the use of a laboratory scale ED system; as an example of low reported current efficiencies, Sadrzadeh & Mohammadi (2009) identified current efficiencies from 0-50% for laboratory scale seawater desalination using an ED cell under different operating parameters.

2.7 Electrodialysis Reversal Optimization

There are several approaches for optimizing the performance of EDR systems, and these approaches – two hydraulic, one electrical, and one chemical – are discussed in Sections 2.7.1 through 2.7.4.

2.7.1 Hydraulic: Improving the Rate of Mass Transfer

With respect to optimization, a key parameter that must be considered in EDR performance is the velocity of the solution flowing through a concentrate or diluate cell. This parameter is called inter-membrane velocity.

Dimensionless parameters associated with the transport rates are the Reynolds and Schmidt numbers. The Reynolds number (Re) characterizes the ratio of inertial and viscous forces of the fluid dynamics, quantifying the relative importance of these two types of forces for given flow conditions. For flow in a tube or channel, Re is related to the flow velocity in the boundary layer at the membrane surface, as shown in Equation 2.23:

$$Re = \frac{\rho\, h\, u}{v} \qquad \text{Eq. 2.23}$$

where ρ is the solution mass-density (kg/m), h is the channel height (spacer

thickness) (m), u is the superficial flow velocity (m/s), and μ is the absolute (dynamic) viscosity of the solution (kg/m.s). Assuming that the solution density and viscosity and the channel height are approximately constant, the Reynolds number is essentially a scalar of velocity for a particular system.

The dimensionless parameter that represents the ratio of viscous and diffusive forces within the solution is the Schmidt number (Sc), defined as in Equation 2.24:

$$Sc = \frac{\mu}{\rho D} \qquad \text{Eq. 2.24}$$

where μ is the absolute (dynamic) viscosity of the solution (kg/m.s), ρ is the solution mass-density (kg/m^3), and D is the ion diffusivity (m^2/s), which depends on solution concentration.

By relating the Schmidt and Reynolds numbers, the non-dimensional mass-transfer coefficient can be created, known as the Sherwood number (Sh). This is defined in Equation 2.25.

$$Sh = \alpha_0 \, Re^{\alpha_1} Sc^{\alpha_2} \qquad \text{Eq. 2.25}$$

where α_0, α_1, and α_2 are positive fitting parameters for which numerous attempts have been made to theoretically approximate and empirically validate these parameters; the present study is not concerned with the specific determination of the mass transfer parameters.

Equation 2.25 indicates the relationship of the hydraulic and electrochemical behavior and demonstrates that the limiting rate of mass-transport in an EDR system increases with increases in the velocity. Consequently, as increasing the inter-membrane velocity in a diluate cell promotes mixing and turbulence, which decreases the diffusion boundary layer thickness in the dilute cell and thereby improves the rate-limiting mass-transport through the diluate diffusion boundary layer, decreases in the electrical resistance of the stack thus improve the electrical efficiency and reduce salt scaling at the membrane surfaces.

Furthermore, an increase in mixing in the concentrate cell can prevent scale formation in the stagnant regions that first show accumulation of precipitates (Berger and Lurie, 1962). However, decreasing the inter-membrane velocity decreases the cost of pumping energy required. In result, there is an optimum value for the flow velocity through the EDR cell pairs, and it needs to be considered while defining the operating solution flowrate values.

2.7.2 Hydraulic: Improving Recovery Ratio

Another important strategy for improving the efficiency of EDR is to increase the recovery ratio. In a single stage EDR system, this improvement can be accomplished by recycling part of the diluate or concentrate to the feed solution. As illustrated in Figure 2.2, the general material balances based on the flows and the species material balance for the total dissolved solids (TDS) are shown in Equation 2.26 and 2.27:

$$Q_f = Q_p + Q_c \quad \text{Eq. 2.26}$$

$$Q_f C_f = Q_p C_p + Q_c C_c \quad \text{Eq. 2.27}$$

Consequently, the waste concentration factor (CF) can be calculated (for the entire system, independently of internal concentrate recycle) by material balance as in Equation 2.28:

$$CF = \frac{C_c}{C_f} = 1 + \frac{rR}{1-r} \quad \text{Eq. 2.28}$$

where C_c is the concentrate waste concentration, C_f is the feed concentration, r is the removal ratio, and R is the recovery ratio.

As the recovery ratio increase, the concentration of salt in the concentrate waste stream increases approaching zero liquid discharge (ZLD), but the challenge in this type of operation is that, as the recovery ratio increases, precipitation in the concentrate stream is more likely to occur because of the elevated ionic concentrations causing problems associated with scaling.

2.7.3 Electrical: Decreasing the Electrical Resistance of the Stack

The resistance of the stack is the summation of the resistances all cell pairs. As illustrated in Figure 2.13, each cell pair of the ED stack can be divided into eight district regions as follows: (1) the CEM, (2) the concentrate diffusion boundary layer adjacent to the CEM, (3) the concentrate bulk, (4) the concentrate diffusion boundary layer adjacent to the AEM, (5) the AEM, (6) the diluate boundary layer adjacent to the AEM, (7) the diluate bulk, and (8) the diluate boundary layer adjacent to the other CEM.

The electrical resistance of an ion-exchange membrane is determined by its capacity and the mobility of ion species in the membrane matrix (Toshikatsu Sata, 2004; Strathmann et al., 2006), and typical values of real resistances in many commercial AEMs and CEMs are in the range of 1-10 Ω-cm^2.

The solution phase resistances are functions of chemical composition, total conductivity, and the dimensions of each solution, as explained in Equations 2.19 and 2.20.

Developing ion exchange membranes with lower electrical resistance can be accomplished by decreasing width and increasing conductivity. Also, as the resistance of the bulk region decreases with increasing salinity, the electrical resistance of the dilute cell can be reduced by sending part of the concentrate to the feed stream. In addition, the electrical resistance of the diluate diffusion boundary layer can be reduced by reducing it thickness through enhanced mixing.

2.7.4 Chemical: Preventing Scaling and Fouling

In order to implement effective scale-control measures in EDR desalination plants, it is necessary to know the permissible water recovery level at which the plant may be operated under given process conditions without the risk of scale

precipitation. Process conditions that influence the permissible water recovery level are numerous and include the supersaturation level of the concentrate stream, the residence time of the concentrated solution, the nature of the antiscalant used, and the dose of the antiscalant used (Hasson, Drak, & Semiat, 2009). Antiscalants are compounds that are added to the concentrate stream of the EDR system in order to alter the precipitation kinetics of low-solubility salts by disrupting one or more aspects of the crystallization stages. Antiscalants inhibit crystal growth through increasing the ion concentration threshold required for clustering, distorting normal crystal growth and produce an irregular crystal structure with poor scale forming ability, or using dispersants which place a surface charge on the crystals. Consequently, the crystals repel one other and are dispersed into the water bulk.

Antiscalants are able to work at relatively low concentrations (< 100 mg/L), where the ion concentrations are stoichiometrically much higher. In many water treatment systems, Phosphonate antiscalants are widely and effectively used to inhibit scale, corrosion and gypsum precipitation (Akyol, Öner, Barouda, & Demadis, 2009; R. P. Allison, 1995).

In another approach to preventing fouling and scaling, the EDR process employs periodic polarity reversal, reducing or eliminating the need for adding acid to the feed water (Fubao, 1985).

2.8 Summary

The fundamentals of the hydraulic, electrical, and chemical phenomena employed in EDR systems are integrally connected to the overall performance, which can be evaluated through different aspects including removal ratio, recovery ratio, current efficiency, specific power consumption and total cost.

As explained in Section 2.6, most of the parameters of the EDR process are inherently overlapping and improving any one aspect could change other aspects in either beneficial or harmful ways.

Within EDR systems, the rate of separation (removal ratio) is proportional to the electrical current density. Since current density is limited by a lack of ions in the diluate diffusion boundary layer and a supersaturation of ions in the concentrate diffusion boundary layer, the diffusion boundary layer thickness must be sufficiently thin and the applied voltage sufficiently low to avoid both cases. The thickness of diffusion boundary layer is controlled by the hydraulic inter-membrane velocity. The scaling tendency of the salts existing in the concentrate stream not only reduces the removal ratio, but also limits high-recovery inland desalination.

The electrical behavior of an EDR system is dominated by the resistance of the stack described in Section 2.6.3, and different stack design parameters and operating parameters can change the total resistance in the stack.

The hydraulic efficiency of an EDR system can be improved by increasing the recovery ratio or velocity of intermembrane streams, which are limited by scale formation and pumping energy, respectively.

Therefore, although experimental and full-scale EDR treatments of brackish waters have been proven technically and economically feasible (American Water

Works Association, 1995; Reahl, 2005; Strathmann, 2004; Tanaka, 2007; Xu et al., 2008), the EDR process still needs to be optimized for removal ratio, recovery ratio, current efficiency, and power consumption in order to improve its efficiency for widespread deployment. Hence, thorough and systematic experimentation and documentation of EDR performance is required for understanding the optimally beneficial use of EDR to treat saline water.

Chapter 3 - Materials and Methods

The objective of the experimental work was to quantitatively observe the hydraulic, electrical, and chemical behavior of EDR treatment of brackish groundwater. The effects of process variables on the performance of the EDR were evaluated through precise EDR experimentation. The experimental plan and descriptions of the experimental design, experimental set-up and location, experimental procedure, characterization and control systems, and data analysis are presented here.

3.1 Experimental Design

Regarding the research goal and objectives presented in Chapter 1 and the fundamental concepts outlined in Chapter 2, the experiments performed sketch the EDR performance sensitivities and limitations with respect to the following variables:

1. Chemical – feed water salinity,
2. Electrical – applied voltage, and
3. Hydraulic – feed flow rate.

Among the different operating conditions that impact the EDR process, four parameters were selected; product flow rate, conductivity, applied voltage, and electrode type. These parameters can be briefly described as:

Flow rate: The volumetric flow rate is the volume of fluid which passes through a given surface per unit time. Although the SI unit for flow rate is cubic meters per second (m^3/s), in the EDR pilot scale plant used for our experimentation, flow rate is measured based on gallons per minute (GPM). The flow rate for each of the inlet and outlet streams, dilute, feed, and concentrate streams, are measured and presented. In our experimental set-up, flow rates are measured by flow meters and can be monitored and read on both the flow meters and on a human-machine interface (HMI) screen on the machine.

Conductivity: Conductivity is a measure of the ability of water to pass an electrical current. How well a solution conducts electricity depends on a number of factors including the concentration of ions, mobility of ions, valence of ions, and the temperature of the solution. The conductivity is linked to the level of total dissolved solids (TDS) and is measured in micro-Siemens per centimeter (µS/cm).

Voltage: The electrical voltage and current applied to the electrodialyzer were controlled and monitored by a switching mode, regulated, and programmable power supply. Voltage increments are modified and increased for every reading of the experiment and the accuracy of the applied voltage and current was verified by a handheld digital multi-meter. The voltage applied to an electrodialyzer is indicated by the Equation 3.1:

$$V = N\,V_{cell} + V_p \qquad \text{Eq. 3.1}$$

where N is the number of cell pairs, V_p the voltage in the electrode cell, and V_{cell} is cell voltage as follows, defined in Equation 3.2:

$$V_{cell} = I\,R + E_M \qquad \text{Eq. 3.2}$$

where I is current, R is the resistance of the cell pair (Eq. 2.18), and E_M is the membrane potential. (Purification & Program, 2003; Rosenberg & Tirrell, 1957). The manufacturer recommended a maximum voltage application of 1.5 V per cell-pair. Voltage increments are modified and increased for every reading of the experiment.

Electrode type: Electrodes are integral to the EDR process, providing the driving force for desalination. It has been hypothesized that the shape of the electrodes, as well as their location with respect to the solution manifolds, could impact both performance and stack life. Manifold shorting current, which is a parasitic current to the overall desalination process and reduces current efficiency, is a function of electrode design. Based on contemporary design practices and historical knowledge of the GE EDR stack configurations, three electrode designs are proposed and classified based on their geometry: full, recessed and tapered.

The motivation for this particular component of the study arises from GE's hypothesis that changing the electrode from full to recessed could result in reduced stray current, higher allowed stack voltage, and more demineralization. Therefore, there is a strong need to evaluate the three proposed electrode designs.

In each test, input parameters are defined for the experiment. The parameters can be changed between different tests, and subsequently change the outputs. All other operating conditions are recorded. To accomplish the

experimental design, three different levels of feed conductivity (salinity) were considered: low, medium, and high. Also, three levels of feed flow rate are considered so that the input flow rate, in its low level, is set to the lowest possible value, and for the high level, it is set to the highest value possible recommended by the manufacturer of the EDR pilot plant used. Since the experimental setup is pilot scale, the single center point is used to check the validity of results from low and high levels. The center points are set to the numbers closely reflecting the average of the low and high levels. The applied voltage has five levels; the highest value is limited by the limiting current values and the lowest is limited by the separation rate.

For flow rate, the values for low, middle and high level were 7, 9 and 11 GPM, respectively. Levels of conductivity were varying among various feed waters depending on the well utilized in the experiment. The lowest value obtained was in Well1 (cold and warm), with low-level conductivity at 1700 µS/cm, and the highest one was with Well2, with high-level conductivity at 6100 µS/cm. Middle points, accordingly, were obtained by a combination of well1 and well2, giving approximately 3700 µS/cm conductivity.

The experimental plan was designed to study the impact of each variable through performing a full factorial design with three replicates. The order of the all tests was randomized in order to raise the level of quality assurance. The resulting design of experiment is shown in Table 3.1.

3.2 Experimental Set-up

The EDR experimental setup is shown in Figure 3.1.

3.3 Experimental Location

The laboratory site is located at the Brackish Groundwater National Desalination Research Facility (BGNDRF), first opened on August 16, 2007, in Alamogordo, New Mexico. BGNDRF is a federal facility that operates under the U.S. Bureau of Reclamation, whose mission is "to promote sustainable advanced water treatment research and technology development for inland brackish groundwater sources". The available feed waters consist of four brackish groundwater wells with TDS levels between 1,000 and 6,400 mg/L. The EDR pilot is located at inside bay #4, where all of the wells – well1, well2, and their combination – are used for performing this experiment. Well1 is a geothermal well with medium salinity (~1700 µS) and well2 is a cold well with very high salinity (~6200 µS).

3.3.1 Influent Pumping Equipment

At the BGNDRF, well water is first pumped from the aquifer to a large outside storage tank, and then to a smaller hydrostatic tank, which pressurizes the water to 350 kPa. When water enters the facility, a valve is used to reduce the feed pump inlet pressure to less than 70 kPa and make it ready to reach the EDR pilot

system. The source water then flows into the pretreatment system comprised of a multi-media filter (MMF) and a 5 micron cartridge filter.

3.3.2 Multimedia Filter System

The discharge from the feed pump is ejected through an MMF prior to entering the cartridge filtration system. The MMF removes suspended solids from the source water as it sieves through the filter's various media layers. The feed water is fed in the top of a container through a header which distributes the water evenly. The filter media start with fine sand on the top and then become gradually coarser sand in a number of layers followed by gravel on the bottom, in progressively larger sizes. The top sand physically removes particles from the water. The job of the subsequent layers is to support the finer layer above and provide efficient drainage.

The utilized MMF starts with anthracite (0.85-0.95 mm) on the top, then gradually coarser sand (0.85 mm), followed by garnet (0.42-0.6 mm) in gradually larger sizes to remove suspended particles from the source water, down to a 10-15 micron size (Fues, 2008).

3.3.3 Cartridge Filtration System

Downstream of the MMF, a cartridge filter (5 μm) is employed to protect the membranes from fine suspended particles in the feed water and prevent damage to either the pumps or the membranes. One of the suspended particles is iron (Fe^{2+}), which reacts strongly with hydrogen peroxide (H_2O_2) to produce hydroxyl radicals (OH^-) that could destroy the function of antiscalants (D.F. Lawler, M. Cobb, 2010; Yang & Ma, 2004).

Although no signs of significant pressure loss were observed during the experiments, the MMF was backwashed and the cartridge filter was replaced approximately every 3 months, between experiments.

After the pretreatment system, the source water enters the EDR hydraulics, which are detailed in Figure 2.1 and explained in Section 2.1.

3.3.4 EDR stack

The EDR Stack is comprised of 40 cell pairs stacked one on top of another. Each cell pair consists of a cation-exchange membrane and an anion-exchange membrane, separated by flow-path spacers, with another spacer on one side of the cell pair.

All the membranes are flexible sheets of cloth-reinforced resin. The properties of the membranes include long life-expectancy, resistance to fouling, impermeability to water under pressure, and operability in temperatures in excess of 46º C.

The spacers separating the membranes, as illustrated in Figure 3.2, provide a U-shaped tortuous path. The solution enters the compartment from the one above it, makes two bends, and finally goes out of the compartment to the one below it.

The spacers are manufactured by using two sheets of low-density polyethylene with die-cut flow channels, which are glued together to form an over-under flow-path that promotes mixing and turbulence (A. von Gottberg, 1998).

These spacers have an effective transfer area of 0.34 m^2 per membrane and been designed specifically to optimize the turbulence and pressure drop.

This basic cell pair is repeated until it is capped on both ends by the electrode compartments, which consist of a heavy flow-path spacer, a heavy cation-exchange membrane, and an electrode. Heavy cation exchange membranes have all the properties of regular cationic membranes but are twice as thick and can withstand a greater degree of hydraulic pressure.

The electrodes are constructed of platinized titanium and act as either a cathode or an anode, depending on the polarity reversal period. GE Water and Process Technologies has manufactured three kinds of electrode (presented in Figure 3.3):

1. Old Design (Full): Electrode area fully covers active membrane area, but also extends into manifold area;
2. Current Design (Recessed): Geometry mismatch between electrode and spacer; and
3. New Design (Tapered): No geometry mismatch between spacer and electrode.

The polarity reversal cycle for this experiment is 15 min. A steady state was achieved in 10 min, so the 15 min polarity setting was acceptable. Table 3.2 summarizes the specifications of the EDR stack components.

3.3.5 Concentrate Recycle and Waste Blowdown System

The concentrate enters the concentrate pump located in the hydraulic section, then part of it is recycled to the stack. The waste is sent to drain, while some feed water is also added to the recycle as makeup to prevent the dissolved solids from precipitating on the membranes.

3.3.6 Chemical Dosing System

The chemical dosing system has the following chemicals added:

1. Hydrochloric Acid (15%): The hydrochloric acid is continuously added to the electrode in stream to neutralize the OH^- ions formed at the cathode, in order to prevent the precipitation of pH dependent salts, such as $CaCO_3$ and $Mg(OH)_2$.
2. Antiscalant, HYPERSPERSE MDC 706: These chemicals are added to concentrate instream control various scaling and precipitation processes occurring in the equipment during operation.

3.4 Experimental procedure

This experiment studied how different operating and design parameters, including applied voltage, electrode type, product flowrate, and salinity of the feed solution, affect the efficiency of the EDR process. The efficiency of EDR systems can be evaluated by studying the salt removal ratio, produced current density, and amount of specific energy consumed. Table 3.3 shows the design of experiment,

where finally the significance of each variable to change the EDR efficiency will be modeled empirically.

In each cycle of polarity reversal, the time is set for a 15 minute reversal. By trial and error, it has been determined that after 10 minutes of reversal, the system attains a steady state. Then, various measurements are taken accordingly. In this study, temperature and recovery ratio have been constant and their effects are not considered to be studied.

Unfortunately, because of the variation in the temperature of the source water coming from the wells, it is difficult to have a constant operating temperature. It was observed that the temperature changes during different seasons in the range of 8-37 ºC and it also changes during the day up to 5 ºC. Therefore, the experiments were conducted in a range of 20-25˚C.

The highest recovery ratio in the EDR pilot-scale located at BGNDRF was determined to be 80%. The product and feed flow rates were monitored closely to ensure constant recovery throughout the long-term experiments; minor variation (< 0.2 GPM) could be observed. The effect of this slight variation was difficult to quantify, and must be considered a noise signal throughout the results.

The feed salinity has been classified as low, medium and high because the feed water quality varies slightly due to its deep-basin origin, leading to variations in conductivity and TDS levels.

Low salinity is the water sourced from well1, high salinity is the water coming from well2, and medium salinity is the combination of the well1 and well2. Table 3.4 shows the composition of each level of salinity considered in this experiments.

The general experimental procedure was as follows:

1. Voltage increments are modified and increased for every reading of the experiment so that they are in ascending order.
2. Measurements for voltage and current for the stage are taken using a voltmeter and an ammeter.
3. The HMI screen gives the measurement of flow rate, temperature, conductivity, and pH of feed, product, and concentrate, and energy consumed.
4. Samples of product, feed, and concentrate water were collected to be subjected to dissolved species analysis. The samples were withdrawn in the final 5 minutes of the polarity reversal period in order to allow enough time for the performance characteristics to stabilize.
5. Water samples were sent to the laboratory of Water and Energy at New Mexico State University and analyzed by ion chromatography.

Prior to the experiments, regarding the study of EDR efficiency factors, it is necessary to achieve the limiting current for each feed flow rate, applied voltage, feed salinity, and electrode type combination. To find the limiting current for each mentioned combination, all of the first three steps have been taken for a large range of voltage values, and then the limiting current was be found based on current-voltage and removal ratio-current curves. Operating current values that exceed the limiting current will be problematic, as discussed in Section 2.4.

3.5 Characterization and Control systems

EDR system conditions – including hydraulic flow rates, the stack voltage and current, the pH, temperature, and electrical conductivity of each process stream – were continuously monitored to ensure stable operation. Table 3.5 represents a data collection log of the system conditions that were recorded daily during all the experiments.

The stage voltage (electrode-to-electrode) was measured using an oscilloscope, and the stage current was measured using a DC current probe. The temperature, conductivity, and pH were measured on site, using in-system probes and bench top laboratory devices. The temperature dependence relationship built into the measurement devices converts all the conductivities measured to conductivities at the temperature of 25 °C.

The monitoring the feed stream provides information on the consistency of the inlet water quality, which was expected to vary slightly due to its deep-basin origin. Measurements of the pH, conductivity, and temperature of outlet streams also provide important information on the system performance.

Conductivity and pH have to be monitored constantly because significant changes in pH can imply that concentration polarization is occurring, leading to water-splitting within the stack. Changes in conductivity can be an indication that concentration polarization or scaling is affecting the removal process. The conductivity measurements of the outlet streams were particularly important during operation to achieve the separation rate of desalination.

3.6 Data Analysis

In the first step of data analysis for this study, the normality of the data was checked using the Shapiro-Wilk test. Additionally, the correlations between independent parameters were examined to eliminate the covariated variables from the regression relationship. Also, regression analysis between the response variables (removal ratio, specific energy consumption, and the current) and independent variables (feed conductivity, applied voltage, feed flow rate, and electrode type) was completed. Results of SAS programming were confirmed using Excel.

In order to find both the correlation between different parameters and a model to predict the characteristics of response variables based on operating conditions, multiple linear regression (MLR) was utilized. MLR is a statistical method to model the linear relationship between a dependent variable (predicted) and one or more independent variables (predictors).

In order to validate that the data have met the regression assumptions and to identify whether the regression model sufficiently represents the data, "regression diagnostics" methods such as R-squared and variance inflation factor (VIF) were used. During the data analysis of this study, the predictors were always

defined in such a way that the regression model gives us the closest R-squared to 1. In addition, the predictors on the regression model could be intercorrelated. Intercorrelation can make it difficult or impossible to determine the relative importance of individual predictors from the estimated coefficients of the regression equation.

Multicollinearity, which is defined as extremely high intercorrelation of predictors, makes the interpretation of the regression coefficients more difficult, and may call for the combination of subsets of predictors into a new set of less-intercorrelated predictors (Curto & Pinto, 2011). Therefore, the VIF method was used to identify multicollinearity in a matrix of predictor variables. Multicollinearity is problematic when the variance inflation factors of one or more predictors becomes large. Therefore, the predictor without which the other VIF numbers would all change to a number close to 1 was eliminated from the list of independent variables.

Once the regression model was estimated, the residuals were defined as the differences between the observed and predicted values in order to measure the closeness of fit of the predicted and actual values (Dowdy, Wearden, & Chilko, 2011).

Chapter 4 - Results and Discussion

Experimentation and empirical modeling were used to systematically and quantitatively analyze the treatment performance of a pilot-scale EDR plant on several brackish groundwater under various electrical, hydraulic, and chemical conditions. The experimental results are described and discussed in Section 4.1, and the modeling results are covered in Section 4.2.

4.1 Experimental Results

Experimental evaluation of EDR's ability to treat brackish groundwater was performed according to the methods detailed in Chapter 3.

The limiting current, which is dependent on flow rate, feed salinity, and temperature, is obtained for each electrode. The effects of electrical, hydraulic, and chemical variables are presented in Sections 4.1.1 through 4.1.4, along with the effect of electrode type in Section 4.1.5.

4.1.1 Electrical: Determining Limiting Current

An applied electrical potential (voltage) is the driving force for ionic separation in EDR, and it is the primary controlling factor for the rate of separation. The current increases along with voltage until the limiting current is reached. Once the system reaches limiting current, the voltage drop across the boundary layer

increases drastically, resulting in water dissociation, and consequently changes in the pH of the solution in dilute and concentrate channels. This may cause precipitation of carbonates and sulphates of calcium and magnesium. Thus, to identify operating parameters for EDR that avoid salt precipitation, the limiting current must be determined.

To avoid the many aforementioned problems associated with exceeding limiting current, it is very important to work with operating current values less than limiting current. Measurements of the limiting current for each combination of variables shown are taken through the following procedure:

1. The flow rates of the feed, product, and concentrate streams are set;
2. Voltage increments are modified and increased for every reading of the experiment in ascending order;
3. The polarity reversal time is set for 15 minutes, and after 10 minutes, a time period which is required for the system to reach stability, measurements are taken;
4. The current for each voltage set is taken;
5. The pH and conductivity of feed, product, and concentrate stream are measured.
6. The current vs. voltage, current vs. stack resistance, and removal ratio vs. current curves are plotted to observe the limiting current.

The limiting current curves measured through the aforementioned approach are shown in Figures 4.1 through 4.3.

As the current density through the EDR stack is increased from zero by increasing the voltage at the electrodes, the concentration gradient in the diffusion boundary layer becomes steeper. If the concentration gradient becomes too steep and consequently the diffusion boundary layer thickness becomes large, then the salt concentration in the dilute diffusion boundary layer approaches zero at the membrane surface; as a result, stack resistance increases drastically, causing a drastic decrease in current produced. As a result of the current decrease, the desalting (removal) ratio decreases. As shown in Figures 4.1 through 4.3, the limiting current is the point where current starts to reach plateau, stack resistance increases drastically, and further increase in removal ratio is prevented.

The resistance, in general, strongly depends on the temperature, since the diffusion boundary layer resistance decreases with increasing temperature due to the increase in ion mobility with increasing temperature. Therefore, since a temperature increase could change the limiting current and this work does not focus on temperature's effect, the temperature has been maintained approximately constant during these experiments (~20° C).

Also, as presented in Eq. 2.11 ($I_{lim} \propto C_f U^{0.8} T^{0.67}$) and indicated in Figures 4.1 through 4.3, the limiting current is influenced by the flow rate, because higher solution flow rates generate turbulence in the bulk of the streams, reducing the diffusion boundary layer thickness at the membrane surface, and resulting directly in an increased limiting current value.

Furthermore, the results show that the resistance strongly depends on the solution concentration. We observe a very strong decrease in the resistance with increasing concentration, leading to an increase in the limiting current. All the plots

presented are for feed water with low-level conductivity (~1700 µS/cm), as summarized in Table 4.1.

In this study, it was not possible to measure the limiting current for feeds with medium (~3700 µS/cm) and high salinity (~6000 µS/cm), because the manufacture has recommended a maximum voltage application of 1.5 V per cell-pair (40 cell pairs used), which limits the total possible applied voltage to 60 V. The experiments conducted indicate that for voltages less than 40 V, the limiting current is not reached, and working with operating current less than 40 V is safe for all levels of flow rate for both medium and high levels of salinity.

Among all the combinations of feed salinity and feed flow rate levels, the lowest limiting current occurs for 7 GPM and low salinity at 45 V. Therefore, the highest voltage applied to the stack was adjusted to be 40 V and the data collected were constantly monitored to make sure that operating currents were in the Ohmic section of the voltage-current curves. In addition, the pH of the dilute and concentrate was monitored constantly, and most significantly, no precipitation occurred in the concentrate solution during the experiments, which demonstrates that the concentration polarization of EDR was sufficiently small.

4.1.2 Electrical: Effects of Stack Voltage

Experiments were performed at five different voltage applications (30, 32.5, 35, 37.5, 40 V) for treating the brackish water from a deep aquifer at BGNDRF in Alamogordo, New Mexico. The measurements were repeated for three levels of feed flow rate, and the experiment simulated 80% single-stage recovery.

4.1.2.1 Chemical Efficiency

The ionic separation of each experiment is shown in Figure 4.4. As the ions were continuously separated from the dilute and transported to the concentrate, the conductivity of the dilute decreased from its initial value and the removal ratio based on dilute conductivity increased.

As expected, the separation rate increased with increasing voltage because the increased electric field strength increases the rate of electromigration, as shown by the Nernst-Planck equation (Equation 2.4). Also, the rate of removal was approximately proportional to the applied stack voltage.

To determine the removal ratio, the concentration of the effluent dilute and the salt concentration of the feed solution are typically measured in the units of mass of salt per volume of solution. Therefore, the relationship between concentration and conductivity must be obtained. Chintakindi (2011) showed that there is a linear relationship between concentration and conductivity, and Table 4.2 provides the conversion factors of conductivity (µS/cm) to concentration (meq./L).

4.1.2.2 Electrical Efficiency

As expected, current increases with voltage increases based on Ohm's law. Also, there is an approximate linearity between current and voltage (Figure 4.5) which can be attributed to the relatively stable resistance within the stack.

The resistance of dilute solution increases as the dilute conductivity

decreases, and conversely, the concentrate resistance decreases as the concentrate conductivity increases. In EDR brackish water treatment systems, the resistance of the ion exchange membranes can be neglected compared to the resistance of dilute and concentrate solutions.

Another metric for evaluating the electrical efficiency of the EDR process is specific energy consumption (SEC), which is the amount of invested energy per unit volume of product water. SEC often is reported in kWh/gallon, and it is approximately proportional to the stack voltage, as shown in Figure 4.6. The SEC includes the electrical energy applied to the stack as well as the hydraulic energy invested to pump the solution through the process.

As shown in Equation 2.16, the actual desalination energy required in an EDR stack is given by the current passing through the stack multiplied by the total voltage drop encountered between the electrodes. Also, the current and voltage have a proportional relationship. Therefore, a voltage increase leads to a higher SEC.

4.1.3 Hydraulic: Effects of Flow Rate

To explore the effect of flow velocity on EDR performance, three different levels of feed flow rate (7, 9, 11 GPM) with a constant recovery ratio (80%) have been considered. In terms of temperature, recovery, stack design parameters, etc., the experiments were performed under conditions equivalent to those listed for the investigations of the effects of stack voltage.

4.1.3.1 Chemical Efficiency

While the applied voltage is the main controlling factor for the rate of separation, the solution velocity controls the residence time limitation. At higher flow rates, removal ratio values fall and separation performance decreases. Because a greater flow rate means a lower residence time, ions that are between the membranes do not have enough time to transfer through the membranes (Mohammadi & Kaviani, 2003; Sadrzadeh & Mohammadi, 2008). The rate of separation was decreased approximately 30% by increasing the feed flow rate from 7 to 11 GPM. The effects of flow rate on ion removal are shown in Figure 4.7.

4.1.3.2 Electrical Efficiency

As the velocity increases, the thickness of the diffusion boundary layer decreases due to the increased shear near the membrane surface. A thinner diffusion boundary layer results in lower electrical resistance, which allows a higher current density, as shown in Figure 4.8. However, flow rate here does not seem to have a very significant effect on current generated (the main effect of flow rate on current will be discussed in detail with the modeling results in Section 4.2).

As shown in Figure 4.9, the specific energy required to achieve a removal ratio is decreases with the velocity based on Equation 2.21.

On average, the hydraulic energy accounted for approximately 15% of the total specific energy consumptions of all 7, 9, and 11 GPM experiments. Therefore, the hydraulic energy required is typically a small fraction of the total EDR energy consumption and final operating cost.

As shown in Figures 4.16 – 4.21, as velocity increases within the conditions of this experimentation, the current and SEC improve, while the separation rate results indicate that the marginal improvement in energy consumption alone is not sufficient to justify the increase in capital and operating costs associated with the increase in superficial velocity. The removal ratio decreases with increased velocity. Therefore, the optimal superficial velocity (for a treatment system operating with similar conditions as these) is expected to be optimized to improve the total performance of EDR process.

4.1.4 Chemical: Effects of Feed Concentration

Inlet conductivity, one of inputs changing from low to high levels, has a direct and proportional impact on product conductivity. In order to investigate the effect of feed inlet concentration, three levels of salinity have been considered. For well1, which has the lowest TDS compared with other well waters, the conductivity ranged between 1600 and 1800 µS/cm; for well2, the conductivity was between 5800 and 6200 µS/cm; and for blend water, conductivities varied from 4700 to 4900 µS/cm. Experiments were conducted under conditions equivalent to those listed for previous investigations.

4.1.4.1 Chemical Efficiency

At higher feed concentrations – in spite of the fact that solution conductivity increases, diminishing resistances of dilute and concentrate compartments in the cell pair – the separation percent decreases (Figure 4.10). Hence, it was demonstrated that EDR is more efficient at lower concentrations and can be applied as a treatment process for desalination.

4.1.4.2 Electrical Efficiency

Generally, higher ionic content of the source water results in lower electrical resistance of the EDR concentrate and dilute cells, allowing a higher current density for the same voltage application based on Ohm's law (Figure 4.11). However, higher current densities create a larger potential loss through membrane resistance and concentration polarization. Thus, it is assumed that the electrical resistance of the membranes was small compared to the electrical resistance of the solutions, which provided the predominant stack resistance drop.

Another key parameter for evaluating the electrical efficiency of the EDR system is SEC, and as illustrated in Figure 4.12, the SEC was proportional to the concentration of ionic content removed from the dilute in streams.

Recognizing that the SEC is correlated with the financial cost of an EDR system, it is important to note that, at some point, the energy required to concentrate a solution by EDR would be greater than the energy required by a thermal process, which is practically insensitive to salinities in this range (brackish water salinity range). In order to achieve a lower SEC for high salinity brackish water, one solution is operating at a lower voltage application.

4.1.5 Design: Effect of Electrode Geometry

Based on current design practices and historical knowledge of the GE EDR stack configurations, three electrode designs are investigated: full, recessed, and tapered.

In this project, to compare the three proposed electrode designs, EDR performance was studied as a function of chemical, electrical and hydraulic operating parameters to introduce optimized electrode design, which directly contributes to higher removal ratio, less current loss, and a lower SEC.

To compare the performances of the three investigated electrodes, analysis of variance (ANOVA) was used with current, removal ratio, and SEC as response (dependent) variables, with the null hypothesis as follows:

$$H_0: \mu_{full} = \mu_{recessed} = \mu_{tapered}$$

The null hypothesis for ANOVA is that the mean (average value of the dependent variable) is the same for all different electrode designs. The alternative or research hypothesis is that the average is not the same for all groups.

For the ANOVA test procedure in this experiment, the p-values obtained from statistical data analyses are shown in Table 4.3.

As shown in Table 4.3, we fail to reject the null hypothesis since the p-values are greater than 0.05. Consequently, it can be concluded that the average of the dependent variable is the same for all groups.

In addition to the p-values, looking at the standard error bars lets us compare the difference between the mean and the amount of scatter within the groups. As shown in Figures 4.13-4.15, since the standard error bars for all three electrode designs overlap, the differences between the three means are statistically insignificant.

Therefore, although it has been hypothesized that the shape of the electrodes and their locations with respect to the solution manifolds could impact EDR performance, based on the statistical results, there is no significant difference between these three electrode designs in terms of current, removal ratio, and specific energy consumption.

However, there is a possibility that experimental errors have affected the accuracy of experimental results and conclusions made based on the results. All measurements are subject to some uncertainty, as several types of errors and inaccuracies can happen.

The main sources of possible experimental errors include:

1. Poorly maintained instruments;
2. Fluctuation of the operating conditions during the measurements;
3. Assumption of linear relationship between conductivity and concentration of sample waters; and
4. Assumption of constant temperature and recovery during all the experiments.

4.2 Modeling Results

Several researchers have developed mathematical simulations of the performance of ED and EDR systems (Kabay et al., 2003; Mohammadi, Moheb, Sadrzadeh, & Razmi, 2005; Moon et al., 2004; Myint et al., 2011; Sadrzadeh et al., 2007; Shaposhnik, 1997; Tanaka, 2009). Unfortunately, many of them are limited to binary ionic solutions, and they are limited to low concentrations of brackish water (up to 1000 mg/L TDS or 0.1 mol/L) or small EDR lab scale systems with low input flow rate values.

In this experiment, statistical modeling of the experimental system was employed using SAS programming to predict characteristics of response variables based on operating conditions and the interactions of the hydraulic, electrical, and chemical phenomena within EDR system.

For all the statistical models provided, residual plots have been evaluated. (Residuals are defined as the difference between the original data and the predicted values from the regression equation.) The residuals should be centered on zero throughout the range of fitted values and have a constant spread throughout the range to make sure that variances of residuals are equal.

In addition, in the regression problem, we are looking for a model that explains a substantial proportion of the variation in the response variable. The analysis of residuals, which is a simple graphic technique (plotting residual vs. predicted value) is required to see if there are any obvious patterns left within the unexplained portion of the variation of the response variable. The emphasis is upon not missing patterns that might suggest a relationship between the predictor and predicted variables.

4.2.1 Chemical Efficiency: Removal Ratio

Based on the results obtained, there is no statistical significance between three different designs of electrode in aspect of EDR performance. Thus, a similar multilinear regression model has been achieved and proposed for all of them. Table 4.4 shows the variation in removal ratio (response) with predictor variables (P-value < 0.05).

The p-value for each term tests the null hypothesis that the coefficient is equal to zero. A low p-value (< 0.05) indicates that the null hypothesis can be rejected. In other words, a predictor that has a low p-value is likely to be a meaningful addition to a model because changes in the predictor's value are related to changes in the response variable.

As shown in the Table 4.4, salinity, flow rate, voltage, and the interactions between them are likely to have a significant effect on removal ratio as a response variable.

However, variance inflation factors (VIF) are another parameter that must be considered while evaluating a regression model. VIF is used to describe how much multicollinearity (correlation between predictors) exists in a regression analysis and measures how much the variances of the estimated regression coefficients are inflated as compared to when the predictor variables are not linearly related.

Multicollinearity is problematic because it can increase the variance of the regression coefficients, making them unstable and difficult to interpret.

In a full factorial design, for estimating removal ratio with stack voltage (V), feed flow rate (GPM) and feed conductivity (mS/cm), the regression model, with the R-square value of 0.95, is:

Removal Ratio = -0.6886 + 0.0122*Voltage + 2.8734/ Flow Rate + 0.8818/Conductivity

The parameter estimates for this regression model are shown in Table 4.5.

Although the interaction of predictors appears to be significant, the high values of VIF indicate that there is a strong multicollinearity between predictors and their interactions.

As illustrated in Figures 4.4, 4.7, and 4.10, and as explained in Section 1.1, removal ratio increases with increasing the voltage, decreasing the feed flow rate, and decreasing the feed conductivity. Figures 4.16, 4.17, and 4.18, show that the regression model introduced to predict the removal ratio fits the experimental data very well.

4.2.2 Electrical Efficiency: Current

Table 4.6 shows the variation in current (response) with predictor variables (P-value < 0.05) for the multilinear regression model.

The regression model in a full factorial design to estimate current with stack voltage (V), feed flow rate (GPM) and feed conductivity (mS/cm) is (R-square = 0.95):

Current = -15.2230+ 3.5116 * Conductivity + 0.6017 * Voltage + 0.0055 * Voltage*Flow Rate

Table 4.7 shows the parameter estimates for this model of current.

As discussed in Section 1.1, current increases as the conductivity of feed increases due to decreases in the resistance of solutions in the cell pair. Based on Ohm's law, there is a linear relationship between voltage and current, and the model confirms that. Also, as Faraday's law indicates, there is an interaction between the dilute mass transfer and dilute flow rate, as shown in the model. Figures 4.19, 4.20, and 4.21 show that the regression model introduced to predict the current fits the experimental data very well.

4.2.3 Electrical Efficiency: Specific Energy Consumption

Table 4.8 shows the variation in specific energy consumption (response) with predictor variable (P-value <0.05) for the multilinear regression model.

The regression model in a full factorial design for estimating specific energy consumption with stack voltage (V), feed flow rate (GPM) and feed conductivity (mS/cm) is (R-square = 0.95):

Specific Energy Consumption = 0.0013 + 0.0413/ Flow Rate + 6.475E-05* Voltage^2* Conductivity/Flow Rate

The parameter estimates for specific energy consumption based on this model are shown in Table 4.9.

The main effects and interaction effects of independent variables on specific energy consumption are quite reasonable and match with Eq. 2.15, Eq. 2.16, and Eq. 2.21. Additionally, Figures 4.22, 4.23, and 4.24 show that the regression model introduced to predict the specific energy consumption fits the experimental data very well.

4.3 Conclusion

The hypothesis for this research is that EDR desalination systems perform differently under changing operating and design conditions, including applied stack voltage, flow rate, source water salinity, and electrode design. The objectives of this research were to:

1. Experimentally determine the sensitivity of EDR to hydraulic, electrical, and chemical operational parameters;
2. Determine and compare how the three electrode designs (full, recessed, and tapered) affect EDR performance;
3. Identify the operating parameters that maximizes the performance of EDR;
4. Perform statistical analyses of the investigated parameters (electrical, hydraulic, and chemical) to determine their impacts on EDR performance.

Objective 1 and 2 were accomplished with a pilot-scale continuous EDR system, the performance of which was investigated with respect to applied stack voltage, flow rate, source water salinity, and electrode design. Objectives 3 and 4 were accomplished through the statistical analysis and development of regression models.

Based on the results obtained, EDR performance depends on the operating conditions (stack voltage, flow rate and feed salinity). However, changing the design of electrodes has no significant effect on EDR performance.

Experiments performed with brackish groundwater demonstrated that stack voltage applications in the range of 30-40 Volts and feed flow rates in the range of 7-11 GPM effectively separated up to 70% of the initial feed salinity in the range of approximately 1000-5500 mg/L at single-stage EDR recovery of 80%.

The stack voltage application is a process controlling parameter, and the rate of separation and current are approximately proportional to the applied voltage. The specific energy consumption increases with increasing the applied voltage.

With the feed flow rates tested here, a decrease in the rate of separation was observed with increases in the feed flow rate, which increase the stack superficial velocity leading to a decrease in residence time. Also, increases in flow rate cause an increase in energy required for pumping and consequently an increase in total energy.

However, the specific energy consumption decreases with increases in the feed flow rate because the pumping energy does not change when recovery is kept constant, while product water volume increases when feed flow rate increases.

As the concentration of solution increases, the removal ratio drops when

feed concentration increases due to the magnification in the concentration factor (i.e., from 0.011 to 0.014) and limited ion exchange capacity of the membranes. Furthermore, since current is proportional to feed conductivity, the specific energy consumption increases as feed water becomes more saline.

In order to increase the removal ratio, lower feed concentrations, higher voltages, and lower flow rates should be utilized. Also, to reduce the specific energy consumption, lower voltages, lower feed concentrations, and higher flow rates are suggested. Table 4.10 summarizes and demonstrates the best choice of voltage, feed flow rate and feed salinity as operating conditions to maximize each EDR performance metric.

It should be noted, however, that the data gathered in these experiments are from conditions that still left salinity levels above 1,000 μS/cm in the product water. Therefore, although the developed regression models do predict the effects of the different parameters, real-world desalination processes would require further treatment to bring the quality of the produced water to acceptable levels. Given that specific energy consumption is strongly determined by the removal ratio, further salt removal to produce truly potable water would significantly increase the specific energy consumption of the systems. Furthermore, as a consequence of an expanded hydrodynamic boundary layer (the results of viscous forces) and concentration boundary layer (the product of mass transfer rates through the desalination membrane), the system is likely to experience progressively poorer electrochemical/hydrodynamic behavior. Additionally, as the removal ratio increases, there is a higher likelihood of salt precipitation in the hydrodynamic/concentration boundary layer, the area in which the most saline part of the solution is moving slowest. For all of these reasons, additional testing should be conducted before designing industrial-scale systems.

4.4 Future Work

Several logical extensions can stem from this work. First, the EDR experimentation could be expanded to study how additional operating conditions, such as temperature and recovery ratio, affect EDR performance. Also, the experiments could be done with more than one hydraulic stage to improve the removal ratio, especially for higher feed salinities, and study how energy consumption changes when more stages are added.

Furthermore, the models for the pilot-scale plant could be extended to simulate full-scale EDR systems. This would allow them to quantify limitations in the tradeoff between energy consumption and removal ratio associated with voltage application and feed flow rate, making it possible to optimize the design of EDR systems.

References

Akyol, E., Öner, M., Barouda, E., & Demadis, K. D. (2009). Systematic Structural Determinants of the Effects of Tetraphosphonates on Gypsum Crystallization. *Crystal Growth & Design*, *9*(12), 5145–5154.

Allison, A. R. P. (2008). Surface and Wastewater Desalination by Electrodialysis Reversal, *86*(0).

Allison, R. P. (1995, November). Electrodialysis reversal in water reuse applications. *Desalination*.

Anderko, A., & Lencka, M. M. (1997). Computation of Electrical Conductivity of Multicomponent Aqueous Systems in Wide Concentration and Temperature Ranges. *Industrial & Engineering Chemistry Research*, *36*(5), 1932–1943.

Balster, J., Stamatialis, D. F., & Wessling, M. (2009). Towards spacer free electrodialysis. *Journal of Membrane Science*, *341*(1-2), 131–138.

Bard, A. J., Faulkner, L. R., Swain, E., & Robey, C. (n.d.). *Fundamentals and Applications*.

Brady, P. V., Kottenstette, R. J., Mayer, T. M., & Hightower, M. M. (2009). Inland Desalination: Challenges and Research Needs. *Journal of Contemporary Water Research & Education*, *132*(1), 46–51.

Chiapello, J.-M., & Bernard, M. (1993). Improved spacer design and cost reduction in an electrodialysis system. *Journal of Membrane Science*, *80*(1), 251–256.

Choi, E., Choi, J., & Moon, S. (2002). An electrodialysis model for determination of the optimal current density, *153*, 399–404.

Choi, J.-H., Lee, H.-J., & Moon, S.-H. (2001). Effects of Electrolytes on the Transport Phenomena in a Cation-Exchange Membrane. *Journal of Colloid and Interface Science*, *238*(1), 188–195.

Hanrahan, C. (2013). *High-Recovery Electrodialysis Reversal for the Desalination of Inland Brackish Waters*. New Mexico State University.

Walker, S. (2010). *Improving recovery in reverse osmosis desalination of inland brackish groundwaters via electrodialysis*. University of Texas at Austin.

Curto, J. D., & Pinto, J. C. (2011). The corrected VIF (CVIF). *Journal of Applied Statistics*, *38*(7), 1499–1507.

D.F. Lawler, M. Cobb, B. F. (2010). *Improving Recovery : A Concentrate Management Strategy for Inland Desalination*. Austin, TX.

Demircio, M., Kabay, N., & Gizli, N. (2001). Cost comparison and efficiency modeling in the electrodialysis of brine, *9164*(01).

Demircioglu, M., Kabay, N., Kurucaovali, I., & Ersoz, E. (2002). Demineralization by electrodialysis (ED) - separation performance and cost comparison for monovalent salts, *153*, 329–333.

Długołęcki, P., Anet, B., Metz, S. J., Nijmeijer, K., & Wessling, M. (2010). Transport limitations in ion exchange membranes at low salt concentrations. *Journal of Membrane Science*, *346*(1), 163–171.

Dowdy, S., Wearden, S., & Chilko, D. (2011). *Statistics for Research* (p. 640). John Wiley & Sons.

Eden, S., Glass, T. W., & Herman, V. (2011). Desalination in Arizona. *Arroyo*.

Electrodialysis and Electrodialysis Reversal: M38. (1995) (p. 62). American Water Works Association.

Elsaid, K., Bensalah, N., & Abdel-wahab, A. (2007). Inland Desalination : Potentials and Challenges. *Rivers*.

Elsaid, K., Bensalah, N., & Abdel-wahab, A. (2012). Inland Desalination : Potentials and Challenges. In Z. Nawaz (Ed.), *Advances in Chemical Engineering* (pp. 449–480). In Tech.

Fubao, Y. (1985). Study on electrodialysis reversal (EDR) process. *Desalination*, *56*, 315–324.

Fues, J. (2008). High-Efficiency Filtration as Pretreatment to Membrane-Based Demineralization Systems. In *American Filtration & Separations Society Annual Conference*. Valley Forge, PA.

Gleick, P. (2012). *The World's Water Volume 7: The Biennial Report on Freshwater Resources*. *The Biennale Report on Freshwater Resources* (Vol. 7). Island Press.

Gleick, P. H. (1993). *Water in Crisis: A Guide to the World's Fresh Water Resources*. New York: Oxford University Press.

Gottberg, A. von. (1998). New High Performance Spacers in Electrodialysis Reversal (EDR) Systems. *Proceedings, American Water Works Assoc. Annual …*.

Gottberg, A. A. Von, & Manager, P. (2010). New High-Performance Spacers in Electro- Dialysis Reversal (EDR) Systems.

Greenlee, L. F., Lawler, D. F., Freeman, B. D., Marrot, B., & Moulin, P. (2009). Reverse osmosis desalination: water sources, technology, and today's challenges. *Water Research*, *43*(9), 2317–48.

Hasson, D., Drak, A., & Semiat, R. (2009). Induction times induced in an RO system by antiscalants delaying CaSO4 precipitation, *157*(May 2003), 193–207.

Helfferich, F. G. (1962). *Ion Exchange* (p. 624). Courier Corporation.

Hwang, J.-Y., & Lai, J.-Y. (2007). The effect of temperature on limiting current density and mass transfer in electrodialysis. *Journal of Chemical Technology & Biotechnology*, *37*(2), 123–132.

Ibanez, R., Stamatialis, D. ., & Wessling, M. (2004). Role of membrane surface in concentration polarization at cation exchange membranes. *Journal of Membrane Science*, *239*(1), 119–128.

Ions, C. A. T., Rod, E., & Is, A. (n.d.). PROCESS A P P L I CAT IONS 0 F ELECT ROD I ALYS IS, (6), 29–35.

Jefferies, M., & Comstock, D. (2001). Predicting calculating scaling tendency in membrane plants. *Desalination*, *139*(1-3), 341–344.

Kabay, N., Ardab, M., Ersoza, E., Kahveci, H., Can, M., Dal, S., … Yuksel, M. (2003). Effect of feed characteristics on the separation performances of monovalent and divalent salts by electrodialysis, *58*, 95–100.

Katz, W. E. (1979). The electrodialysis reversal (EDR) process. *Desalination*, *28*(1), 31–40.

Kim, Y., Walker, W. S., & Lawler, D. F. (2012). Competitive separation of di- vs. mono-valent cations in electrodialysis: effects of the boundary layer properties. *Water Research*, *46*(7), 2042–56.

Lee, H. J., Strathmann, H., & Moon, S. H. (2006). Determination of the limiting current density in electrodialysis desalination as an empirical function of linear velocity. *Desalination*, *190*(1-3), 43–50.

Lee, H.-J., Hong, M.-K., Han, S.-D., Cho, S.-H., & Moon, S.-H. (2009). Fouling of an anion exchange membrane in the electrodialysis desalination process in the presence of organic foulants. *Desalination*, *238*(1-3), 60–69.

Mandersloot, W. G. B., & Hicks, R. E. (1966). Leakage currents in electrodialytic desalting and brine production. *Desalination*, *1*(2), 178–193.

Martin-lagardette, B. J. L. (2003). Desalination of Seawater. *Water Engineering and Managment*.

Mcgovern, R. K., Zubair, S. M., & V, J. H. L. (2014). The cost effectiveness of electrodialysis for diverse salinity applications, *348*, 57–65.

Meng, H., Deng, D., Chen, S., & Zhang, G. (2005). A new method to determine the optimal operating current (Ilim') in the electrodialysis process. *Desalination*, *181*(1-3), 101–108.

Miller, A. W. S., Water, G. E., & Technolo-, P. (2009). Understanding Ion-Exchange Resins For Water Treatment Systems.

Miller, J. E. (2003). Review of Water Resources and Desalination Technologies. *Exchange Organizational Behavior Teaching Journal*, (March), 3–54.

Mohammadi, T., & Kaviani, A. (2003). Water shortage and seawater desalination by electrodialysis. *Desalination*, *158*(1-3), 267–270.

Mohammadi, T., Moheb, A., Sadrzadeh, M., & Razmi, A. (2005). Modeling of metal ion removal from wastewater by electrodialysis. *Separation and Purification Technology*, *41*(1), 73–82.

Moon, P., Sandí, G., Stevens, D., & Kizilel, R. (2004). Computational Modeling of Ionic Transport in Continuous and Batch Electrodialysis. *Separation Science and Technology*, *39*(11), 2531–2555.

Murray, P. (1995). *Electrodialysis and Electrodialysis Reversal (M38): AWWA Manual of Water Supply Practice*. American Water Works Association.

Myint, M. T., Ghassemi, A., & Nirmalakhandan, N. (2011). Modeling in desalination—electro-dialysis reversal. *Desalination and Water Treatment*, *27*(1-3), 255–267.

National Ground Water Association. (2010). NGWA Information Brief: Brackish Groundwater, 1–4.

Nicot, J.-P., & Chowdhury, A. H. (2005). Disposal of brackish water concentrate into depleted oil and gas fields: a texas study. *Desalination*, *181*(1-3), 61–74.

Pankratz, T. (2012). *IDA Desalination Yearbook 2011-2012*. Oxford, UK.

Philibert, J. (2005). One and a Half Century of Diffusion : Fick , Einstein , before and beyond, *2*, 1–10.

Pilat, B. (2001). Practice of water desalination by electrodialysis, *139*(May), 385–392.

Process Technologies for Water Treatment. (2013) (p. 239). Springer Science & Business Media.

Purification, W., & Program, D. (2003). Handbook, (72).

Reahl, A. E. R. (2006). Half A Century of Desalination With Electrodialysis.

Rosenberg, N. W., & Tirrell, C. E. (1957). Limiting Currents in Membrane Cells. *Industrial & Engineering Chemistry*, *49*(4), 780–784.

Rubinstein, I., & Shtilman, L. (1979). Voltage against current curves of cation exchange membranes. *Journal of the Chemical Society, Faraday Transactions 2*, *75*, 231.

Sadrzadeh, M., Kaviani, A., & Mohammadi, T. (2007). Mathematical modeling of desalination by electrodialysis. *Desalination*, *206*(1-3), 538–546.

Sadrzadeh, M., & Mohammadi, T. (2008). Sea water desalination using electrodialysis. *Desalination*, *221*(1-3), 440–447.

Sadrzadeh, M., & Mohammadi, T. (2009). Treatment of sea water using electrodialysis: Current efficiency evaluation. *Desalination*, *249*(1), 279–285.

Sata, T. (1986). Recent trends in ion exchange membrane research. *Pure Appl. Chem*, *58*(1), 1613–1626.

Sata, T. (2004). *Ion Exchange Membranes: Preparation, Characterization, Modification and Application* (p. 314). Royal Society of Chemistry.

Scott, K. (1996). *Industrial Membrane Separation Technology* (p. 305). Springer Science & Business Media.

Shaffer, L. H., & Mintz, M. S. (1966). Electrodialysis. In K. S. Spiegler (Ed.), *Principles of Desalination* (pp. 199–289). Academic Press.

Shaposhnik, V. (1997). Analytical model of laminar flow electrodialysis with ion-exchange membranes. *Journal of Membrane Science*, *133*(1), 27–37.

Shaposhnik, V. a., & Grigorchuk, O. V. (2010). Mathematical model of electrodialysis with ion-exchange membranes and inert spacers. *Russian Journal of Electrochemistry*, *46*(10), 1182–1188.

Ślezak, A., Ślezak, I. H., & Ślezak, K. M. (2005). Influence of the concentration boundary layers on membrane potential in a single-membrane system. *Desalination*, *184*(1-3), 113–123.

Staff, A. (1996). *Electrodialysis and Electrodialysis Reversal (M38)* (p. 72). American Water Works Association.

Strathmann, H. (2004a). Assessment of Electrodialysis Water Desalination Process Costs. *Proceedings of the International Conference on Desalination Costing*, 32–54.

Strathmann, H. (2004b). *Ion-Exchange Membrane Separation Processes* (p. 360). Elsevier.

Strathmann, H. (2010). Electrodialysis, a mature technology with a multitude of new applications. *Desalination*, *264*(3), 268–288.

Strathmann, H. (2011). *Introduction to Membrane Science and Technology*. Weinheim, Germany: Wiley-VCH.

Strathmann, H., Giorno, L., & Drioli, E. (n.d.). An Introduction to Membrane.

Stuttgart, U. (2002). Designing of an electrodialysis desalination plant, *142*, 267–286.

Subcommittee, A. M. R. M. (2004). Committee Report: Current Perspectives on Residuals Management for Desalting Membranes. *Journal - American Water Works Association*, *96*(12), 73–87.

Tanaka, Y. (1991, April). Concentration polarization in ion exchange membrane electrodialysis. *Journal of Membrane Science*.

Tanaka, Y. (2009). A computer simulation of continuous ion exchange membrane electrodialysis for desalination of saline water. *Desalination*, *249*(2), 809–821.

Tanaka, Y. (2015). *Ion Exchange Membranes: Fundamentals and Applications* (p. 522). Elsevier Science.

Tanaka, Y., Uchino, H., & Murakami, M. (2012). Continuous ion-exchange membrane electrodialysis of mother liquid discharged from a salt-manufacturing plant and transport of Cl - ions and SO 42- ions, *3*(1), 63–76.

Tsiakis, P., & Papageorgiou, L. G. (2005). Optimal design of an electrodialysis brackish water desalination plant. *Desalination*, *173*(2), 173–186.

Turek, M. (2002). Cost effective electrodialytic seawater desalination, *153*, 371–376.

Turek, M., & Dydo, P. (2001). O PTIMISATION OF E LECTRODIALYTIC D ESALINATION.

Valerdi-pcrez, R. (2001). Current-voltage curves for an electrodialysis reversal pilot plant : determination of limiting currents, *141*, 23–37.

VALERDI-PÉREZ, R., BERNÁ-AMORÓS, L. M., & IBÁÑEZ-MENGUAL, J. A. (2000). Determination of the Working Optimum Parameters for an Electrodialysis Reversal Pilot Plant. *Separation Science and Technology*, *35*(5), 651–666.

Valerdi-Pérez, R., López-Rodríguez, M., & Ibáñez-Mengual, J. A. (2001). Characterizing an electrodialysis reversal pilot plant. *Desalination*, *137*(1-3), 199–206.

Valero, F., & Arbós, R. (2010). Desalination of brackish river water using Electrodialysis Reversal (EDR). *Desalination*, *253*(1-3), 170–174.

Valero, F., Barceló, A., & Arbós, R. (2010). Theory and Applications ., 3–22.

Veerman, J., Post, J. W., Saakes, M., Metz, S. J., & Harmsen, G. J. (2008). Reducing power losses caused by ionic shortcut currents in reverse

electrodialysis stacks by a validated model. *Journal of Membrane Science*, *310*(1-2), 418–430.

Verbrugge, M. W., & Hill, R. F. (1990). Ion and Solvent Transport in Ion-Exchange Membranes) F (~), *137*(3), 886–893.

Walker, S. (2010). *Improving recovery in reverse osmosis desalination of inland brackish groundwaters via electrodialysis*. University of Texas at Austin.

Walton, H. F. (1962). Ion Exchange. F. G. Helfferich. McGraw-Hill, New York, 1962. ix + 624 pp. Illus. $16. *Science*, *138*(3537), 133–133.

Yang, Q., & Ma, Z. (2004). DESTRUCTION OF ANTI-SCALANTS IN RO CONCENTRATES BY ELECTROCHEMICAL OXIDATION. *Journal of Chemical Industry and Engineering (China)*, *55*(2), 339–340.

Younos, T., & Tulou, K. E. (2009). Overview of Desalination Techniques. *Journal of Contemporary Water Research & Education*, *132*(1), 3–10.

Zhou, Y., & Tol, R. S. J. (2005). Evaluating the costs of desalination and water transport. *Water Resources Research*, *41*(3), n/a–n/a.

Tables

Table 3-1. Experimental variables and discrete value ranges

Variables	Levels
Stack voltage (V)	30, 32.5, 35, 37.5, 40
Feed flow rate (GPM)	7, 9, 11
Feed water	Low, Medium, High
Electrode type	Full, Recessed, Tapered

Table 3-2. EDR stack specifications

Type	Filter press	GE MkIV 2
EDR Stack	Number	1
	Polarity reversal cycle	15 min
	Electric stage	1
	Hydraulic stage	1/electric stage
	Number of cell pairs	40
Membrane	Heavy cation-exchange	GE CR67-HMR
	Cation-exchange	GE CR67-LLMR
	Anion-exchange	GE AR204-SZRA
	Membrane dimensions	102*46 *0.6 cm
	Effective membrane area	0.47 m^2/membrane
	Spacer model	Mk-IV
	Spacer surface area	0.34m^2/membrane (flow path = 2 m)
Electrode Information	Type and active area	Full : 511.4 in^2
		Recessed: 493.4 in^2
		Tapered: 511.4 in^2

Table 3-3. Design of experiments

Factors	Levels	Values
Electrode type	3	Full, Recessed, Tapered
Feed flowrate (GPM)	3	7, 9 ,11
Feed salinity classification	3	Low, Medium, High
Applied voltage (V)	5	30, 32.5, 35, 37.5, 40

Table 3-4. Composition and concentration of feed water at BGNDRF

Parameter Name	**Units**	**Low**	**High**	**Medium**

Bicarbonate	mg/L	150	250	200
Chloride	mg/L	34	580	305
Fluoride	mg/L	2.40	0.35	1.38
Sulfate	mg/L	730	3000	1870
Calcium	mg/L	63	550	306
Magnesium	mg/L	16	320	169
Potassium	mg/L	5.0	2.9	3.9
Silicon Dioxide	mg/L	25	24	24
Sodium	mg/L	320	640	480
Strontium	mg/L	2.0	8.8	5.40
Total Concentration	meq/L	37	160	99
pH	pH units	8.16	7.25	7.40
Conductivity	µs/cm	1700	6100	3900
Total Dissolved Solids	mg/L	1240	5550	3395
Water Temperature	º C	22	21	23

Table 3-5. Data collection log

	Daily Record
Date	-
Time	-
Comment	-
Polarity	-
Feed Conductivity (µS/cm)	-
Feed Temperature (°C)	-
Feed pH	-
Inter-Stage Dilute pH	-
Product Conductivity (µS/cm)	-
Product pH	-
Concentrate Conductivity (µS/cm)	-
Concentrate pH	-

Stage 1 Voltage (V)	-
Stage 1 Current (A)	-
Product Flow Rate (GPM)	-
Concentrate Blow-Down Flow Rate (GPM)	-

Table 3-6. Material specifications

Product	Model	Manufacturer
Pretreatment		
Pressure Reducing Valve	PR150-EP	Plastomatic, Cedar Grove, NJ
Cartridge Filter	Zplex MuniZ 5µm	GE WPT, Minnetonka, MN
Multi-Media Filter	Professional Series Tanks	GE WPT, Minnetonka, MN
Water Measurement		
Flow Meters	Polysulfone Flowmeter	King Instrument Company, Garden Grove, CA
System Conductivity Meters	Elec.inpro 4260/120/PT1000	Thorton Medler Toledo, Bedford, MA
Handheld Conductivity Meter	Sension5	HACH, Loveland, CO
Electrical Measurement		
Oscilloscope	Industrial Scopemeter	Fluke, Everett, WA
Handheld Voltmeter	115 True RMS Multimeter	Fluke, Everett, WA

Table 4-1. Limiting current values for low-level salinity

Electrode Type	Feed Flow Rate	Limiting Current
Full	7 GPM	15.6
	9 GPM	19.0
	11 GPM	26.6
Recessed	7 GPM	14.8
	9 GPM	18.9
	11 GPM	23.8
Tapered	7 GPM	14.9

9 GPM	18.1
11 GPM	24.0

Table 4-2. Conversion factors of conductivity to concentration.

Feed Salinity Level	Conversion Factor
Low	0.011
Medium	0.012
High	0.014

Table 4-3. P-values for different dependent variables

Response variable	P-value
Current	0.1596
Removal Ratio	0.2218
Specific Energy Consumption	0.0815

Table 4-4. Analysis of variance for removal ratio

Source	DF	SS	MS	F value	P value
Salinity	1	2.74463	2.74463	1443.11	<.0001
Flow Rate	1	0.50242	0.50242	264.17	<.0001
Voltage	1	0.25328	0.25328	133.17	<.0001
Salinity*Flow Rate	1	0.02277	0.02277	11.97	0.0007
Flow Rate*Voltage	1	0.00564	0.00564	2.96	0.0876
Salinity*Voltage	1	0.02083	0.02083	10.95	0.0012
Salinity*Flow Rate*Voltage	1	0.00188	0.00188	0.99	0.3216

Error	127	0.24154	0.0019
Total	134	3.79297	

Table 4-5. Parameter estimates for removal ratio

	DF	Parameter Estimate	Standard Error	P-value	VIF
Intercept	1	-0.6886	0.03651	<.0001	0
Voltage	1	0.0122	0.0009	<.0001	1
1/Flow Rate	1	2.8734	0.14874	<.0001	1
1/Conductivity	1	0.8818	0.01929	<.0001	1

Table 4-6. Analysis of variance for current

Source	DF	SS	MS	F-value	P-value
Conductivity	1	4819.44	4819.44	3188.78	<.0001
Flow Rate	1	12.0167	12.0167	7.95	0.0056
Voltage	1	715.457	715.457	473.38	<.0001
Salinity*Flow Rate	1	17.7158	17.7158	11.72	0.0008
Flow Rate*Voltage	1	17.7158	17.7158	11.72	0.0008
Salinity*Voltage	1	3.67753	3.67753	2.43	0.1213
Salinity*Flow Rate*Voltage	1	5.4E-05	5.4E-05	0	0.9952
Error	127	191.945	1.51138		
Total	134	5819.78			

Table 4-7. Parameter estimates - current

	DF	Parameter Estimate	Standard Error	P-value	VIF
Intercept	1	-15.223	1.26678	<.0001	0
Conductivity	1	3.5116	0.073	<.0001	1
Voltage	1	0.6017	0.04013	<.0001	1.3068
Voltage*Flow Rate	1	0.0055	0.00216	0.0128	1.3068

Table 4-8. Analysis of variance for specific energy consumption

Source	DF	SS	MS	F value	P value
Conductivity	1	4819.44	4819.44	3188.78	<.0001
Flow Rate	1	12.0167	12.0167	7.95	0.0056

Voltage	1	715.457	715.457	473.38	<.0001
Salinity*Flow Rate	1	17.7158	17.7158	11.72	0.0008
Flow Rate*Voltage	1	3.67753	3.67753	2.43	0.1213
Salinity*Voltage	1	59.5278	59.5278	39.39	<.0001
Salinity*Flow Rate*Voltage	1	5.4E-05	5.4E-05	0	0.9952
Error	127	191.945	1.51138		
Total	134	5819.78			

Table 4-9. Parameter estimates for specific energy consumption

	DF	Parameter Estimate	Standard Error	P-value	VIF
Intercept	1	0.00127	0.00052	0.0156	0
Voltage^2*Conductivity/Flow Rate	1	1.4E-05	3.44E-07	<.0001	1.1405
1/Flow Rate	1	0.05419	0.00473	<.0001	1.1405

Table 4-10. Best choices of the operating conditions

Response Variable	Minimum Value	Maximum Value
SEC (kWh/Gallon)	0.0075 (30 V, 11 GPM, Low Salinity)	0.0279 (40 V, 7 GPM, High Salinity)
Current (A)	10.2 (30 V, 7 GPM, Low Salinity)	32.5 (40 V, 11 GPM, High Salinity)
Removal Ratio	0.11 (30 V, 11 GPM, High Salinity)	0.73 (40 V, 7 GPM, Low Salinity)

Figures

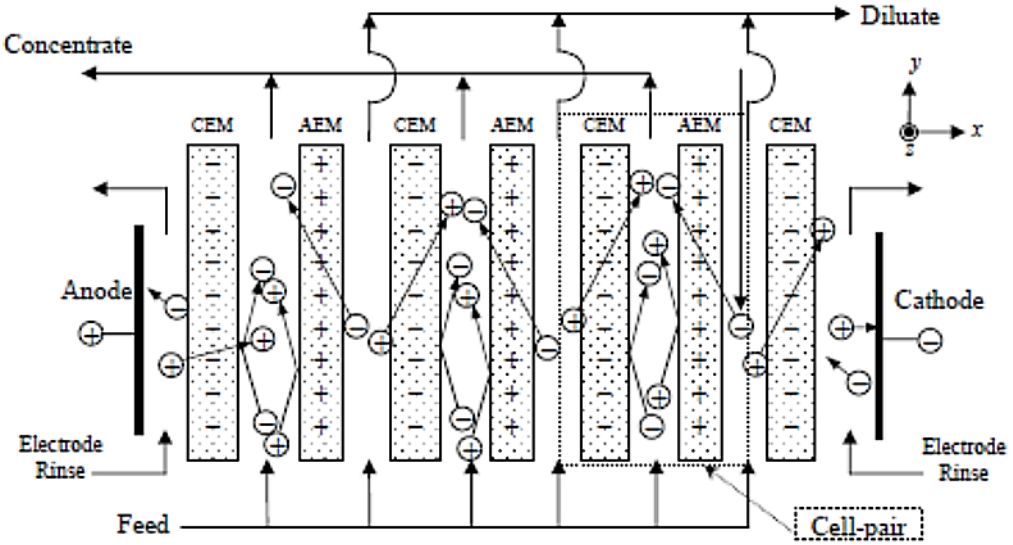

Figure 2.1. Schematic of EDR System. Reprinted from Walker, 2010.

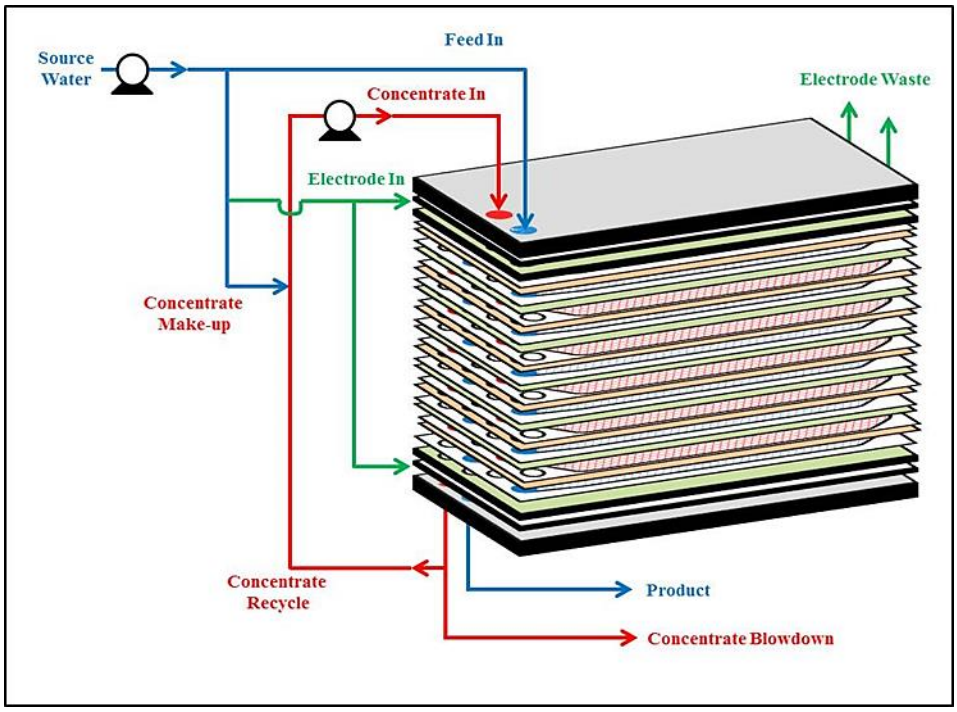

Figure 2.2. Electrodialysis Process Schematic. Reprinted from Hanrahan, 2013.

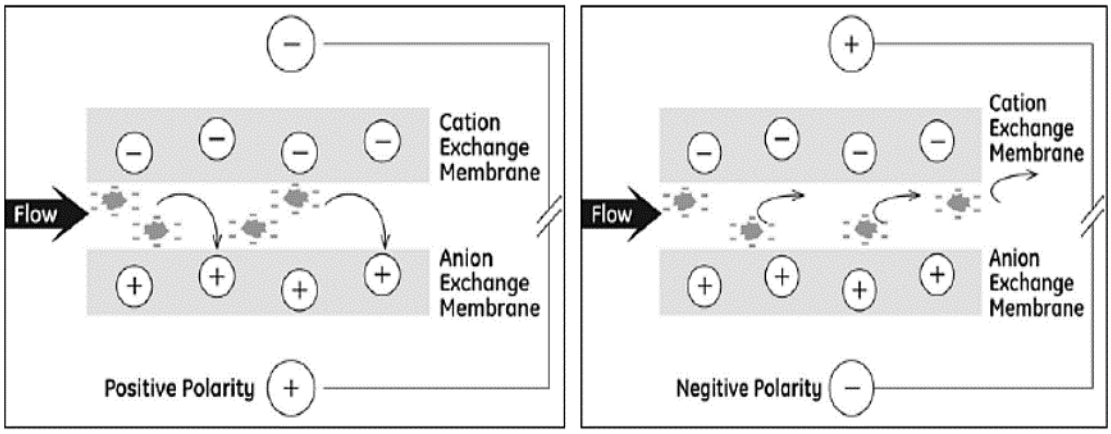

Figure 2.3. Scale Deposition and Scale Removal in EDR. Reprinted from A. R. P. Allison, 2008.

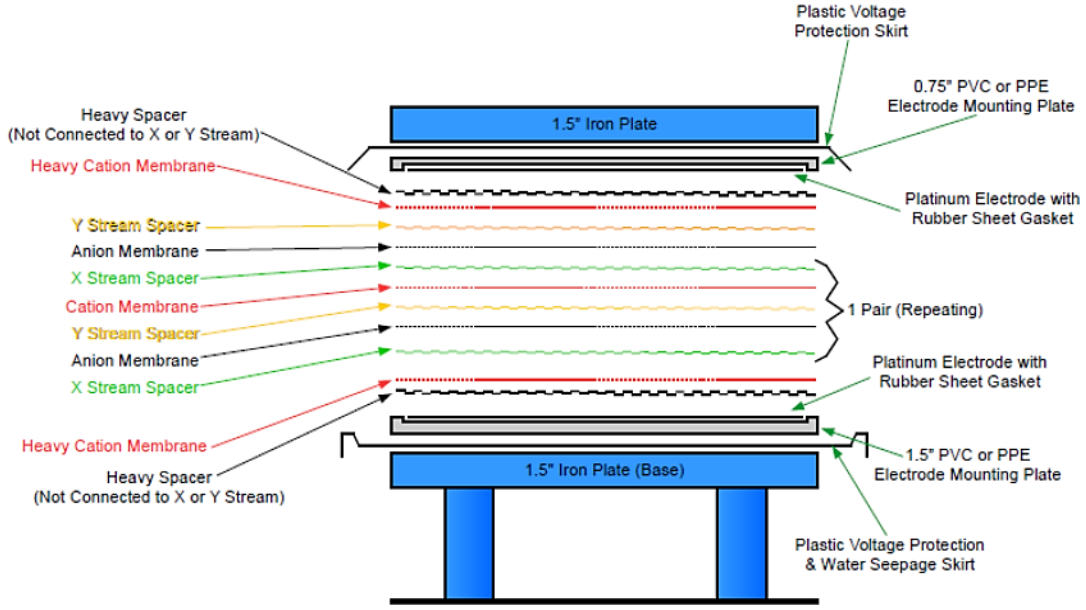

Figure 2.4. EDR Stack Diagram

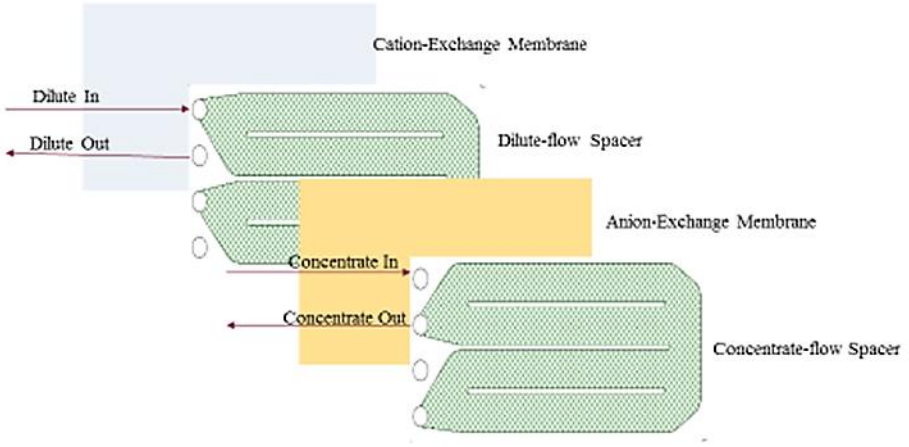

Figure 2.5. Cell Pair Schematic.

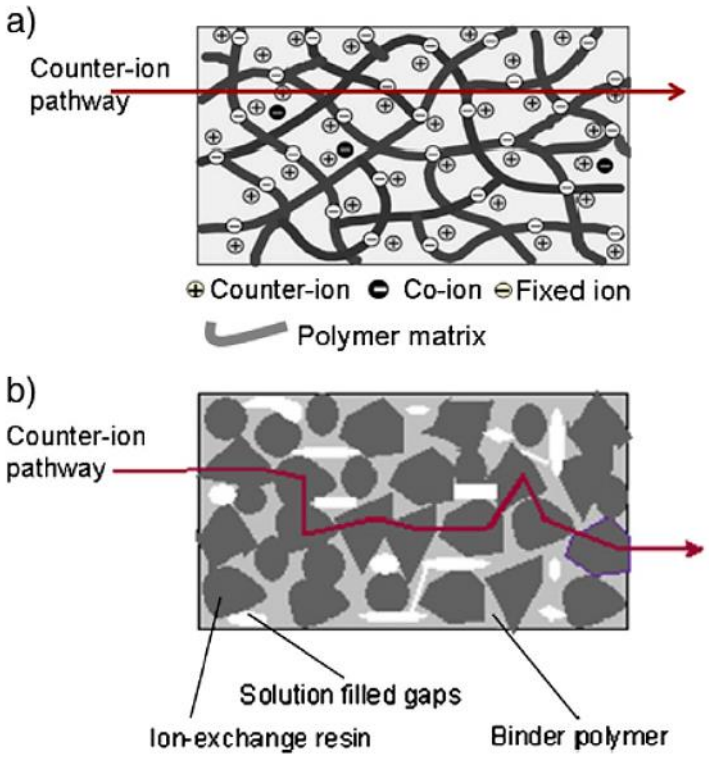

Figure 2.6. Schematic drawing illustrating a) a cation-exchange membrane with a homogeneous structure and b) an ion-exchange membrane with a heterogeneous structure prepared from anion-exchange resin powder and a binder polymer. Reprinted from Strathmann, 2004.

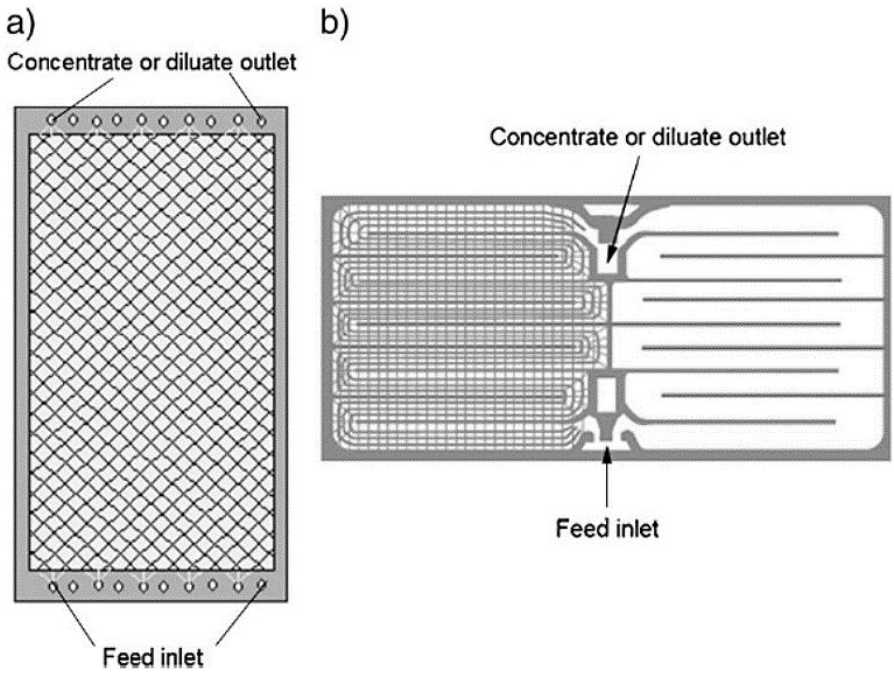

Figure 2.7. Schematic drawing illustrating a) the design of a sheet flow and b) a tortuous path flow spacer. Reprinted from Strathmann, 2010.

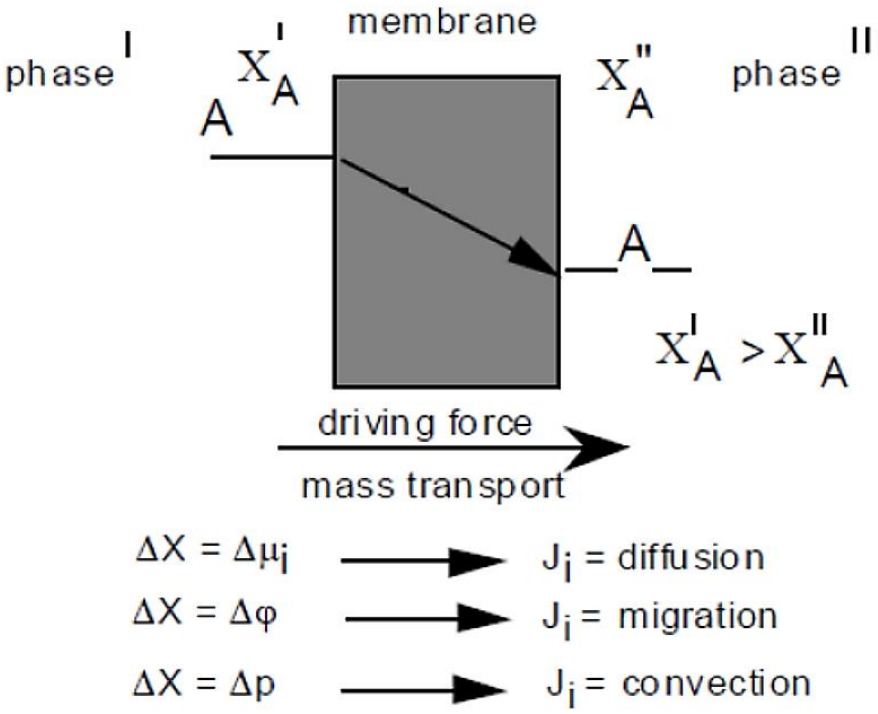

Figure 2.8. General forms of mass transport through the membrane. Reprinted from *Introduction to Membrane Science and Technology*, by H. Strathmann, 2011, Weinheim, Germany: Wiley-VCH.

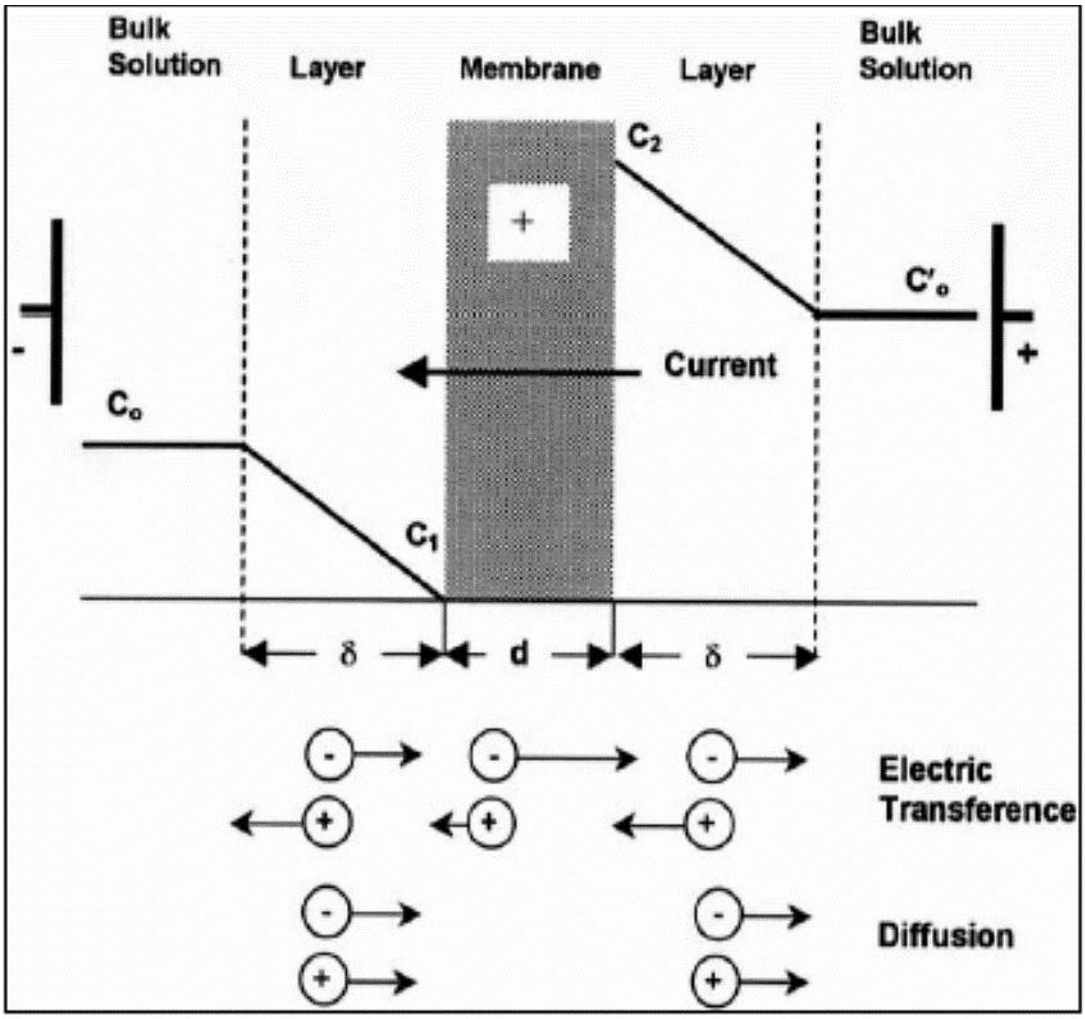

Figure 2.9. Counterion Concentration Profile in the Polarization Layers of an Ion-Exchange Membrane. Reprinted from Valerdi-Pérez et al., 2001.

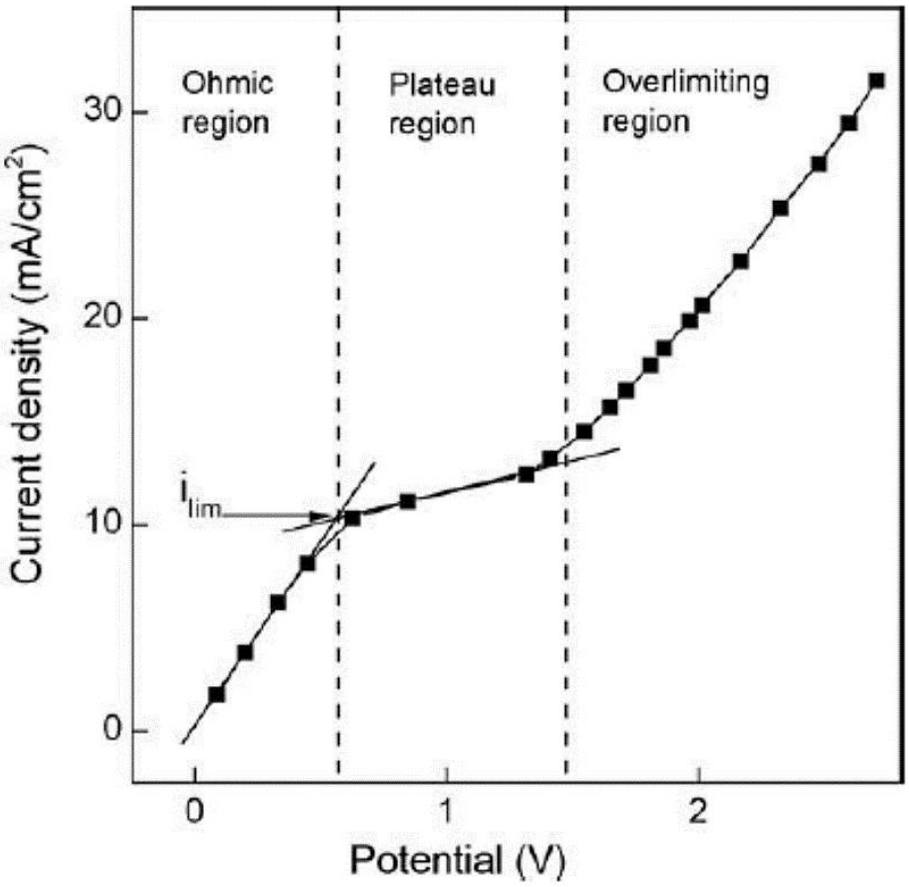

Figure 2.10. Typical Example of a Current-Voltage Curve. Reprinted from Długołęcki et al., 2010.

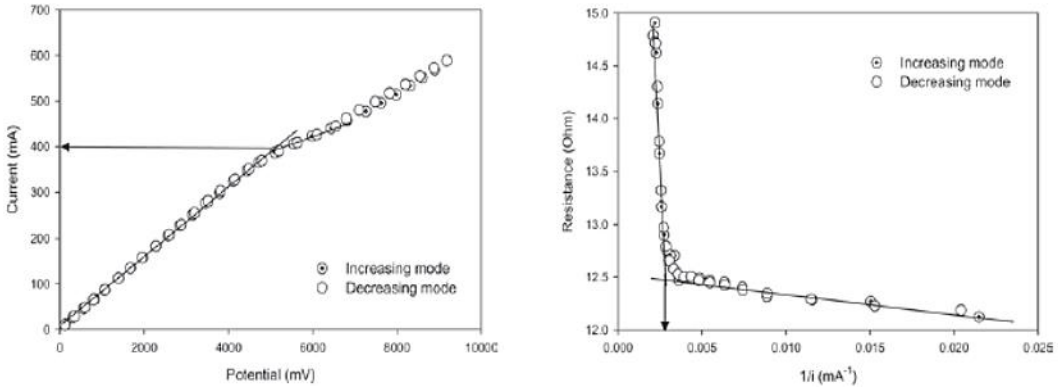

Figure 2.11. a) Current-Potential Relationship, and b) Cell Resistance-1/current Relationship Reprinted from H. J. Lee et al., 2006.

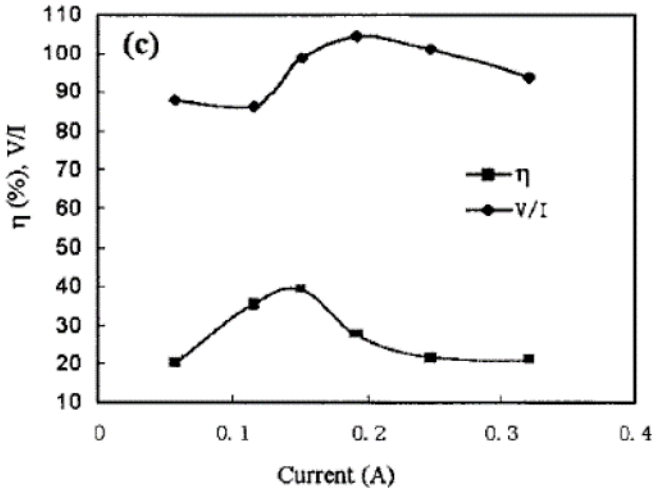

Figure 2.5. Removal Ratio-Current Relationship. Reprinted from Meng et al., 2005.

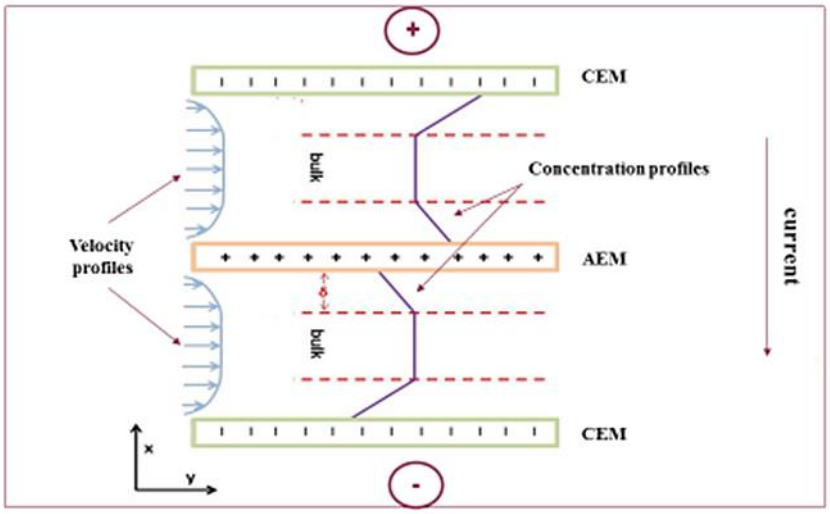

Figure 2.13. Schematic of Regions in a Cell Pair. Adapted from Moon et al., 2004

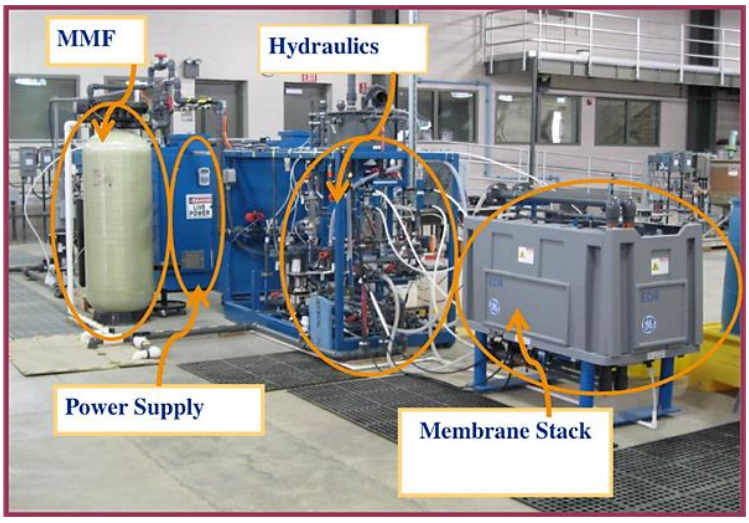

Figure 3.1. EDR pilot-scale set-up

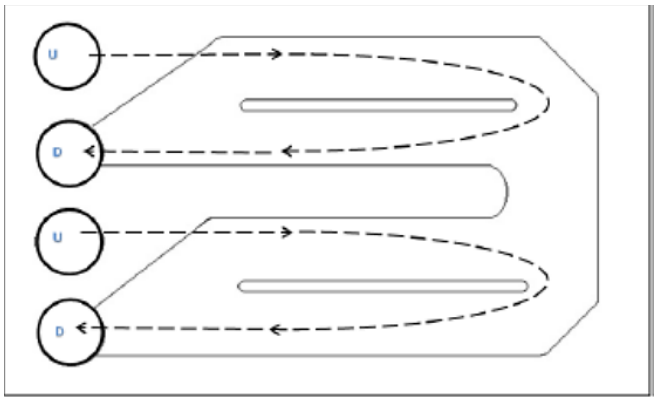

Figure 3.2. GE "MkIV-2" tortuous path spacer

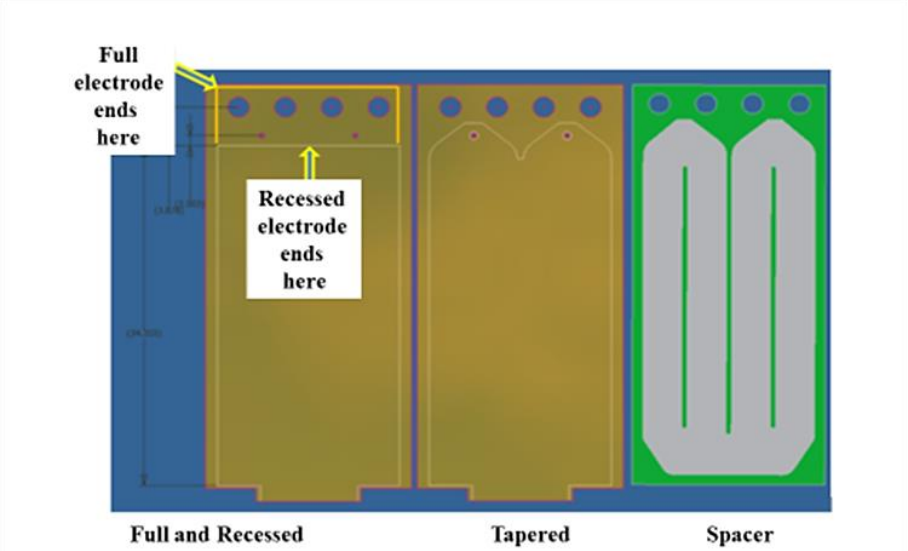

Figure 3.3. Illustration of electrode shapes

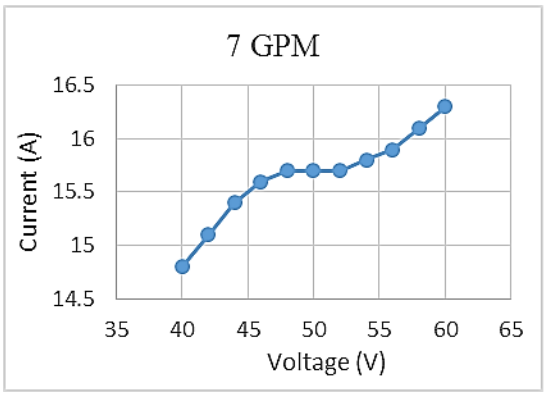
7 GPM
Current (A)
16.5
16
15.5
15
14.5
35 40 45 50 55 60 65
Voltage (V)

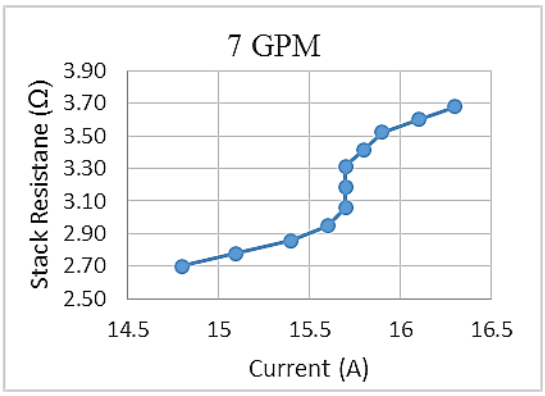
7 GPM
Stack Resistane (Ω)
3.90
3.70
3.50
3.30
3.10
2.90
2.70
2.50
14.5 15 15.5 16 16.5
Current (A)

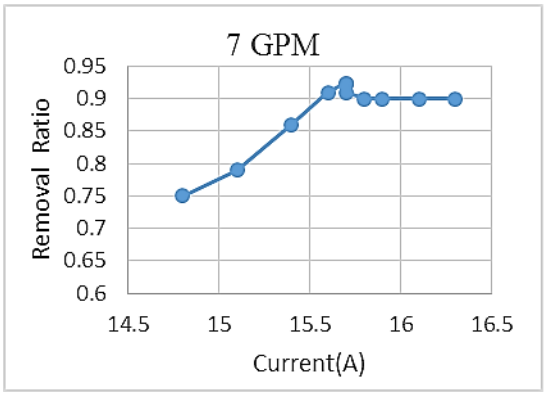
7 GPM
Removal Ratio
0.95
0.9
0.85
0.8
0.75
0.7
0.65
0.6
14.5 15 15.5 16 16.5
Current(A)

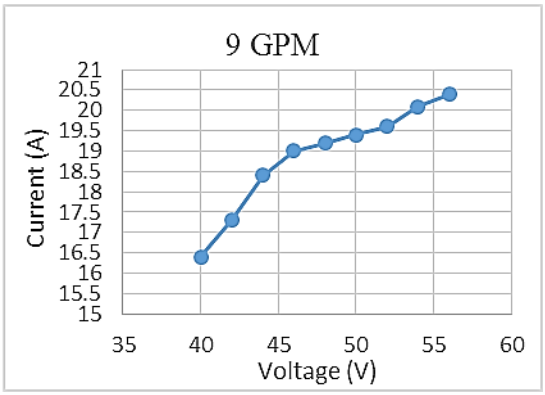
9 GPM
Current (A)
21
20.5
20
19.5
19
18.5
18
17.5
17
16.5
16
15.5
15
35 40 45 50 55 60
Voltage (V)

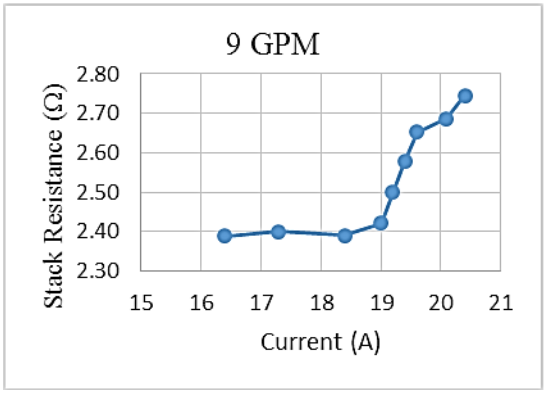
9 GPM
Stack Resistance (Ω)
2.80
2.70
2.60
2.50
2.40
2.30
15 16 17 18 19 20 21
Current (A)

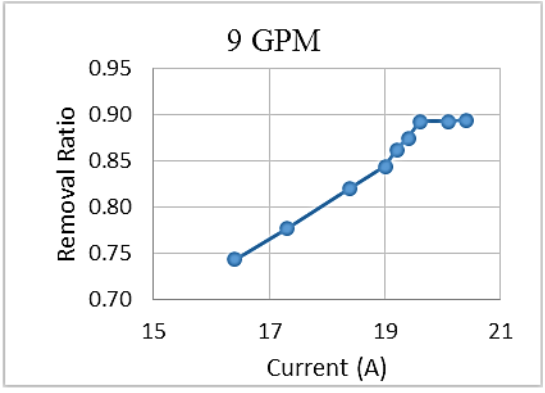
9 GPM
Removal Ratio
0.95
0.90
0.85
0.80
0.75
0.70
15 17 19 21
Current (A)

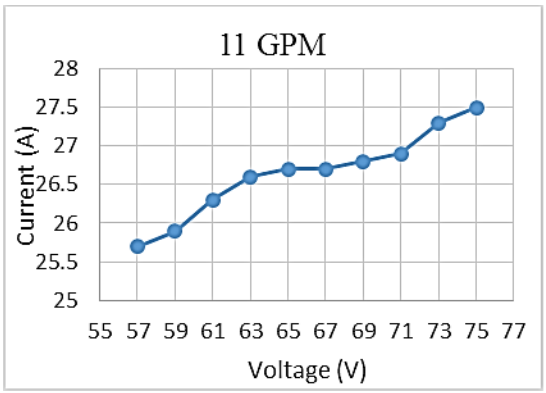
11 GPM
Current (A)
28
27.5
27
26.5
26
25.5
25
55 57 59 61 63 65 67 69 71 73 75 77
Voltage (V)

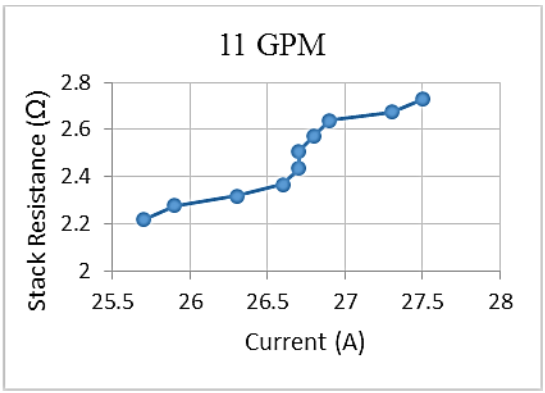
11 GPM
Stack Resistance (Ω)
2.8
2.6
2.4
2.2
2
25.5 26 26.5 27 27.5 28
Current (A)

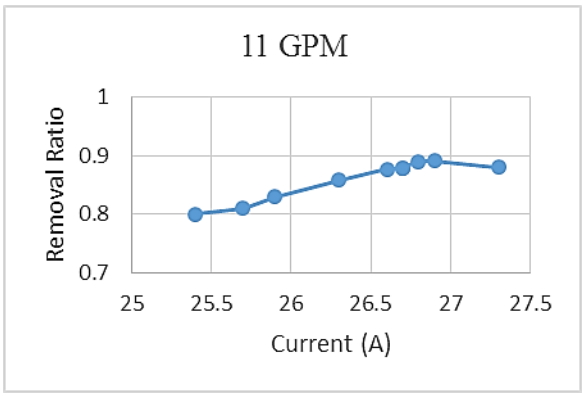

Figure 4.1. Limiting current curves for different feed flow rates – full electrode

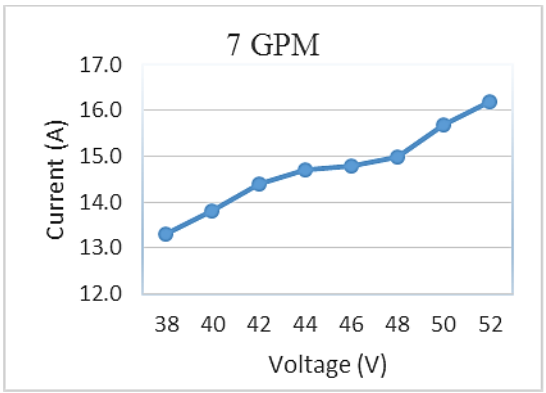

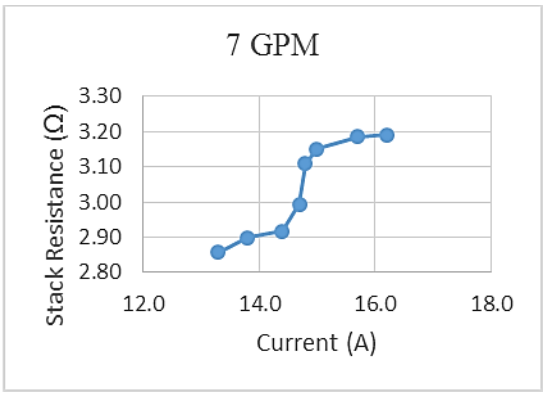

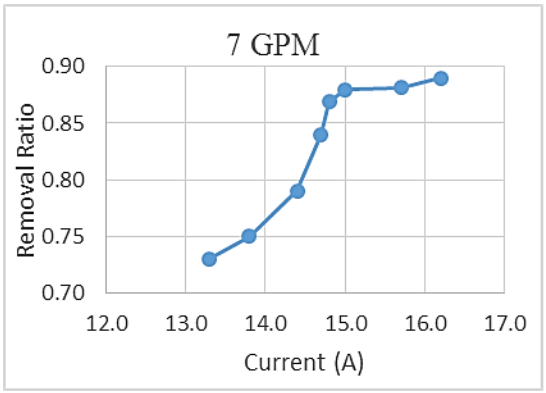

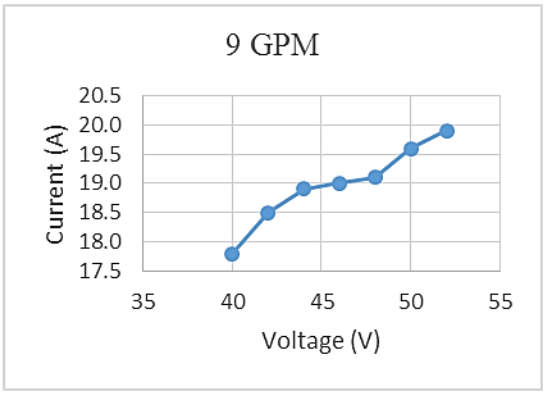

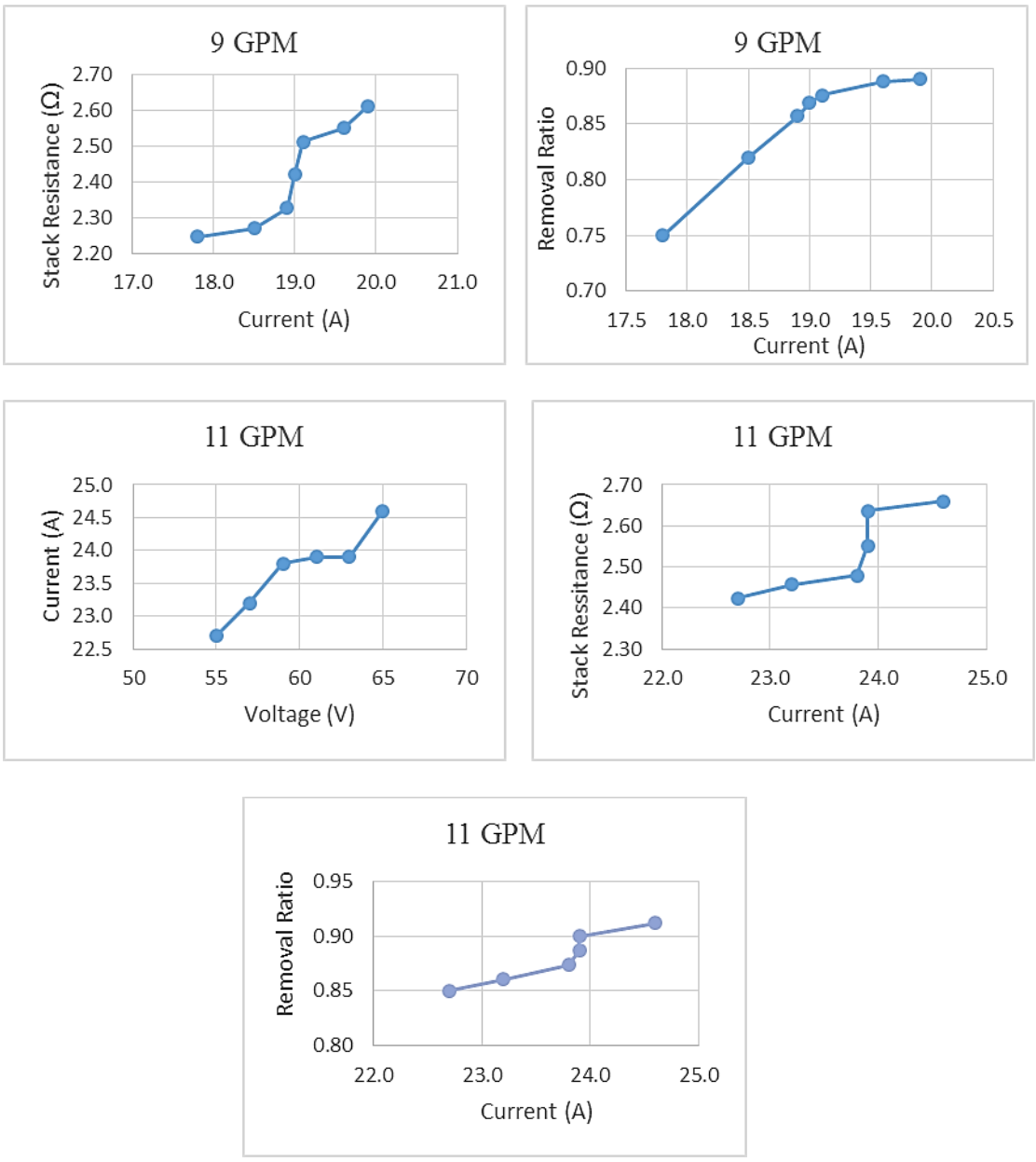

Figure 4.2. Limiting current curves for different feed flow rates – recessed electrode

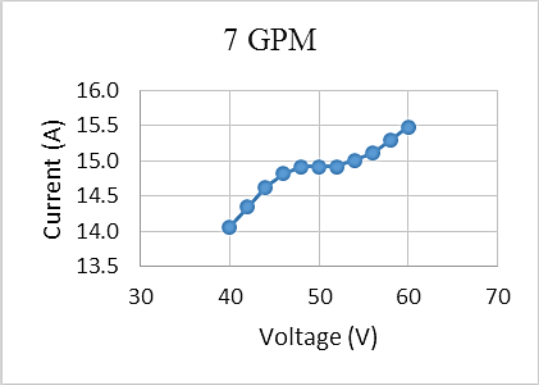
7 GPM
Current (A)
16.0
15.5
15.0
14.5
14.0
13.5
30
40
50
60
70
Voltage (V)

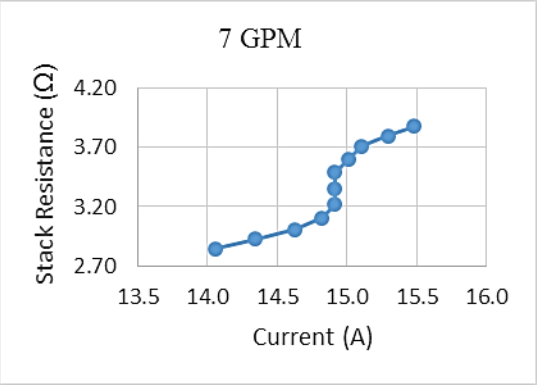
7 GPM
Stack Resistance (Ω)
4.20
3.70
3.20
2.70
13.5
14.0
14.5
15.0
15.5
16.0
Current (A)

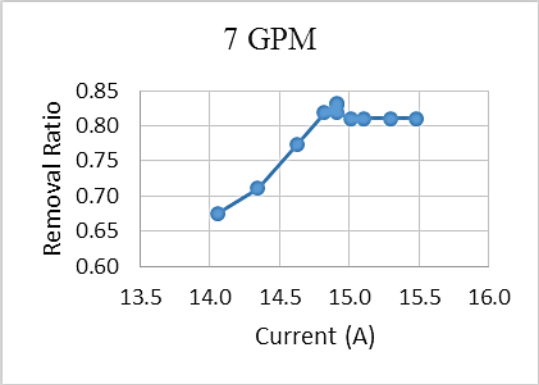
7 GPM
Removal Ratio
0.85
0.80
0.75
0.70
0.65
0.60
13.5
14.0
14.5
15.0
15.5
16.0
Current (A)

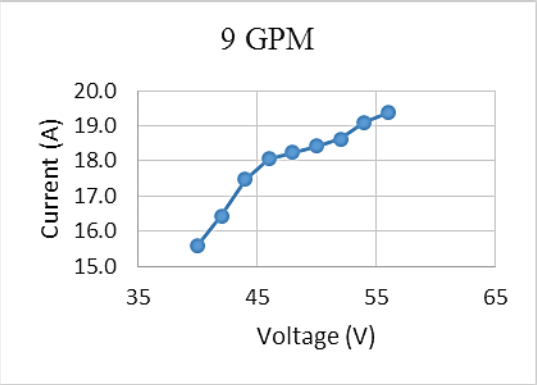
9 GPM
Current (A)
20.0
19.0
18.0
17.0
16.0
15.0
35
45
55
65
Voltage (V)

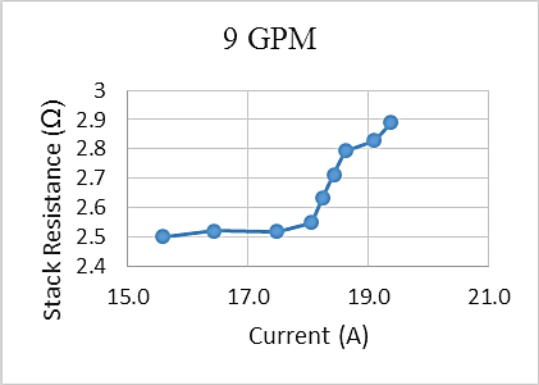
9 GPM
Stack Resistance (Ω)
3
2.9
2.8
2.7
2.6
2.5
2.4
15.0
17.0
19.0
21.0
Current (A)

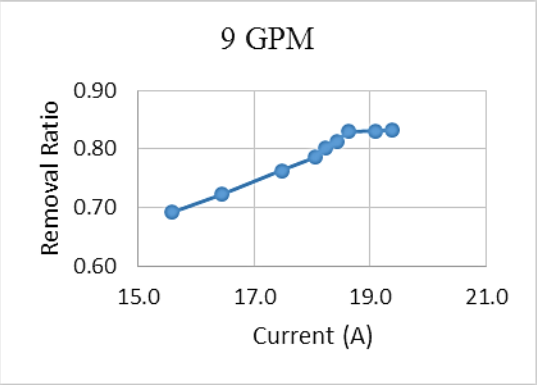
9 GPM
Removal Ratio
0.90
0.80
0.70
0.60
15.0
17.0
19.0
21.0
Current (A)

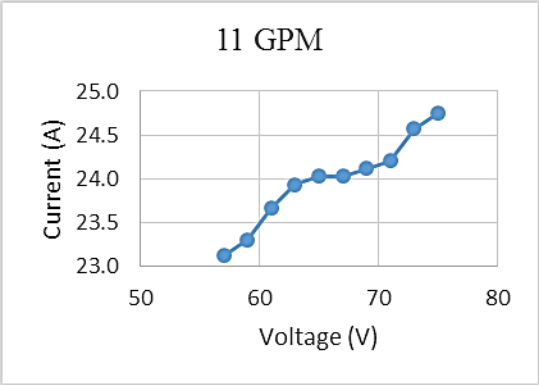
11 GPM
Current (A)
25.0
24.5
24.0
23.5
23.0
50
60
70
80
Voltage (V)

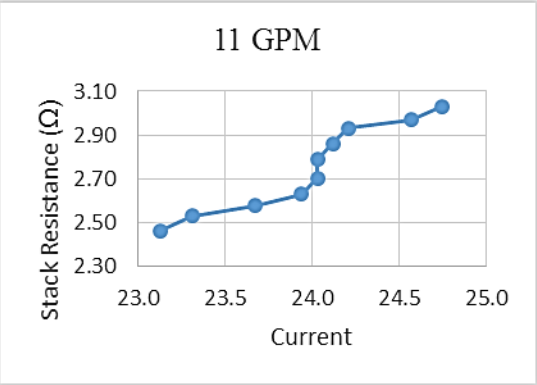
11 GPM
Stack Resistance (Ω)
3.10
2.90
2.70
2.50
2.30
23.0
23.5
24.0
24.5
25.0
Current

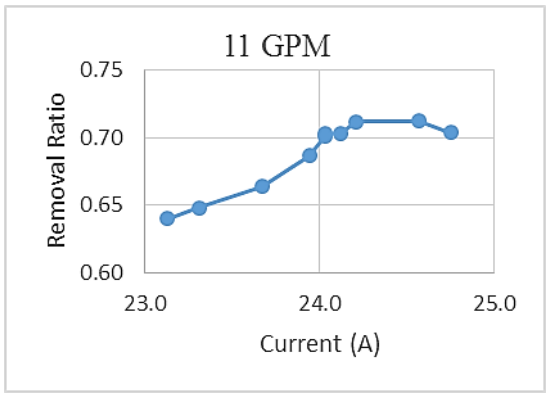

Figure 4.3. Limiting current curves for different feed flow rates – tapered electrode

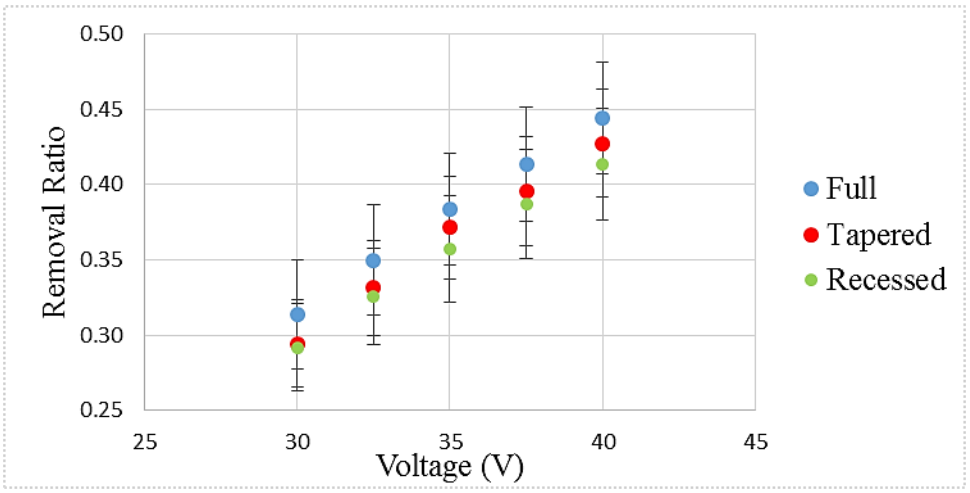

Figure 4.4. Effect of stack voltage on removal ratio

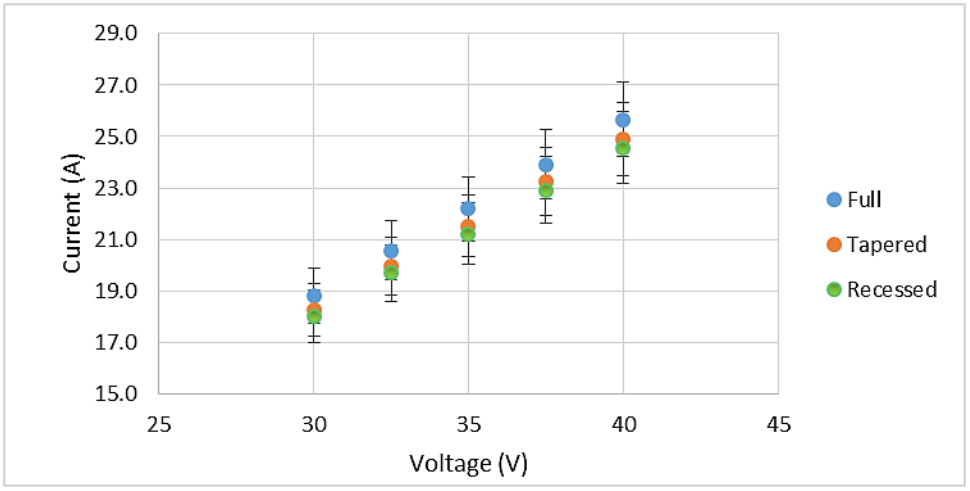

Figure 4.5. Effect of stack voltage on current

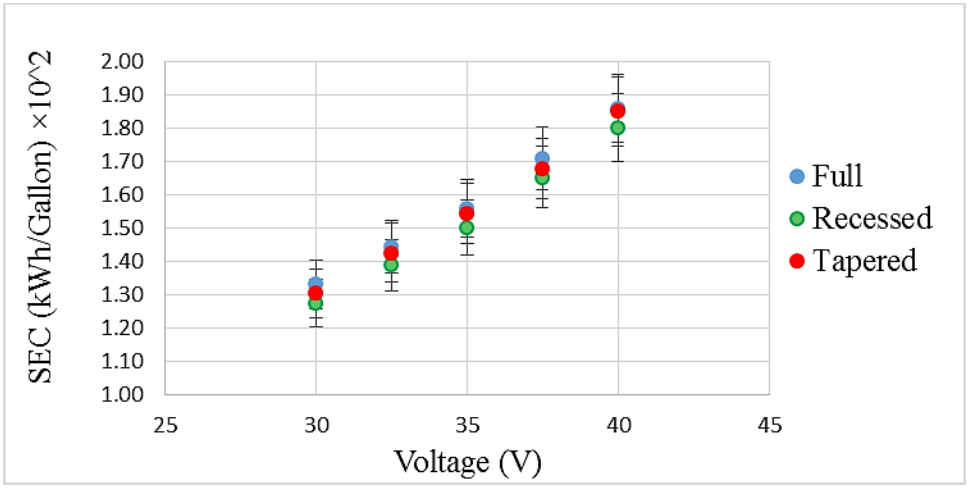

Figure 4.6. Effect of stack voltage on specific energy consumption

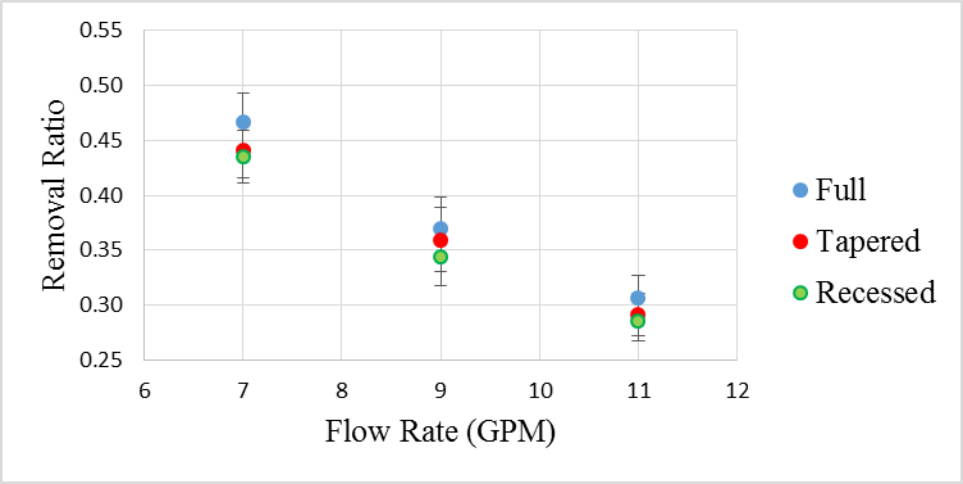

Figure 4.7. Effect of flow rate on removal ratio

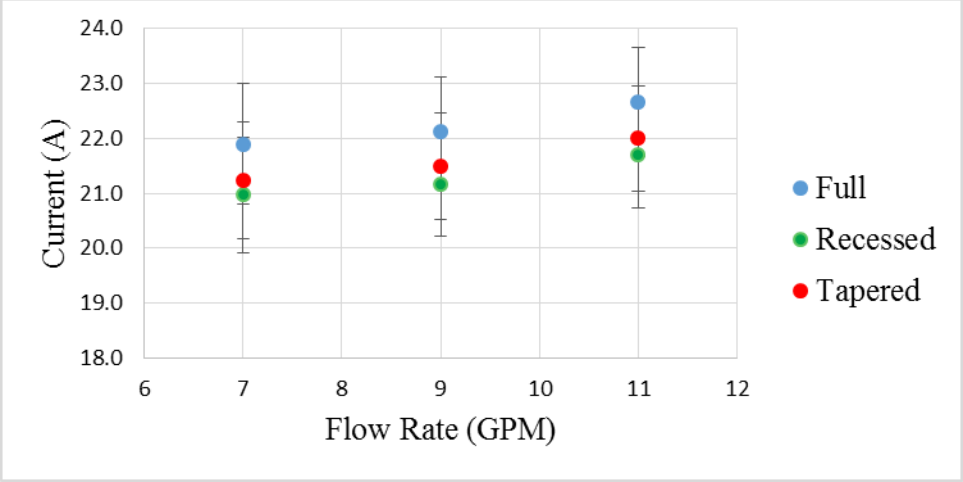

Figure 4.8. Effect of flow rate on current

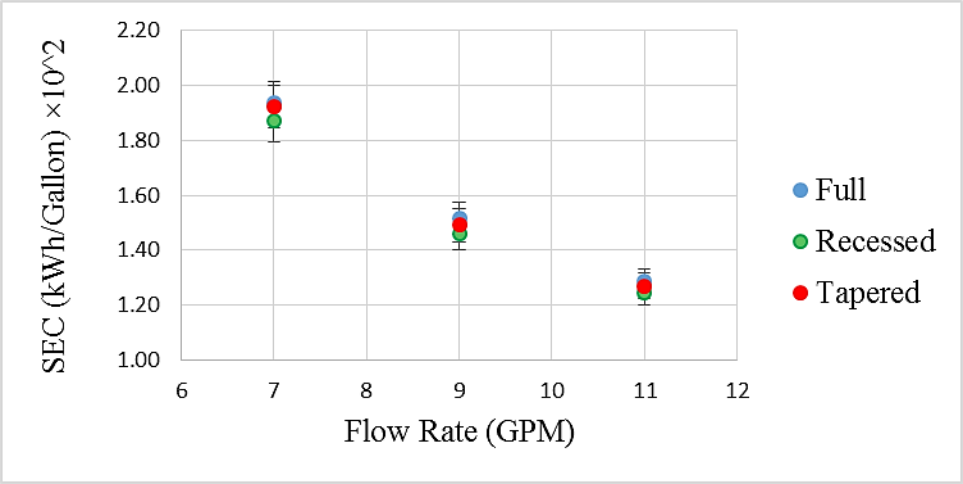

Figure 4.9. Effect of flow rate on specific energy consumption

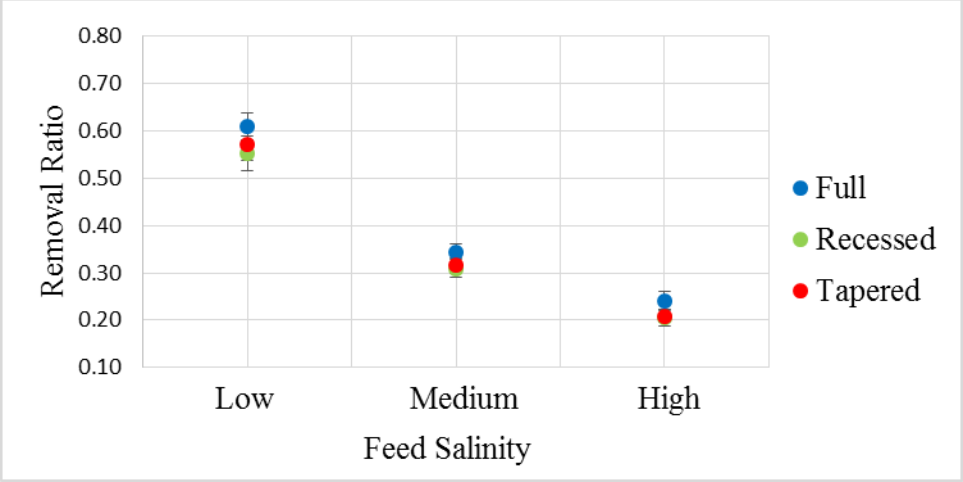

Figure 4.10. Effect of feed salinity on removal ratio

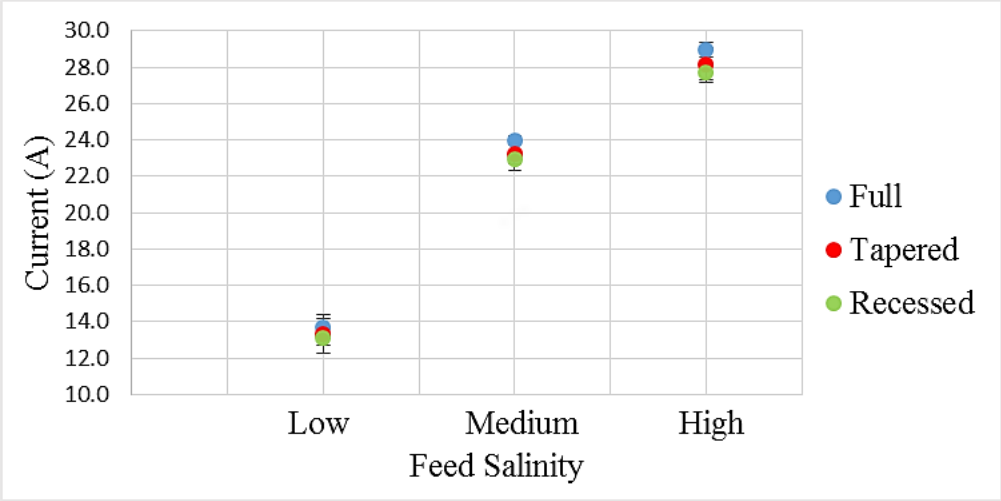

Figure 4.11. Effect of feed salinity on current

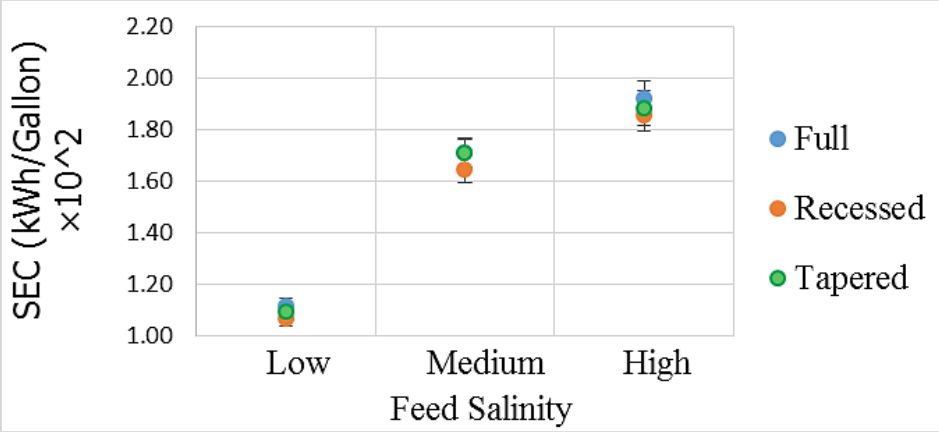

Figure 4.12. Effect of feed salinity on specific energy consumption

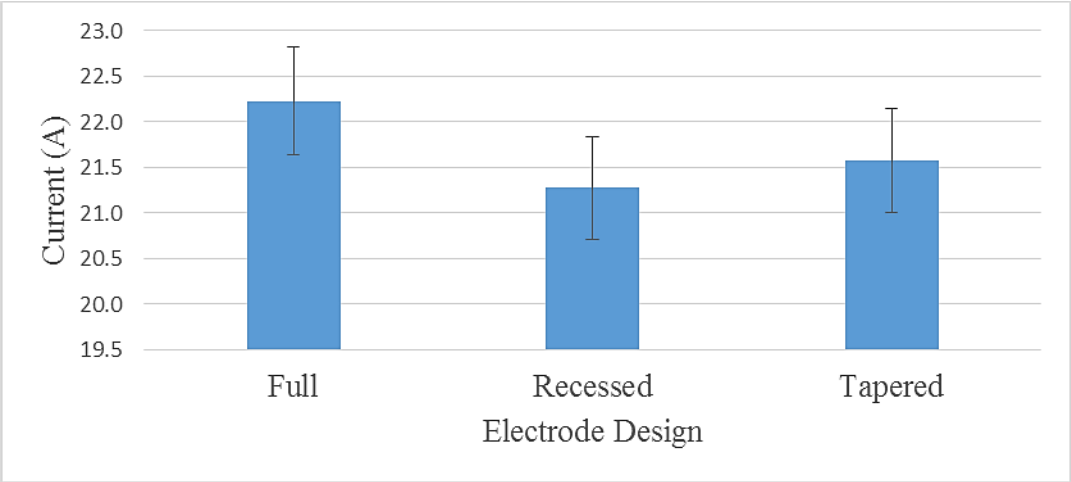

Figure 4.13. Effect of electrode design on current

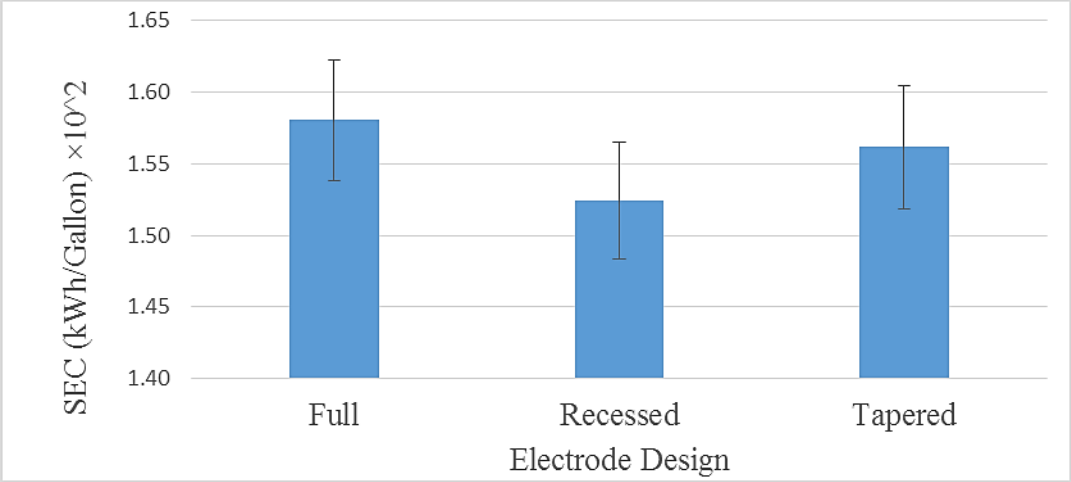

Figure 4.14. Effect of electrode design on specific energy consumption

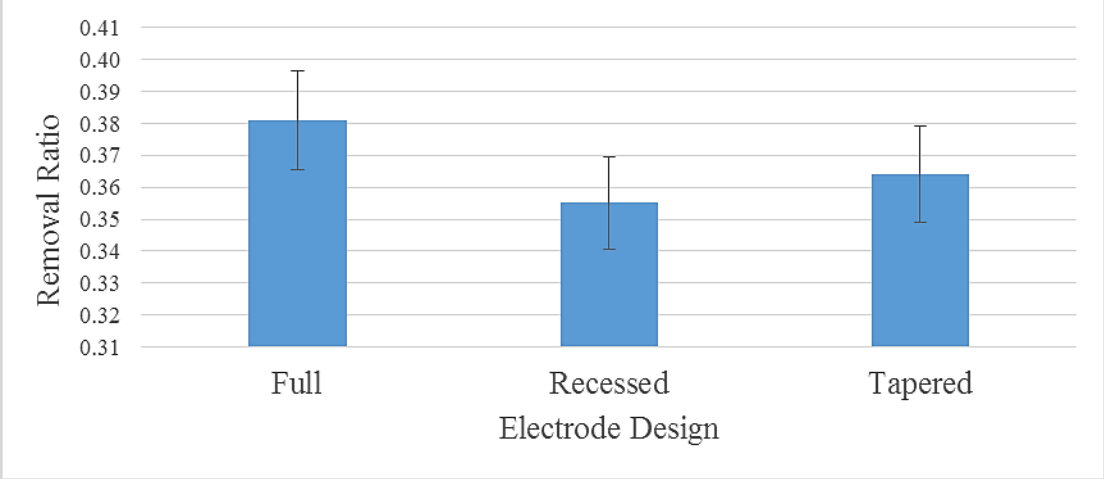

Figure 4.15. Effect of electrode design on removal ratio

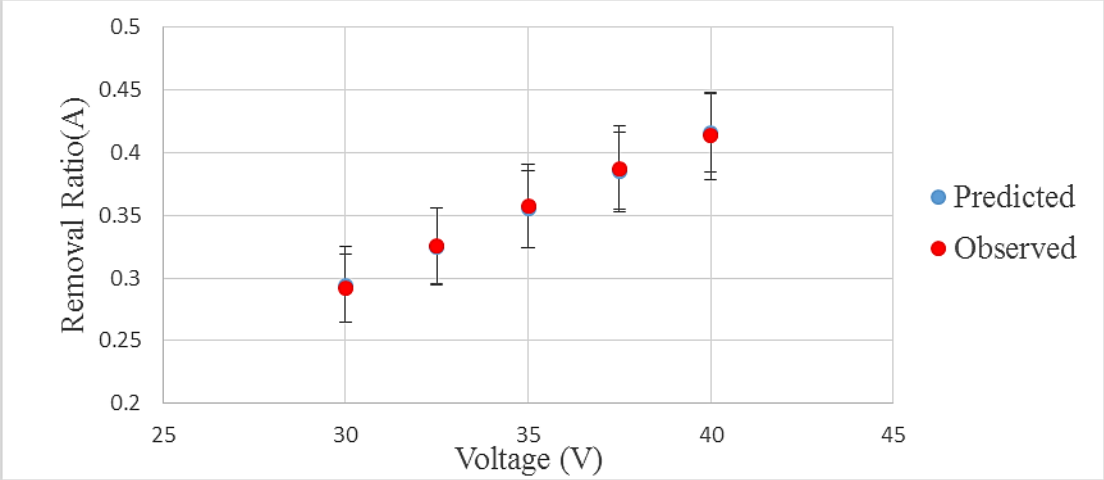

Figure 4.16. Effect of voltage on observed and predicted removal ratio

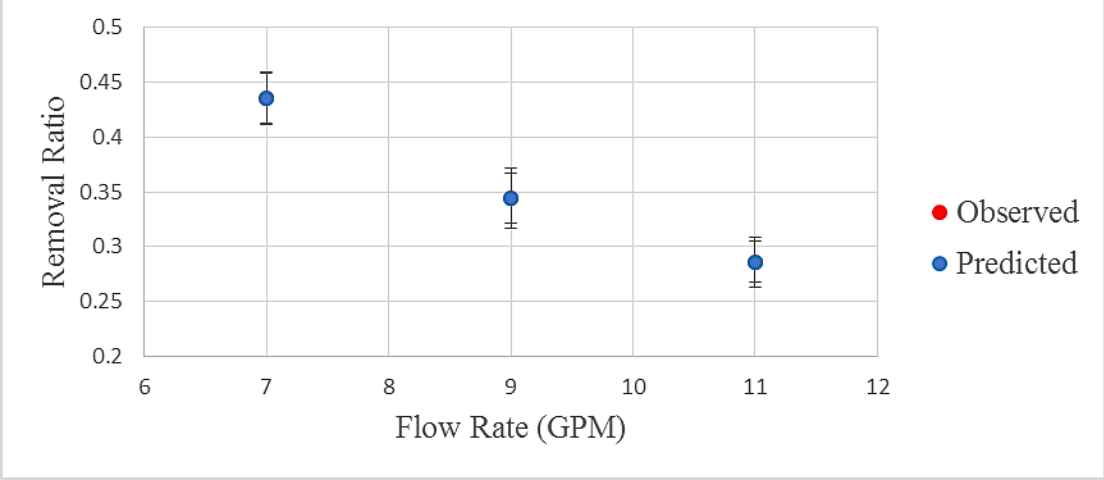

Figure 4.17. Effect of flow rate on observed and predicted removal ratio

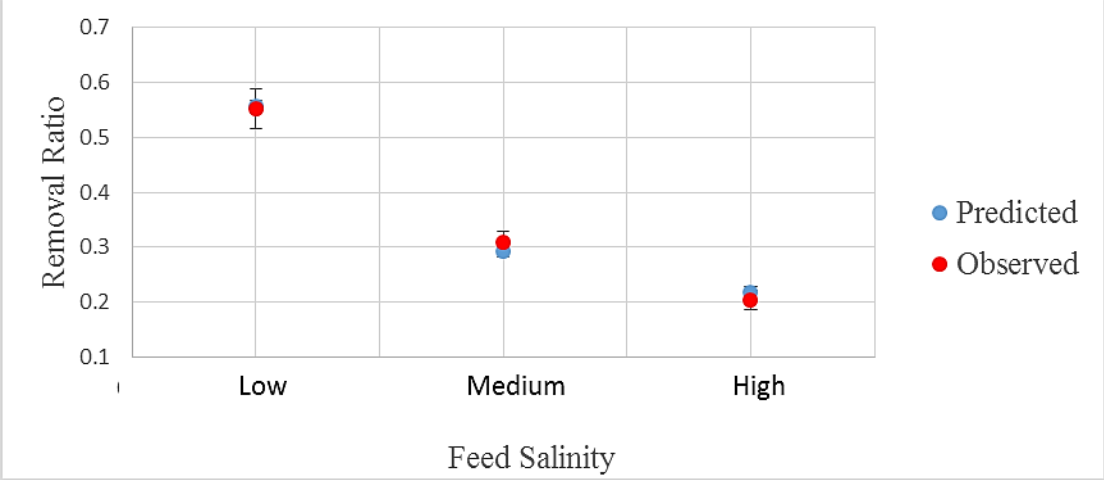

Figure 4.18. Effect of feed salinity on observed and predicted removal ratio

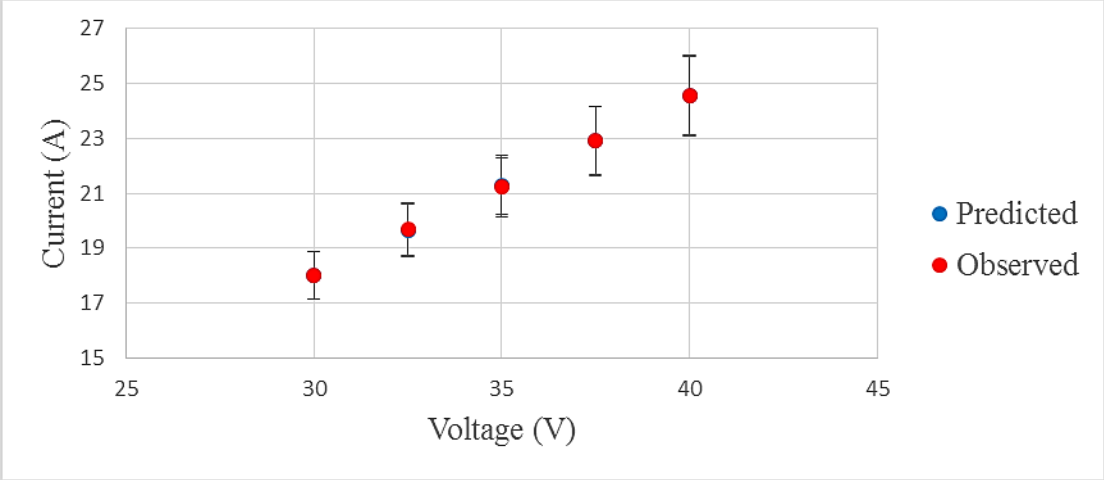

Figure 4.19. Effect of voltage on observed and predicted current

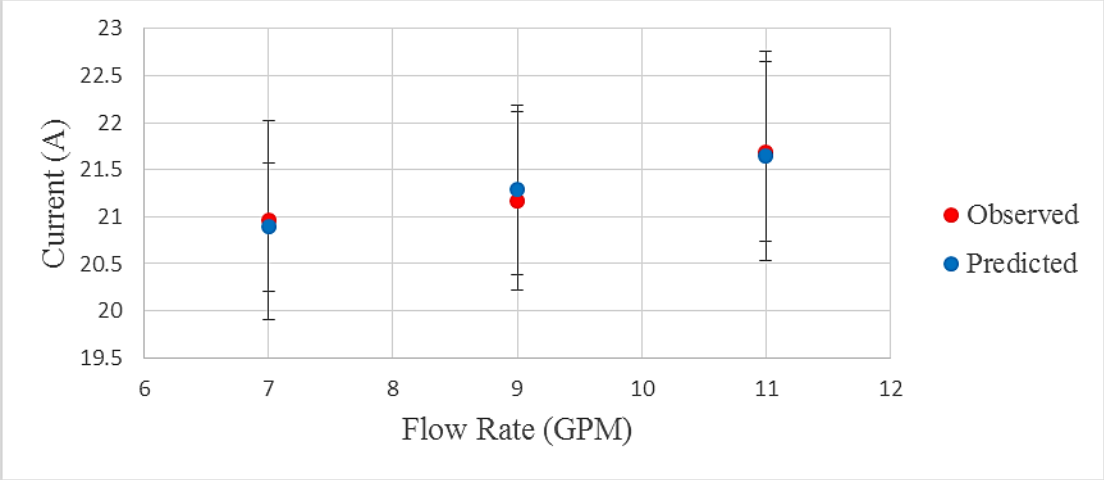

Figure 4.20. Effect of flow rate on observed and predicted current

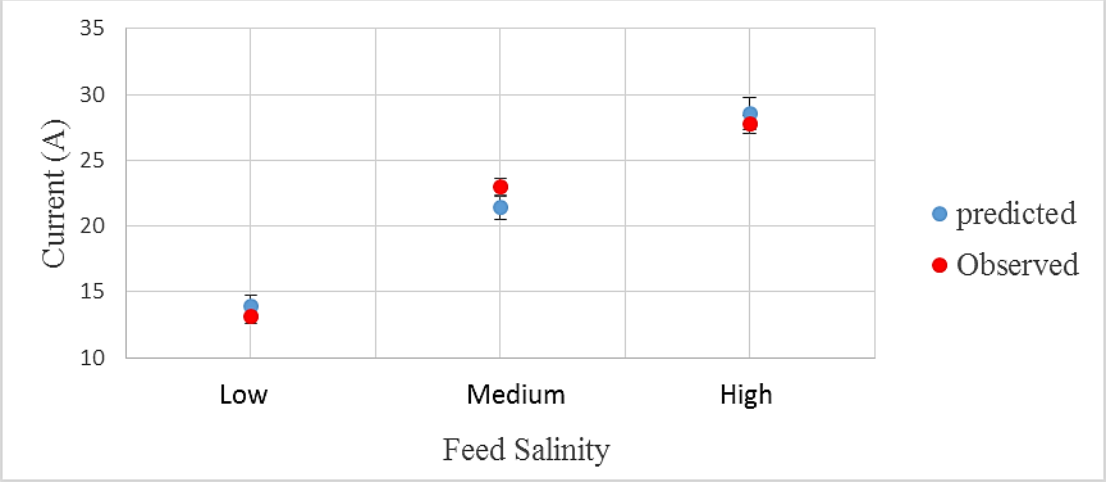

Figure 4.21. Effect of feed salinity on observed and predicted current

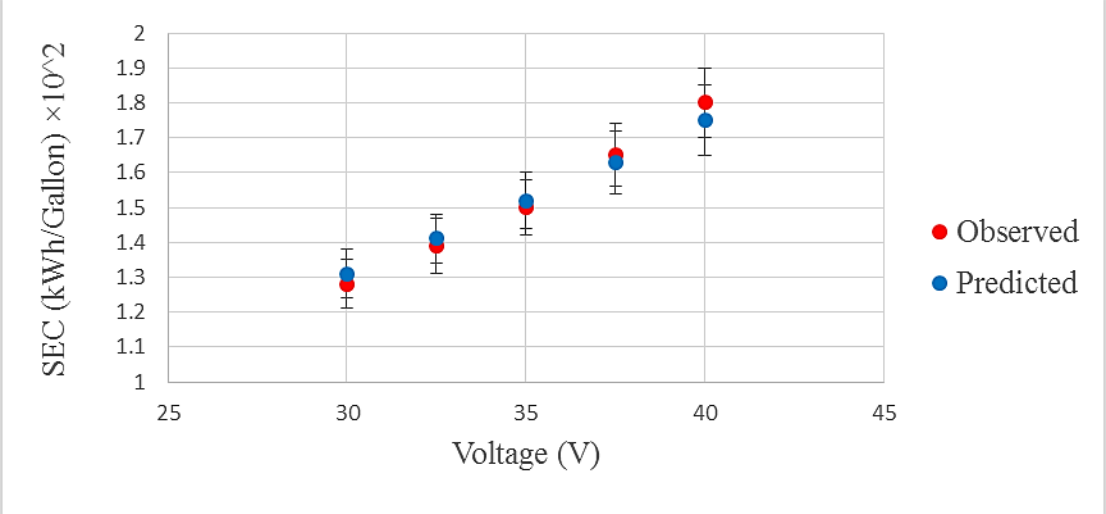

Figure 4.22. Effect of voltage on observed and predicted specific energy consumption

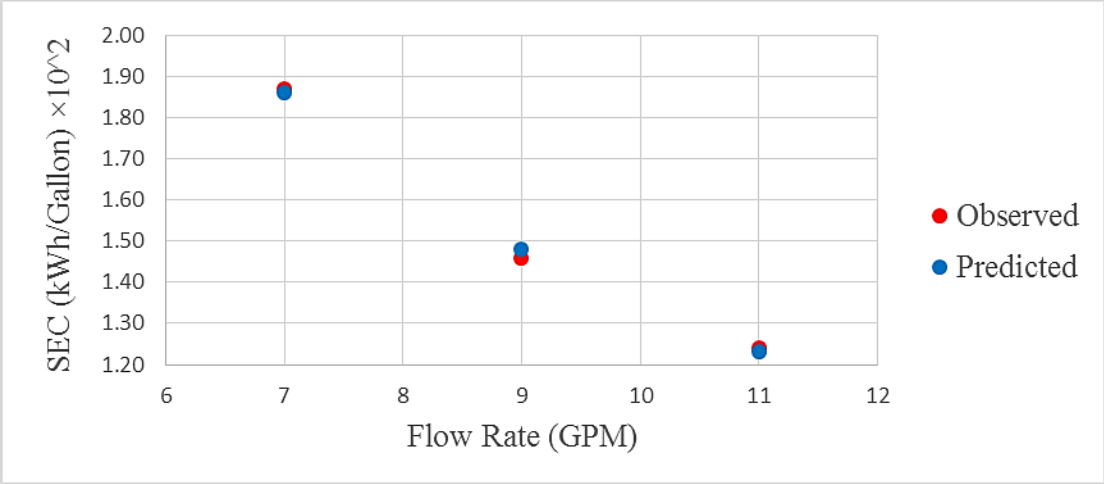

Figure 4.23. Effect of flow rate on observed and predicted specific energy consumption

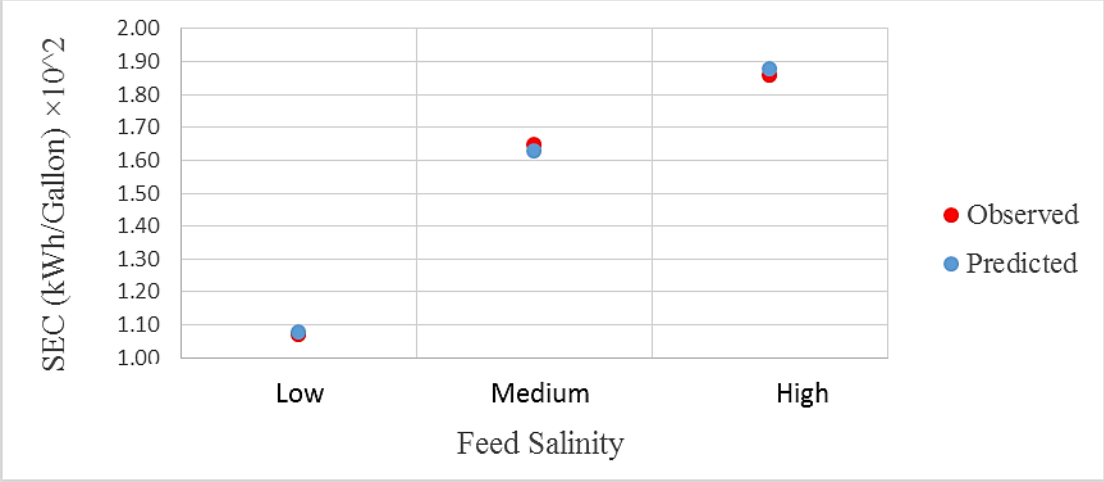

Figure 4.24. Effect of feed salinity on observed and predicted specific energy consumption

Appendices

Data Record

Table-1 data table for response variables

Electrode Type	Well Salinity	Feed Flow Rate (GPM)	Feed Conductivity (ms/cm)	Voltage (V)	Current (A)	Removal Ratio	SEC (kWh/GPM)
Recessed	Low	7	1.811	30.0	10.4	0.52	0.0115
Recessed	Low	7	1.814	32.5	11.2	0.59	0.0121
Recessed	Low	7	1.814	35.0	12.0	0.66	0.0128
Recessed	Low	7	1.813	37.5	12.8	0.69	0.0133
Recessed	Low	7	1.816	40.0	13.6	0.72	0.0137
Recessed	Low	9	1.813	30.0	11.6	0.50	0.0080
Recessed	Low	9	1.813	32.5	12.8	0.54	0.0092
Recessed	Low	9	1.814	35.0	13.4	0.59	0.0103
Recessed	Low	9	1.813	37.5	14.4	0.62	0.0116
Recessed	Low	9	1.814	40.0	15.4	0.64	0.0129
Recessed	Low	11	1.816	30.0	11.6	0.36	0.0082
Recessed	Low	11	1.815	32.5	12.8	0.40	0.0083
Recessed	Low	11	1.815	35.0	13.9	0.43	0.0084
Recessed	Low	11	1.814	37.5	15.1	0.50	0.0095
Recessed	Low	11	1.814	40.0	16.2	0.53	0.0106
Recessed	Low	7	1.809	30.0	10.6	0.54	0.0120
Recessed	Low	7	1.811	32.5	11.3	0.62	0.0125
Recessed	Low	7	1.810	35.0	12.3	0.67	0.0132
Recessed	Low	7	1.807	37.5	13.0	0.71	0.0139
Recessed	Low	7	1.809	40.0	14.0	0.73	0.0141

Recessed	Low	9	1.811	30.0	11.9	0.51	0.0085
Recessed	Low	9	1.810	32.5	12.9	0.57	0.0096
Recessed	Low	9	1.807	35.0	13.6	0.61	0.0108
Recessed	Low	9	1.809	37.5	14.7	0.63	0.0120
Recessed	Low	9	1.806	40.0	15.7	0.67	0.0133
Recessed	Low	11	1.810	30.0	12.0	0.39	0.0086
Recessed	Low	11	1.811	32.5	13.0	0.41	0.0086
Recessed	Low	11	1.807	35.0	14.0	0.44	0.0087
Recessed	Low	11	1.809	37.5	15.4	0.52	0.0100
Recessed	Low	11	1.807	40.0	16.5	0.56	0.0111
Recessed	Low	7	1.811	30.0	10.2	0.50	0.0109
Recessed	Low	7	1.809	32.5	11.1	0.57	0.0117
Recessed	Low	7	1.810	35.0	11.7	0.65	0.0124
Recessed	Low	7	1.808	37.5	12.6	0.66	0.0126
Recessed	Low	7	1.809	40.0	13.2	0.70	0.0133
Recessed	Low	9	1.811	30.0	11.3	0.48	0.0075
Recessed	Low	9	1.808	32.5	12.6	0.52	0.0087
Recessed	Low	9	1.809	35.0	13.2	0.57	0.0098
Recessed	Low	9	1.810	37.5	14.1	0.60	0.0112
Recessed	Low	9	1.809	40.0	15.1	0.61	0.0125
Recessed	Low	11	1.810	30.0	11.2	0.34	0.0078
Recessed	Low	11	1.807	32.5	12.6	0.38	0.0079
Recessed	Low	11	1.807	35.0	13.8	0.41	0.0080
Recessed	Low	11	1.809	37.5	14.8	0.48	0.0091
Recessed	Low	11	1.808	40.0	15.9	0.51	0.0102
Recessed	Medium	7	3.940	30.0	19.3	0.32	0.0168
Recessed	Medium	7	3.930	32.5	21.2	0.36	0.0186
Recessed	Medium	7	3.940	35.0	22.8	0.39	0.0203

Recessed	Medium	7	3.950	37.5	24.6	0.41	0.0221
Recessed	Medium	7	3.940	40.0	26.2	0.45	0.0238
Recessed	Medium	9	3.930	30.0	18.8	0.24	0.0125
Recessed	Medium	9	3.930	32.5	20.8	0.27	0.0141
Recessed	Medium	9	3.930	35.0	22.7	0.30	0.0156
Recessed	Medium	9	3.940	37.5	24.5	0.33	0.0172
Recessed	Medium	9	3.940	40.0	26.4	0.35	0.0188
Recessed	Medium	11	3.940	30.0	19.6	0.20	0.0113
Recessed	Medium	11	3.930	32.5	21.6	0.22	0.0124
Recessed	Medium	11	3.940	35.0	23.5	0.24	0.0134
Recessed	Medium	11	3.950	37.5	25.3	0.27	0.0145
Recessed	Medium	11	3.950	40.0	27.1	0.29	0.0156
Recessed	Medium	7	3.940	30.0	19.7	0.35	0.0174
Recessed	Medium	7	3.930	32.5	21.5	0.38	0.0190
Recessed	Medium	7	3.940	35.0	23.2	0.41	0.0210
Recessed	Medium	7	3.940	37.5	24.9	0.44	0.0227
Recessed	Medium	7	3.940	40.0	26.4	0.47	0.0245
Recessed	Medium	9	3.940	30.0	19.1	0.26	0.0129
Recessed	Medium	9	3.940	32.5	21.0	0.28	0.0146
Recessed	Medium	9	3.940	35.0	23.1	0.31	0.0160
Recessed	Medium	9	3.940	37.5	24.8	0.35	0.0176
Recessed	Medium	9	3.940	40.0	26.7	0.36	0.0192
Recessed	Medium	11	3.940	30.0	19.9	0.21	0.0115
Recessed	Medium	11	3.930	32.5	21.9	0.24	0.0127
Recessed	Medium	11	3.950	35.0	23.9	0.27	0.0137
Recessed	Medium	11	3.950	37.5	25.5	0.29	0.0148
Recessed	Medium	11	3.950	40.0	27.2	0.32	0.0160
Recessed	Medium	7	3.930	30.0	18.9	0.30	0.0163

Recessed	Medium	7	3.930	32.5	20.9	0.33	0.0181
Recessed	Medium	7	3.940	35.0	22.4	0.37	0.0196
Recessed	Medium	7	3.940	37.5	24.3	0.39	0.0215
Recessed	Medium	7	3.940	40.0	26.0	0.43	0.0231
Recessed	Medium	9	3.930	30.0	18.5	0.22	0.0121
Recessed	Medium	9	3.930	32.5	20.6	0.26	0.0136
Recessed	Medium	9	3.930	35.0	22.3	0.28	0.0153
Recessed	Medium	9	3.930	37.5	24.2	0.30	0.0168
Recessed	Medium	9	3.940	40.0	26.1	0.34	0.0183
Recessed	Medium	11	3.940	30.0	19.3	0.19	0.0110
Recessed	Medium	11	3.940	32.5	21.3	0.20	0.0120
Recessed	Medium	11	3.940	35.0	23.1	0.21	0.0132
Recessed	Medium	11	3.940	37.5	25.1	0.24	0.0142
Recessed	Medium	11	3.940	40.0	27.0	0.26	0.0153
Recessed	High	7	5.990	30.0	24.7	0.21	0.0196
Recessed	High	7	5.990	32.5	26.3	0.25	0.0211
Recessed	High	7	5.987	35.0	27.8	0.29	0.0225
Recessed	High	7	5.945	37.5	29.8	0.32	0.0250
Recessed	High	7	5.945	40.0	31.8	0.35	0.0274
Recessed	High	9	5.950	30.0	22.7	0.13	0.0144
Recessed	High	9	5.975	32.5	25.0	0.14	0.0158
Recessed	High	9	6.000	35.0	27.2	0.15	0.0172
Recessed	High	9	6.005	37.5	29.7	0.18	0.0195
Recessed	High	9	6.010	40.0	32.2	0.20	0.0217
Recessed	High	11	5.935	30.0	23.3	0.15	0.0125
Recessed	High	11	5.940	32.5	25.5	0.16	0.0135
Recessed	High	11	5.965	35.0	27.7	0.17	0.0146
Recessed	High	11	5.990	37.5	30.0	0.18	0.0161

Recessed	High	11	5.990	40.0	32.2	0.19	0.0177
Recessed	High	7	5.990	30.0	24.9	0.23	0.0200
Recessed	High	7	5.990	32.5	26.4	0.26	0.0215
Recessed	High	7	5.987	35.0	28.0	0.31	0.0231
Recessed	High	7	5.945	37.5	29.9	0.33	0.0255
Recessed	High	7	5.945	40.0	31.9	0.37	0.0279
Recessed	High	9	5.950	30.0	23.0	0.14	0.0149
Recessed	High	9	5.975	32.5	25.4	0.16	0.0163
Recessed	High	9	6.000	35.0	27.5	0.18	0.0175
Recessed	High	9	6.005	37.5	29.9	0.20	0.0199
Recessed	High	9	6.010	40.0	32.5	0.22	0.0220
Recessed	High	11	5.935	30.0	23.7	0.16	0.0128
Recessed	High	11	5.940	32.5	25.7	0.18	0.0140
Recessed	High	11	5.965	35.0	27.9	0.20	0.0150
Recessed	High	11	5.990	37.5	30.2	0.19	0.0165
Recessed	High	11	5.990	40.0	32.4	0.22	0.0179
Recessed	High	7	5.990	30.0	24.5	0.19	0.0192
Recessed	High	7	5.990	32.5	26.2	0.24	0.0207
Recessed	High	7	5.987	35.0	27.6	0.27	0.0220
Recessed	High	7	5.945	37.5	29.7	0.30	0.0245
Recessed	High	7	5.945	40.0	31.7	0.33	0.0269
Recessed	High	9	5.950	30.0	22.4	0.11	0.0139
Recessed	High	9	5.975	32.5	24.6	0.12	0.0153
Recessed	High	9	6.000	35.0	26.9	0.13	0.0169
Recessed	High	9	6.005	37.5	29.5	0.15	0.0190
Recessed	High	9	6.010	40.0	31.9	0.17	0.0214
Recessed	High	11	5.935	30.0	22.9	0.13	0.0122
Recessed	High	11	5.940	32.5	25.3	0.14	0.0131

Recessed	High	11	5.965	35.0	27.5	0.14	0.0142
Recessed	High	11	5.990	37.5	29.8	0.17	0.0157
Recessed	High	11	5.990	40.0	32.0	0.17	0.0174
Full	Low	7	1.76	30.0	10.9	0.56	0.0116
Full	Low	7	1.76	32.5	11.7	0.64	0.0123
Full	Low	7	1.765	35.0	12.5	0.71	0.0135
Full	Low	7	1.765	37.5	13.4	0.74	0.0139
Full	Low	7	1.765	40.0	14.1	0.77	0.0145
Full	Low	9	1.763	30.0	12.1	0.54	0.0086
Full	Low	9	1.763	32.5	13.4	0.58	0.0095
Full	Low	9	1.763	35.0	14.0	0.64	0.0109
Full	Low	9	1.763	37.5	15.1	0.67	0.0120
Full	Low	9	1.763	40.0	16.0	0.69	0.0133
Full	Low	11	1.77	30.0	12.1	0.39	0.0085
Full	Low	11	1.768	32.5	13.4	0.43	0.0086
Full	Low	11	1.76	35.0	14.5	0.46	0.0089
Full	Low	11	1.758	37.5	15.7	0.54	0.0100
Full	Low	11	1.759	40.0	17.0	0.57	0.0111
Full	Low	7	1.751	30.0	11.1	0.58	0.0126
Full	Low	7	1.752	32.5	11.8	0.67	0.0131
Full	Low	7	1.751	35.0	12.8	0.72	0.0135
Full	Low	7	1.753	37.5	13.6	0.76	0.0148
Full	Low	7	1.751	40.0	14.7	0.79	0.0150
Full	Low	9	1.756	30.0	12.4	0.55	0.0091
Full	Low	9	1.751	32.5	13.5	0.61	0.0103
Full	Low	9	1.754	35.0	14.2	0.65	0.0112
Full	Low	9	1.751	37.5	15.3	0.68	0.0130

Full	Low	9	1.752	40.0	16.5	0.72	0.0139
Full	Low	11	1.756	30.0	12.6	0.42	0.0093
Full	Low	11	1.758	32.5	13.6	0.44	0.0090
Full	Low	11	1.757	35.0	14.6	0.47	0.0088
Full	Low	11	1.752	37.5	16.1	0.56	0.0108
Full	Low	11	1.758	40.0	17.3	0.60	0.0120
Full	Low	7	1.768	30.0	10.6	0.54	0.0117
Full	Low	7	1.762	32.5	11.6	0.61	0.0123
Full	Low	7	1.763	35.0	12.2	0.70	0.0130
Full	Low	7	1.763	37.5	13.2	0.71	0.0136
Full	Low	7	1.762	40.0	13.8	0.75	0.0139
Full	Low	9	1.762	30.0	11.8	0.52	0.0077
Full	Low	9	1.765	32.5	13.2	0.56	0.0092
Full	Low	9	1.763	35.0	13.8	0.61	0.0101
Full	Low	9	1.762	37.5	14.7	0.64	0.0112
Full	Low	9	1.762	40.0	15.7	0.66	0.0129
Full	Low	11	1.765	30.0	11.6	0.37	0.0082
Full	Low	11	1.764	32.5	13.2	0.41	0.0083
Full	Low	11	1.762	35.0	14.4	0.44	0.0083
Full	Low	11	1.762	37.5	15.5	0.52	0.0096
Full	Low	11	1.763	40.0	16.7	0.55	0.0109
Full	Medium	7	3.710	30.0	20.3	0.35	0.0175
Full	Medium	7	3.700	32.5	22.2	0.39	0.0192
Full	Medium	7	3.700	35.0	23.8	0.42	0.0208
Full	Medium	7	3.700	37.5	25.8	0.44	0.0236
Full	Medium	7	3.700	40.0	27.4	0.48	0.0254
Full	Medium	9	3.710	30.0	19.7	0.26	0.0129
Full	Medium	9	3.700	32.5	21.7	0.29	0.0146

Full	Medium	9	3.700	35.0	23.7	0.32	0.0158
Full	Medium	9	3.700	37.5	25.6	0.35	0.0184
Full	Medium	9	3.700	40.0	27.6	0.38	0.0194
Full	Medium	11	3.710	30.0	20.6	0.22	0.0119
Full	Medium	11	3.700	32.5	22.5	0.24	0.0127
Full	Medium	11	3.700	35.0	24.7	0.26	0.0140
Full	Medium	11	3.700	37.5	26.4	0.29	0.0155
Full	Medium	11	3.700	40.0	28.3	0.31	0.0159
Full	Medium	7	3.710	30.0	20.7	0.38	0.0182
Full	Medium	7	3.700	32.5	22.6	0.41	0.0196
Full	Medium	7	3.710	35.0	24.2	0.44	0.0213
Full	Medium	7	3.700	37.5	26.0	0.47	0.0236
Full	Medium	7	3.710	40.0	27.5	0.51	0.0246
Full	Medium	9	3.700	30.0	19.9	0.28	0.0136
Full	Medium	9	3.710	32.5	21.9	0.30	0.0154
Full	Medium	9	3.710	35.0	24.2	0.33	0.0166
Full	Medium	9	3.710	37.5	26.0	0.38	0.0190
Full	Medium	9	3.710	40.0	28.0	0.39	0.0198
Full	Medium	11	3.710	30.0	20.8	0.23	0.0118
Full	Medium	11	3.700	32.5	22.9	0.26	0.0127
Full	Medium	11	3.700	35.0	24.9	0.29	0.0147
Full	Medium	11	3.700	37.5	26.7	0.31	0.0152
Full	Medium	11	3.700	40.0	28.4	0.35	0.0163
Full	Medium	7	3.710	30.0	19.7	0.32	0.0171
Full	Medium	7	3.710	32.5	21.8	0.36	0.0186
Full	Medium	7	3.710	35.0	23.3	0.40	0.0206
Full	Medium	7	3.700	37.5	25.5	0.42	0.0223
Full	Medium	7	3.700	40.0	27.1	0.46	0.0246

Full	Medium	9	3.700	30.0	19.3	0.24	0.0130
Full	Medium	9	3.710	32.5	21.5	0.28	0.0141
Full	Medium	9	3.710	35.0	23.3	0.30	0.0159
Full	Medium	9	3.710	37.5	25.4	0.32	0.0181
Full	Medium	9	3.710	40.0	27.4	0.37	0.0197
Full	Medium	11	3.700	30.0	20.3	0.20	0.0118
Full	Medium	11	3.700	32.5	22.2	0.21	0.0129
Full	Medium	11	3.700	35.0	24.1	0.23	0.0135
Full	Medium	11	3.710	37.5	26.1	0.26	0.0150
Full	Medium	11	3.700	40.0	28.2	0.28	0.0158
Full	High	7	6.060	30.0	25.9	0.23	0.0197
Full	High	7	6.070	32.5	27.5	0.27	0.0221
Full	High	7	6.090	35.0	29.0	0.31	0.0233
Full	High	7	6.020	37.5	31.0	0.34	0.0266
Full	High	7	6.060	40.0	33.2	0.37	0.0276
Full	High	9	6.110	30.0	23.8	0.14	0.0152
Full	High	9	6.100	32.5	26.2	0.15	0.0162
Full	High	9	6.090	35.0	28.4	0.16	0.0185
Full	High	9	6.110	37.5	31.1	0.19	0.0202
Full	High	9	6.110	40.0	33.8	0.21	0.0225
Full	High	11	6.100	30.0	24.3	0.16	0.0129
Full	High	11	6.100	32.5	26.6	0.17	0.0135
Full	High	11	6.100	35.0	29.0	0.18	0.0152
Full	High	11	6.100	37.5	31.4	0.19	0.0168
Full	High	11	6.100	40.0	33.5	0.20	0.0189
Full	High	7	6.060	30.0	26.0	0.25	0.0208
Full	High	7	6.070	32.5	27.7	0.28	0.0221
Full	High	7	6.090	35.0	29.3	0.33	0.0235

Full	High	7	6.020	37.5	31.3	0.36	0.0274
Full	High	7	6.060	40.0	33.2	0.40	0.0295
Full	High	9	6.110	30.0	24.1	0.15	0.0161
Full	High	9	6.100	32.5	26.5	0.17	0.0164
Full	High	9	6.090	35.0	28.7	0.19	0.0189
Full	High	9	6.110	37.5	31.3	0.21	0.0212
Full	High	9	6.060	40.0	34.0	0.24	0.0229
Full	High	11	6.100	30.0	24.8	0.17	0.0129
Full	High	11	6.100	32.5	26.9	0.19	0.0148
Full	High	11	6.060	35.0	29.1	0.21	0.0157
Full	High	11	6.100	37.5	31.7	0.20	0.0170
Full	High	11	6.090	40.0	33.7	0.24	0.0180
Full	High	7	6.060	30.0	25.6	0.20	0.0206
Full	High	7	6.070	32.5	27.4	0.26	0.0221
Full	High	7	6.090	35.0	28.9	0.29	0.0222
Full	High	7	6.020	37.5	31.0	0.32	0.0255
Full	High	7	6.060	40.0	33.1	0.36	0.0280
Full	High	9	6.110	30.0	23.5	0.12	0.0144
Full	High	9	6.100	32.5	25.7	0.13	0.0156
Full	High	9	6.090	35.0	28.2	0.14	0.0177
Full	High	9	6.110	37.5	30.8	0.16	0.0203
Full	High	9	6.090	40.0	33.3	0.18	0.0225
Full	High	11	6.100	30.0	24.0	0.14	0.0126
Full	High	11	6.100	32.5	26.3	0.15	0.0134
Full	High	11	6.090	35.0	28.7	0.15	0.0151
Full	High	11	6.100	37.5	31.2	0.18	0.0167
Full	High	11	6.100	40.0	33.4	0.18	0.0179

Tapered	Low	7	1.685	30.0	10.5	0.47	0.0129
Tapered	Low	7	1.650	32.5	11.4	0.60	0.0137
Tapered	Low	7	1.648	35.0	12.1	0.72	0.0141
Tapered	Low	7	1.647	37.5	13.0	0.78	0.0139
Tapered	Low	7	1.644	40.0	13.8	0.76	0.0152
Tapered	Low	9	1.654	30.0	11.7	0.47	0.0084
Tapered	Low	9	1.648	32.5	13.2	0.59	0.0105
Tapered	Low	9	1.647	35.0	13.7	0.58	0.0104
Tapered	Low	9	1.648	37.5	14.8	0.71	0.0116
Tapered	Low	9	1.648	40.0	15.6	0.58	0.0138
Tapered	Low	11	1.647	30.0	11.7	0.38	0.0089
Tapered	Low	11	1.644	32.5	13.1	0.41	0.0090
Tapered	Low	11	1.654	35.0	14.2	0.47	0.0090
Tapered	Low	11	1.648	37.5	15.4	0.52	0.0091
Tapered	Low	11	1.647	40.0	16.4	0.55	0.0110
Tapered	Low	7	1.645	30.0	10.7	0.50	0.0111
Tapered	Low	7	1.644	32.5	11.5	0.59	0.0123
Tapered	Low	7	1.645	35.0	12.3	0.65	0.0145
Tapered	Low	7	1.645	37.5	13.3	0.74	0.0144
Tapered	Low	7	1.646	40.0	14.1	0.83	0.0127
Tapered	Low	9	1.640	30.0	12.1	0.46	0.0094
Tapered	Low	9	1.611	32.5	13.0	0.52	0.0102
Tapered	Low	9	1.636	35.0	13.8	0.65	0.0104
Tapered	Low	9	1.617	37.5	15.0	0.66	0.0113
Tapered	Low	9	1.624	40.0	16.0	0.75	0.0151
Tapered	Low	11	1.647	30.0	12.3	0.39	0.0099
Tapered	Low	11	1.644	32.5	13.0	0.44	0.0086
Tapered	Low	11	1.654	35.0	14.4	0.46	0.0082

Tapered	Low	11	1.648	37.5	15.8	0.51	0.0104
Tapered	Low	11	1.647	40.0	17.0	0.61	0.0100
Tapered	Low	7	1.650	30.0	10.4	0.45	0.0107
Tapered	Low	7	1.645	32.5	11.3	0.52	0.0130
Tapered	Low	7	1.647	35.0	11.7	0.66	0.0121
Tapered	Low	7	1.646	37.5	12.8	0.65	0.0129
Tapered	Low	7	1.646	40.0	13.4	0.77	0.0123
Tapered	Low	9	1.601	30.0	11.5	0.53	0.0079
Tapered	Low	9	1.609	32.5	12.7	0.52	0.0093
Tapered	Low	9	1.644	35.0	13.6	0.64	0.0111
Tapered	Low	9	1.641	37.5	14.5	0.66	0.0112
Tapered	Low	9	1.620	40.0	15.3	0.57	0.0143
Tapered	Low	11	1.647	30.0	11.5	0.31	0.0073
Tapered	Low	11	1.644	32.5	13.0	0.36	0.0083
Tapered	Low	11	1.654	35.0	14.2	0.40	0.0072
Tapered	Low	11	1.648	37.5	15.0	0.54	0.0099
Tapered	Low	11	1.647	40.0	16.1	0.48	0.0115
Tapered	Medium	7	3.710	30.0	19.6	0.33	0.0170
Tapered	Medium	7	3.680	32.5	21.6	0.40	0.0206
Tapered	Medium	7	3.670	35.0	23.5	0.38	0.0222
Tapered	Medium	7	3.680	37.5	25.1	0.40	0.0199
Tapered	Medium	7	3.680	40.0	27.0	0.48	0.0223
Tapered	Medium	9	3.700	30.0	19.3	0.26	0.0144
Tapered	Medium	9	3.680	32.5	21.2	0.29	0.0150
Tapered	Medium	9	3.680	35.0	23.0	0.31	0.0163
Tapered	Medium	9	3.680	37.5	24.8	0.31	0.0155
Tapered	Medium	9	3.670	40.0	26.8	0.35	0.0215
Tapered	Medium	11	3.680	30.0	19.6	0.23	0.0107

Tapered	Medium	11	3.680	32.5	21.9	0.22	0.0135
Tapered	Medium	11	3.680	35.0	23.6	0.25	0.0129
Tapered	Medium	11	3.680	37.5	25.3	0.29	0.0137
Tapered	Medium	11	3.680	40.0	27.5	0.32	0.0142
Tapered	Medium	7	3.710	30.0	20.0	0.34	0.0181
Tapered	Medium	7	3.680	32.5	21.9	0.37	0.0185
Tapered	Medium	7	3.700	35.0	23.5	0.46	0.0216
Tapered	Medium	7	3.680	37.5	24.9	0.44	0.0216
Tapered	Medium	7	3.680	40.0	26.5	0.44	0.0221
Tapered	Medium	9	3.700	30.0	19.3	0.26	0.0133
Tapered	Medium	9	3.700	32.5	21.5	0.27	0.0143
Tapered	Medium	9	3.710	35.0	23.6	0.30	0.0150
Tapered	Medium	9	3.680	37.5	25.0	0.38	0.0188
Tapered	Medium	9	3.680	40.0	27.4	0.38	0.0175
Tapered	Medium	11	3.680	30.0	20.4	0.24	0.0123
Tapered	Medium	11	3.680	32.5	22.5	0.25	0.0140
Tapered	Medium	11	3.670	35.0	23.9	0.25	0.0145
Tapered	Medium	11	3.680	37.5	26.1	0.27	0.0157
Tapered	Medium	11	3.680	40.0	27.6	0.35	0.0174
Tapered	Medium	7	3.670	30.0	19.4	0.32	0.0168
Tapered	Medium	7	3.680	32.5	21.2	0.31	0.0192
Tapered	Medium	7	3.670	35.0	22.6	0.37	0.0218
Tapered	Medium	7	3.680	37.5	24.3	0.43	0.0209
Tapered	Medium	7	3.680	40.0	26.1	0.47	0.0216
Tapered	Medium	9	3.680	30.0	19.0	0.20	0.0124
Tapered	Medium	9	3.680	32.5	21.0	0.29	0.0126
Tapered	Medium	9	3.670	35.0	22.4	0.25	0.0161
Tapered	Medium	9	3.680	37.5	24.9	0.28	0.0159

Tapered	Medium	9	3.670	40.0	26.2	0.33	0.0210
Tapered	Medium	11	3.680	30.0	19.7	0.20	0.0122
Tapered	Medium	11	3.680	32.5	21.9	0.19	0.0136
Tapered	Medium	11	3.670	35.0	23.7	0.22	0.0120
Tapered	Medium	11	3.680	37.5	25.8	0.27	0.0129
Tapered	Medium	11	3.680	40.0	27.2	0.28	0.0173
Tapered	High	7	6.020	30.0	25.0	0.24	0.0199
Tapered	High	7	6.020	32.5	26.6	0.25	0.0220
Tapered	High	7	6.000	35.0	28.5	0.29	0.0228
Tapered	High	7	6.000	37.5	30.2	0.35	0.0256
Tapered	High	7	6.020	40.0	32.4	0.33	0.0279
Tapered	High	9	6.030	30.0	23.3	0.12	0.0132
Tapered	High	9	6.030	32.5	25.1	0.16	0.0166
Tapered	High	9	6.030	35.0	27.8	0.16	0.0193
Tapered	High	9	6.030	37.5	29.9	0.18	0.0183
Tapered	High	9	6.030	40.0	33.1	0.21	0.0207
Tapered	High	11	6.040	30.0	23.7	0.15	0.0121
Tapered	High	11	6.040	32.5	26.2	0.18	0.0147
Tapered	High	11	6.040	35.0	28.0	0.16	0.0160
Tapered	High	11	6.030	37.5	30.0	0.20	0.0182
Tapered	High	11	6.030	40.0	32.4	0.19	0.0180
Tapered	High	7	6.030	30.0	25.5	0.25	0.0198
Tapered	High	7	6.020	32.5	26.8	0.27	0.0214
Tapered	High	7	6.010	35.0	28.8	0.33	0.0240
Tapered	High	7	6.010	37.5	30.0	0.34	0.0290
Tapered	High	7	6.010	40.0	32.4	0.39	0.0310
Tapered	High	9	6.020	30.0	23.5	0.13	0.0160
Tapered	High	9	6.000	32.5	26.1	0.18	0.0177

Tapered	High	9	6.030	35.0	27.9	0.17	0.0172
Tapered	High	9	6.010	37.5	30.2	0.23	0.0206
Tapered	High	9	6.020	40.0	32.6	0.21	0.0239
Tapered	High	11	6.000	30.0	24.0	0.15	0.0131
Tapered	High	11	6.020	32.5	25.9	0.21	0.0130
Tapered	High	11	6.030	35.0	28.2	0.23	0.0160
Tapered	High	11	6.010	37.5	30.5	0.20	0.0152
Tapered	High	11	6.010	40.0	33.3	0.24	0.0184
Tapered	High	7	6.010	30.0	25.0	0.20	0.0189
Tapered	High	7	6.010	32.5	26.5	0.25	0.0202
Tapered	High	7	6.020	35.0	28.1	0.27	0.0217
Tapered	High	7	6.010	37.5	30.0	0.34	0.0226
Tapered	High	7	6.020	40.0	32.6	0.38	0.0294
Tapered	High	9	6.010	30.0	22.6	0.11	0.0126
Tapered	High	9	6.030	32.5	25.0	0.12	0.0160
Tapered	High	9	6.040	35.0	27.6	0.15	0.0157
Tapered	High	9	6.020	37.5	29.5	0.14	0.0218
Tapered	High	9	6.010	40.0	32.2	0.17	0.0246
Tapered	High	11	6.020	30.0	22.9	0.14	0.0140
Tapered	High	11	6.030	32.5	25.6	0.13	0.0124
Tapered	High	11	6.010	35.0	28.0	0.14	0.0152
Tapered	High	11	6.030	37.5	30.1	0.18	0.0179
Tapered	High	11	6.020	40.0	32.0	0.16	0.0163

Table-2 Data table for limiting current (A)

Electrode Type	Flow Rate (GPM)	Voltage (V)	Current (A)	Removal Ratio	Stack Resistance (Ω)
Full	7	40.0	14.8	0.75	2.70
Full	7	42.0	15.1	0.79	2.78
Full	7	44.0	15.4	0.86	2.86
Full	7	46.0	15.6	0.91	2.95
Full	7	48.0	15.7	0.92	3.06
Full	7	50.0	15.7	0.92	3.18
Full	7	52.0	15.7	0.91	3.31
Full	7	54.0	15.8	0.90	3.42
Full	7	56.0	15.9	0.90	3.52
Full	7	58.0	16.1	0.90	3.60
Full	7	60.0	16.3	0.90	3.68
Full	9	40.0	16.4	0.59	2.44
Full	9	42.0	17.3	0.59	2.43
Full	9	44.0	18.4	0.58	2.39
Full	9	46.0	19.0	0.59	2.42
Full	9	48.0	19.2	0.60	2.50
Full	9	50.0	19.4	0.61	2.58
Full	9	52.0	19.6	0.62	2.65
Full	9	54.0	20.1	0.63	2.69
Full	9	56.0	20.4	0.64	2.75
Full	11	57.0	25.7	0.80	4.97
Full	11	59.0	25.9	0.81	4.97
Full	11	61.0	26.3	0.83	4.98
Full	11	63.0	26.6	0.86	4.98
Full	11	65.0	26.7	0.88	4.98
Full	11	67.0	26.7	0.88	6.08
Full	11	69.0	26.8	0.88	6.07
Full	11	71.0	26.9	0.89	6.09
Full	11	73.0	27.3	0.89	6.08
Full	11	75.0	27.5	0.88	6.09
Tapered	7	40.0	14.1	0.68	2.84
Tapered	7	42.0	14.3	0.71	2.93
Tapered	7	44.0	14.6	0.77	3.01
Tapered	7	46.0	14.8	0.82	3.10
Tapered	7	48.0	14.9	0.83	3.22
Tapered	7	50.0	14.9	0.83	3.35
Tapered	7	52.0	14.9	0.82	3.49
Tapered	7	54.0	15.0	0.81	3.60
Tapered	7	56.0	15.1	0.81	3.71

Tapered	7	58.0	15.3	0.81	3.79
Tapered	7	60.0	15.5	0.81	3.87
Tapered	9	40.0	15.6	0.69	2.57
Tapered	9	42.0	16.4	0.72	2.56
Tapered	9	44.0	17.5	0.76	2.52
Tapered	9	46.0	18.1	0.79	2.55
Tapered	9	48.0	18.2	0.80	2.63
Tapered	9	50.0	18.4	0.81	2.71
Tapered	9	52.0	18.6	0.83	2.79
Tapered	9	54.0	19.1	0.83	2.83
Tapered	9	56.0	19.4	0.83	2.89
Tapered	11	57.0	23.1	0.64	2.46
Tapered	11	59.0	23.3	0.65	2.53
Tapered	11	61.0	23.7	0.66	2.58
Tapered	11	63.0	23.9	0.69	2.63
Tapered	11	65.0	24.0	0.70	2.70
Tapered	11	67.0	24.0	0.70	2.79
Tapered	11	69.0	24.1	0.70	2.86
Tapered	11	71.0	24.2	0.71	2.93
Tapered	11	73.0	24.6	0.71	2.97
Tapered	11	75.0	24.8	0.70	3.03
Recessed	7	38.0	13.3	0.73	2.86
Recessed	7	40.0	13.8	0.75	2.90
Recessed	7	42.0	14.4	0.79	2.92
Recessed	7	44.0	14.7	0.84	2.99
Recessed	7	46.0	14.8	0.87	3.11
Recessed	7	48.0	15.0	0.88	3.15
Recessed	7	50.0	15.7	0.88	3.18
Recessed	7	52.0	16.2	0.89	3.19
Recessed	9	40.0	17.8	0.75	2.25
Recessed	9	42.0	18.5	0.82	2.27
Recessed	9	44.0	18.9	0.86	2.33
Recessed	9	46.0	19.0	0.87	2.42
Recessed	9	48.0	19.1	0.88	2.51
Recessed	9	50.0	19.6	0.89	2.55
Recessed	9	52.0	19.9	0.89	2.61
Recessed	11	55.0	22.7	0.85	2.42
Recessed	11	57.0	23.2	0.86	2.46
Recessed	11	59.0	23.8	0.87	2.48
Recessed	11	61.0	23.9	0.89	2.55
Recessed	11	63.0	23.9	0.90	2.64
Recessed	11	65.0	24.6	0.91	2.66